

Decoding the Functional Relevance of Intrinsic Brain Activity with (TMS-)EEG

Sarah Glim

Dissertation

der Graduate School of Systemic Neurosciences

der Ludwig-Maximilians-Universität München



Graduate School of
Systemic Neurosciences
LMU Munich

September 05, 2018

Supervisor:

Dr. Afra M. Wohlschläger

Department of Neuroradiology

Technische Universität München

First Reviewer: Dr. Afra M. Wohlschläger

Second Reviewer: Dr. Christian Sorg

External Reviewer: Prof. Dr. Dr. Kai Vogele

Date of Submission: September 05, 2018

Date of Defense: March 14, 2019

ABSTRACT

While the human brain had long been considered a reflexive organ that operates primarily in response to stimulation, more and more recent evidence instead points to a proactive role of it. Among such evidence is the observation that the brain exhibits striking patterns of activation also in the absence of any external stimulus, with these patterns being highly organized in both time and space. The overarching aim of the current thesis is to contribute to a better understanding of this so-called intrinsic brain activity, as measured non-invasively with electroencephalography (EEG). To this end, two original research projects were conducted. By examining the functional relevance of low-frequency fluctuations in intrinsic activity on the one hand and by exploring an experimental design able to enhance the measurability of intrinsic cross-frequency coupling on the other hand, these projects were targeted at dynamically evolving intrinsic brain activity in terms of both content and methodology.

In the first project of the current thesis, a visual backward-masking task was carried out in combination with EEG. During each trial of this task, participants localized the missing part of a briefly presented target stimulus and subsequently indicated their confidence as a proxy for the stimulus' access to conscious awareness. We found that this access was related to the evolution of low-frequency fluctuations in electrophysiological activity, so-called slow cortical potentials (SCPs), seconds before stimulus presentation. After stimulus presentation, conscious access came along with enhancements of established correlates of visual consciousness, namely the visual awareness negativity, the P3 component, and associated positive SCPs. These findings provide evidence for the functional relevance of SCPs, which seem to be optimally positioned for integrative processes leading up to the formation of unified conscious experiences, and are in support of a considerable impact of intrinsic brain activity on human perception, cognition, and behavior.

In the second project of the current thesis, EEG was combined with concurrent transcranial magnetic stimulation (TMS), implemented as single-pulse TMS (sTMS) and repetitive TMS (rTMS) at 5, 11, and 23 Hz over the left motor cortex and the right visual cortex of healthy participants. We investigated the influence of this stimulation on theta-gamma, alpha-gamma, and beta-gamma phase-amplitude coupling and found that, relative to sham stimulation, TMS pulses caused transient coupling increases in all assessed conditions. This effect arose not only at the stimulation site but also over various other cortical regions, with the propagation induced by rTMS outperforming that induced by sTMS. The obtained findings support considerations according to which TMS synchronizes natural neural oscillators and thereby enhances the detectability of associated intrinsic signals at the EEG-recorded population level. It stands to reason that concurrent TMS-EEG thus constitutes an effective methodological tool to assess (the functional relevance of) intrinsic brain activity non-invasively at a considerably improved signal-to-noise ratio.

Together, the projects presented in the current thesis complement contemporary research efforts to decode the human brain's intrinsic activity. By providing novel insights into both the functional relevance and the measurability of the fluctuating/oscillating features of such activity, the current thesis paves the way for future studies that might capitalize on these findings in order to target joint overall research objectives: a detailed understanding of the time-frequency-resolved mechanisms generating and maintaining intrinsic brain activity as well as knowledge of this activity's precise role in the dynamic neural processes underlying human perception, cognition, and behavior. In the end, such comprehension has the potential to produce path-breaking advancements in the context of healthy brains, diseased neuronal structures, and artificial neural systems.

TABLE OF CONTENTS

ABSTRACT	i
TABLE OF CONTENTS	iii
1 Introduction: The Human Brain’s Intrinsic Activity	1
1.1 The Human Brain during Rest	2
1.1.1 Discovering Intrinsic Brain Activity	2
1.1.2 Temporo-Spatial Properties of Intrinsic Brain Activity	3
1.1.3 Intrinsic Brain Activity in Clinical Populations	6
1.2 The Human Brain during Active Tasks	7
1.2.1 Intrinsic Brain Activity Impacts on Human Performance	7
1.2.2 Relating Intrinsic Brain Activity in V1 to Visual Consciousness ...	10
1.3 Aims of the Thesis	11
2 Project I: The Evolution of Pre-Stimulus Slow Cortical Potentials is Associated with an Upcoming Stimulus’ Access to Visual Consciousness	15
3 Project II: Phase-Amplitude Coupling of Neural Oscillations can be Effectively Probed with Concurrent TMS-EEG	51
4 Discussion: Decoding the Restless Brain	83
4.1 Advancing Research on Intrinsic Brain Activity	83
4.2 Methodological Considerations	87
4.3 Future Directions and Already Accomplished Steps	90
4.4 Conclusions	94
REFERENCES	v
ACKNOWLEDGMENTS	xix
CURRICULUM VITAE	xxi

LIST OF PUBLICATIONS	xxiii
EIDESSTATTLICHE VERSICHERUNG/AFFIDAVIT	xxv
DECLARATION OF AUTHOR CONTRIBUTIONS	xxvii

1

Introduction: The Human Brain's Intrinsic Activity

The human brain is inherently restless (Raichle 2011). It exhibits highly organized, dynamic patterns of activation not only during active stimulus processing but also in the absence of any external stimulation or overt task. Over the past decades, the complex temporal and spatial properties of such ongoing or intrinsic brain activity have become a major focus of attention in systems neuroscience (e.g., Allen et al. 2014; Biswal et al. 1995; Massimini et al. 2005; Mitra et al. 2015), with evidence for this activity's pronounced influence on human perception, cognition, and behavior rapidly accumulating (e.g., Devrim et al. 1999; Fox et al. 2007; Hesselmann et al. 2008a, 2008b; Schölvinck et al. 2012; Wohlschläger et al. 2016). The operations performed by the brain's intrinsic activity have been proposed to reflect information processing for interpreting, responding to, and specifically also predicting the external environment (Raichle 2010, 2015). Consequently, the traditionally reflexive view of brain functions is more and more substituted by a proactive view of the human brain as an intrinsic prediction machine (Clark 2013). In this introductory chapter, seminal discoveries, hypotheses, and implications relating to the brain's intrinsic activity mode will be presented in order to pave the way for the current thesis' two main projects. By (1) demonstrating a pronounced relationship between low-frequency fluctuations in intrinsic pre-stimulus activity and subsequent stimulus perception in the visual domain and by (2) introducing a novel experimental technique to effectively probe intrinsic cross-frequency coupling in humans, these projects are aimed at enabling a more sophisticated understanding of the spectral characteristics of dynamically fluctuating/oscillating intrinsic brain activity. Ultimately, such

decoding of the restless brain is going to be indispensable for a general understanding of the brain in both the healthy and diseased state.

1.1 The Human Brain during Rest

While the human brain is restless by its very nature, this nature is best investigated during so-called resting state measurements, in which the participant's brain activity is recorded in the absence of any explicit task. In the current section, essential insights into the brain's condition during resting state are presented by portraying (1) a short history of such measurements, (2) the temporo-spatial properties of intrinsic brain activity that were identified through them, and (3) the potential of human resting state data for the assessment of different psychiatric and neurological disorders, whose diagnosis and treatment monitoring might be crucially facilitated through the study of intrinsic brain activity.

1.1.1 Discovering Intrinsic Brain Activity

It has been noted early on that mental work adds only a small increment to the continuous stream of cortical activity measurable non-invasively in human electroencephalography (EEG; Berger 1929). Rather than focusing on this dominant facet of measurable activity though, neuroscientists have traditionally dismissed it as unsystematic noise and consequently sought to attenuate its power during data collection or processing (see e.g., Dawson 1954). In 1995, the functional significance of intrinsic brain activity eventually received broader recognition, when the advancement of functional magnetic resonance imaging (fMRI; Kwong et al. 1992; Ogawa et al. 1990) allowed for the detection of coherent patterns in spontaneous blood-oxygen-level-dependent (BOLD) signal time courses (Biswal et al. 1995). By demonstrating high temporal correlations among low-frequency signals in distributed sensorimotor cortical regions, Biswal and colleagues found evidence for the depiction of meaningful neural communication in resting state data and thereby initiated a long line of

research aimed at identifying the human brain's intrinsic functional connectome (for reviews, see Smith et al. 2013; van den Heuvel and Hulshoff Pol 2010). Up to the present, manifold methods for associated signal analyses and the treatment of potentially confounding non-neuronal signals (e.g., fluctuations originating from cardiac and respiratory cycles) have been actively developed (e.g., Allen et al. 2014; Chang et al. 2009; Friston et al. 2014; Murphy et al. 2013). Novel technological advancements, especially the simultaneous collection of EEG and fMRI data and the involved combination of high temporal and high spatial data resolution (see Huster et al. 2012), promise further remarkable discoveries in the near future, with the research potential in the field of intrinsic brain activity being far from exhausted.

1.1.2 Temporo-Spatial Properties of Intrinsic Brain Activity

With several state-of-the-art methodologies at hand, research has begun to identify a sophisticated web of temporo-spatial mechanisms inherent to intrinsic brain activity, which is ever growing in its explanatory power. In terms of temporal properties, dominant arrhythmic fluctuations and rhythmic oscillations in brain activity have been characterized using (time-) frequency decompositions of electrophysiological resting state data (e.g., Alahmadi et al. 2016; He et al. 2008; Papagiannopoulou and Lagopoulos 2016). Among the traditionally employed frequency bands (encompassing the delta, theta, alpha, beta, and gamma range), alpha activity, which is typically defined as rhythmic activity between 8 and 12 Hz, constitutes the most salient signal during wakeful resting state (Berger 1929) and has thus been ascribed a particularly prominent role in the maintenance of healthy brain functioning. In their inhibition-timing hypothesis, Klimesch and colleagues (Klimesch et al. 2007) associated the alpha band with the inhibitory control and timing of cortical processes. In a similar vein, the group around Jensen (Jensen and Mazaheri 2010; Mazaheri and Jensen 2010; Scheeringa et al. 2012) proposed that alpha activity operates in a pulsed manner to provide rhythmic functional inhibition, the dynamic reduction of processing capabilities in a particular brain

region or set of regions, as a means of effective information gating. As active information processing is by contrast associated with neural activity in the faster gamma band (approximately 30-100 Hz; Henrie and Shapley 2005; Melloni et al. 2007; Pesaran et al. 2002), cross-frequency interactions between both bands are considered a fundamental tool of intrinsic neural coordination (Bonfond and Jensen 2015; Jensen and Mazaheri 2010; Osipova et al. 2008). More generally, such interactions, implemented in particular as coupling between a slower oscillation's phase and a faster oscillation's amplitude (Canolty et al. 2006; Lakatos et al. 2005; Tort et al. 2010), enable the integration of functional systems across different temporo-spatial scales, with high-frequency activity typically reflecting local cortical processing and low-frequency activity arising from the computations of large-scale brain networks (Canolty and Knight 2010). At the lower end of such low-frequency activity and outside of the traditionally employed frequency bands, so-called slow cortical potentials (SCPs; typically ≤ 1 Hz) have lately received broad attention and are now increasingly considered in the context of neural information processing (He and Raichle 2009; Khader et al. 2008; Northoff 2017). Based on their slow time scale, SCPs have been proposed to be optimally positioned for the synchronization of distributed brain regions and to consequently carry out large-scale information integration in the brain (He and Raichle 2009).

As illustrated by these examples of spectral brain organization, coupled oscillations and fluctuations of different frequencies are an effective tool to dynamically control the processing, gating, and integration of neural information, with the temporal properties of brain activity being closely interwoven with this activity's spatial characteristics. The close link between temporal and spatial mechanisms is further illustrated by observations according to which the degree of interaction between certain highly connected cortical areas and the rest of the brain changes at various time scales (de Pasquale et al. 2017) and by a recent whole-brain model that accounts for interregional communication patterns by means of local oscillations

on multiple frequency channels (Deco et al. 2017). To illuminate the precise specifics of such communication patterns, modern neuroimaging research is taking advantage of the wide spatial range of low-frequency signal transmission in particular and has so far produced a number of seminal findings on the brain's global architecture, as detailed next.

To date, multiple networks of functionally connected brain regions have been identified in the human resting state (see van den Heuvel and Hulshoff Pol 2010). Most prominent among these is the so-called default mode network, which comprises, among other areas, the posterior cingulate and adjacent precuneus and the medial prefrontal cortex and is supposed to be tonically active in the baseline state of wakeful rest (Greicius et al. 2003; Raichle et al. 2001; Shulman et al. 1997). As proposed by Raichle and colleagues (Raichle et al. 2001), activity in this network may reflect the brain's continuous gathering and evaluation of internal and external information that is attenuated only when an attention-demanding overt task is performed. From a cognitive perspective, default mode network activation relates to the engagement in internally focused actions such as autobiographical memory retrieval, with the network being crucially involved in the consolidation of past experiences to predict future demands (Buckner et al. 2008). Besides the default mode network and its fundamental role in the human resting state, further networks of spatially separate yet functionally connected brain regions can be consistently observed, including the frontoparietal control network, the ventral and dorsal attention networks, as well as the somatomotor, visual, and language networks (Lee et al. 2012). While functional connectivity within such networks is traditionally understood in terms of zero-lag, non-dynamic temporal synchrony among the activity time courses of contained brain regions (dating back to Biswal et al. 1995), novel approaches have recently emerged that challenge this perspective. In a seminal study, Allen and colleagues (Allen et al. 2014) demonstrated that connectivity patterns are dynamic rather than stationary over time and thus argued for flexibility in neural coordination that contradicts the notion of

distinct stable networks. Taking a different approach, Mitra and colleagues (Mitra et al. 2015) broke the conventional resting state networks down into sequences of propagating activity and identified so-called temporal lag threads as a fundamental organizing property of intrinsic brain activity. By applying analysis techniques based on graph theory, others have characterized the complex topological properties of intrinsic brain networks, including small-world organization with deeply connected hub regions (for a review, see Wang et al. 2010). When taking these extensive temporo-spatial mechanisms of intrinsic brain activity into consideration, it should come as no surprise that their maintenance accounts for the majority of the brain's energy consumption (Raichle and Mintun 2006).

1.1.3 Intrinsic Brain Activity in Clinical Populations

Also unsurprisingly, a structure as complex as the human brain's intrinsic temporo-spatial layout is particularly prone to disturbances and dysfunctional alterations. Changes in intrinsic brain activity have indeed been reported in a number of clinical conditions such as schizophrenia (e.g., Dong et al. 2018; Karbasforoushan and Woodward 2012; Kirino et al. 2017), major depressive disorder (e.g., Sacchet et al. 2016; Workman et al. 2017; Zhou et al. 2017), Alzheimer's disease (e.g., Brueggen et al. 2017; de Vos et al. 2018; Wang et al. 2017), and autism spectrum disorder (e.g., Khan et al. 2015; Ye et al. 2014; Yerys et al. 2017). Most of these studies identified aberrant connectivity patterns within and/or between functional brain networks as a neural correlate of disease (see also Greicius 2008). An imbalance in intrinsic information coordination, manifested in the case of schizophrenia, e.g., as decreased communication within systems involved in salience processing, information gating, internal thought, emotion processing, and perception (among other aspects; Dong et al. 2018), entails a novel, intrinsic-activity-based perspective on pathophysiology. This paradigm shift is substantiated by an influential model unifying major psychiatric and neurological disorders under the framework of disturbances in three interacting core networks - the default mode

network, the salience network, as well as the central executive network (Menon 2011). Since resting state data have thus good potential as a significant marker of disease and treatment response and can be collected easily in clinical populations (relative to task-based examinations), their assessment together with an elevated understanding of intrinsic brain activity might be able to drive personalized medicine in the context of brain-related disorders to a new and enduring high.

1.2 The Human Brain during Active Tasks

In everyday life though, the brain rarely operates in a state of task-free rest. Instead, it continuously receives sensory input, actively processes and evaluates information, forms decisions, and plans and executes motor commands. Intrinsic brain activity does not cease to exist during these routines but runs alongside them and interacts with associated stimulation- or task-related activations and resulting overt output. In the current section, the form of such interactions is discussed in order to convey a detailed picture of how intrinsic brain activity influences human perception, cognition, and behavior. This is achieved by portraying (1) a broad overview of neuroscientific studies that contributed to the field and (2) a close-up view of one particular fMRI study that examined the tight relationship between intrinsic brain activity in early visual areas and the conscious perception of a briefly presented visual target stimulus (Wohlschläger et al. 2016). The latter study is highlighted as it is part of the research work of the current thesis' author and a direct precursor of this thesis' first main project.

1.2.1 Intrinsic Brain Activity Impacts on Human Performance

When investigating the interplay between intrinsic brain activity, stimulus-related brain activity, and behavior, one needs to find an adequate technique to isolate the former signal in brain recordings obtained during task performance. A straightforward way to implement this is to assess brain activity immediately before or right at stimulus onset, an interval that is

naturally free of any effects directly evoked by the stimulus, and to examine how this activity influences subsequent post-stimulus activity and/or relevant behavioral outcome measures (e.g., Britz et al. 2014; Busch et al. 2009; Devrim et al. 1999; Ergenoglu et al. 2004; Hesselmann et al. 2008a, 2008b; Scheeringa et al. 2011). Given a sufficient spatial resolution, one can also use activity time courses of non-engaged brain regions that exhibit high resting state functional connectivity to the engaged region of interest as a proxy for ongoing intrinsic activity in that very region not only before but also during active processing (e.g., Fox et al. 2006, 2007; Schölvinck et al. 2012; Wohlschläger et al. 2016). Recently, Huang and colleagues (Huang et al. 2017) furthermore proposed a novel signal correction approach, based on the subtraction of stimulation-free pseudo-trials, to analyze the interaction between intrinsic and evoked brain activity without the need to assume that certain brain regions are entirely unaffected by stimulation. While findings can vary among analysis techniques (see Huang et al. 2017), they are all in all suited to draw a comprehensive picture of the eminent functional relevance of intrinsic brain activity.

This relevance is most often assessed in the context of visual perception. The power of alpha activity prior to visual stimulation near sensory threshold has been shown to be lower before detected than before undetected stimuli, with detected stimuli triggering a stronger evoked neural response (Ergenoglu et al. 2004). Others have related low pre-stimulus alpha power to enhanced visual discrimination ability (van Dijk et al. 2008) and high confidence in visual discrimination decisions (Samaha et al. 2017). Besides such power effects, intrinsic alpha oscillations have been shown to exert influence particularly via their phase (Busch et al. 2009; Mathewson et al. 2009; Sherman et al. 2016), with stimulus presentation during the alpha wave's trough coming along with decreased visual detection performance (Mathewson et al. 2009). Consistent with this finding is the observation that, during a certain period of a cognitive task, high-frequency gamma power is lower at the trough than at the peak of alpha

oscillations (Bonfond and Jensen 2015). The prominent role of intrinsic alpha activity and alpha-gamma coupling is in line with the oscillation's abovementioned inhibitory function, presumably serving efficient information gating (Jensen and Mazaheri 2010), and suggests that the alpha rhythm is an apt marker of cortical excitability (e.g., Ergenoglu et al. 2004). Interestingly, a relation to visual perception has also been reported for the abovementioned SCPs, which are more negative before detected than before undetected stimuli and have thus been similarly related to fluctuations in the excitability state of neural networks (Devrim et al. 1999). From a spatial perspective, such fluctuations seem to be relevant first and foremost in those brain regions locally engaged in the task. Hesselmann and colleagues demonstrated that pre-stimulus BOLD activity is higher in the fusiform face area when a subsequently presented ambiguous vase-faces picture is perceived as two faces (Hesselmann et al. 2008a) and higher in the right motion-sensitive occipito-temporal cortex when perilliminal coherent motion is perceived as coherent rather than random (Hesselmann et al. 2008b). The authors furthermore showed that pre- and post-stimulus activity interact in a non-additive fashion during these tasks, a finding arguing against a simple linear superposition of evoked and intrinsic brain activity (e.g., brought forward by Fox et al. 2006) and instead supporting an account according to which evoked activity is dependent on the phase cycles of intrinsic activity (Huang et al. 2017). More globally, differences in the perceptual awareness of visual stimuli near sensory threshold have been related to distinct pre-stimulus EEG microstates, i.e., brief states of stable scalp topography that might represent activity in specific neural networks (Britz et al. 2014). The importance of large-scale topological network architecture is also supported by Ekman and colleagues (Ekman et al. 2012), who demonstrated that the anticipatory reconfiguration of communication patterns between a densely connected, frontally dominated network core and task-relevant visual regions is predictive of the success in subsequent visual perception. Together, these studies have started to shed light on the pronounced relationship between intrinsic brain activity at different temporal and spatial

scales and the brain's operations and outputs during active (visual) tasks. Yet, numerous open questions remain to be explored.

1.2.2 Relating Intrinsic Brain Activity in V1 to Visual Consciousness

One of these questions is whether and how intrinsic activity fluctuations within occipital networks covering the early visual areas V1 (primary visual cortex) and V2 (secondary visual cortex) can account for an incoming visual stimulus' access to conscious awareness. To answer this question, Wohlschläger and colleagues (Wohlschläger et al. 2016) collected fMRI measurements from 16 healthy adults during (1) 6 min of resting state, with a limited field of view focusing on the occipital cortex at a specifically high spatial resolution, (2) another 6 min of resting state, this time encompassing the entire brain, and (3) 4 blocks of 20 trials each of a visual backward-masking task. Each trial of this task started with the presentation of a sound cue for 25 ms. After a variable interval of 2, 4, or 6 s, the target stimulus, a honeycomb pattern with a missing comb either at its top or bottom, was presented for 16.5 ms in either the upper or lower left visual field. Following an interval of 66 ms, a negative image of the complete honeycomb pattern appeared for 16.5 ms at the same location, acting as a masking stimulus. Participants then indicated the position of the target's missing comb and whether they had been sure or unsure via button presses. Trials were separated by an inter-target interval of 28 ± 6 s (mean \pm SD). Throughout the trials, fixation was maintained on a centrally presented cross. In order to examine whether conscious awareness of the target stimulus was related to BOLD fluctuations in early visual areas, the authors defined cortical regions of interest in the following manner. By performing an independent component analysis of the high-resolution resting state fMRI data with a subsequent comparison of independent components to cytoarchitecturally defined occipital areas, two bilateral intrinsic brain networks centered on V1 and V2, respectively, were defined. Given that visual stimulation was restricted to the left visual field and consequently the right visual cortex, activity in the

unstimulated left-hemispheric parts of these networks served as a proxy for intrinsic brain activity. In addition, sites of significant activation by the target in the right-hemispheric network parts were extracted to examine stimulation-related brain activity. Analyzing the BOLD signal time courses within these regions of interest revealed the following main findings. In trials where the target was consciously perceived as compared to missed, (1) intrinsic brain activity in V2 was significantly lower before target presentation, (2) intrinsic brain activity in V1 was significantly higher during the interval of active target processing, and (3) stimulation-related activity in both V1 and V2 was significantly higher during active target processing. Interestingly, in V1, intrinsic activity before target presentation was significantly correlated with stimulation-related activity during target processing on a trial-by-trial basis, with lower pre-target intrinsic activity accompanying higher stimulation-related activity. An additional analysis of the intrinsic BOLD signal time courses, filtered narrowly to the dominant frequency of the whole-brain resting state data in order to eliminate any remaining task effects, moreover revealed a significant relation between V1's intrinsic signal evolution before target presentation and the access to consciousness, with a predominant pre-target signal decrease preceding a lack of conscious awareness. Together, these findings vividly illustrate the strong connection between fMRI-based fluctuations in intrinsic brain activity, especially within the primary visual cortex/V1, and the neural and behavioral markers of conscious visual perception. Since the fate of sensory information seems to critically depend on the particular intrinsic state that it meets when entering the human cortex, it becomes obvious now that intrinsic brain activity is not a mere by-product of normal brain functioning but an elementary building block of this very condition.

1.3 Aims of the Thesis

The current thesis is aimed at further advancing our understanding of the complex functional properties of dynamically evolving intrinsic brain activity, especially with regard to its

spectral characteristics. This activity is assessed non-invasively with scalp EEG, whose high temporal data resolution and relatively easy and cost-efficient application make the method attractive for a wide range of scientific and clinical practices. The thesis is subdivided into two main projects, with the first project directly continuing our fMRI study on the relation between low-frequency fluctuations in intrinsic brain activity and the emergence of visual consciousness (Wohlschläger et al. 2016; see above) and the second project putting forth a novel experimental technique based on the combination of EEG and transcranial magnetic stimulation (TMS) to enhance the measurability of intrinsic brain activity, in the form of intrinsic phase-amplitude coupling, in non-invasive brain recordings. The two presented projects examine the dynamics of prevalent fluctuations and oscillations within the restless brain and thereby contribute directly to the ever-growing field of interest surrounding intrinsic brain activity. Together, they open the door for future studies aimed at demonstrating the relevance of this activity for emerging perception at a considerably improved signal-to-noise ratio.

While we were able to show before that the evolution of slow fluctuations in the intrinsic BOLD signal is relevant for visual perception (Wohlschläger et al. 2016), the direct translation of this effect, with the BOLD signal being merely an indirect measure of neural activity, into more direct electrophysiological markers remained to be understood. Several studies attending to this issue proposed relations between the hemodynamic signal and different faster electrophysiological oscillations (Mantini et al. 2007; Scheeringa et al. 2016), e.g., in the alpha and beta (Ritter et al. 2009) as well as the gamma range (Niessing et al. 2005). Yet, the closest electrophysiological correlate of the fMRI signal in its raw fluctuations might be the equally slow but traditionally underappreciated SCPs, which have been reported to exhibit temporal correlations with BOLD activity and overall similar (task-related) activation patterns (He and Raichle 2009; Khader et al. 2008). In the current thesis' first main

project, it was tested whether this link holds true for intrinsic brain activity in the context of conscious visual perception. Using a visual backward-masking paradigm similar to the one used by Wohlschläger and colleagues (Wohlschläger et al. 2016) with concurrent EEG, we addressed the following research question. Do intrinsic fluctuations in SCPs, in particular their relative evolution toward stimulus presentation (rather than their sheer magnitude; see Devrim et al. 1999), relate to whether that stimulus will reach conscious awareness? Substantiated insights into this matter can advance our understanding of the neurophysiological basis and functional relevance of fluctuating intrinsic brain activity while further illuminating the variability in sensory experiences omnipresent in everyday life.

One mechanism in particular is a striking candidate for how slow long-range changes in intrinsic brain activity can influence fast local stimulus processing, the phase-to-amplitude coupling of neural oscillations, which is assumed to coordinate neural processing across multiple temporo-spatial scales (Canolty and Knight 2010; Canolty et al. 2006; Lakatos et al. 2005; Tort et al. 2010). The reliable and preferably non-invasive measurement of this mechanism is therefore of uttermost importance for a further advancement of neuroscience in the field of intrinsic information processing, with the minimal data length that yields a sufficient signal-to-noise ratio in this context depending critically on the wavelength of the involved oscillations. Following a previous approach of including at least 200 oscillatory cycles (Tort et al. 2010), a phase frequency of interest at 0.1 Hz would in this regard already require over 30 min of stable recordings. Better signal-to-noise ratios in scalp EEG measurements are fundamentally hindered by the method's inherent property of capturing not individual neural oscillators but their population-level sum, which involves considerable signal nullifications. In the current thesis' second main project, we therefore aimed at bringing forward a novel TMS-based experimental paradigm that can overcome this deficit by increasing the macroscopic brain signal through an alignment of individual oscillators. In

particular, the following research question was addressed. Does TMS cause a transient enhancement of the macroscopic phase-amplitude coupling of neural oscillations, as measured with concurrent EEG? Evidence for such a modulation can enable a new surge of studies successfully demonstrating intrinsic phase-amplitude coupling in the human brain and relating this mechanism to healthy and/or pathological brain functioning.

The current thesis targets two different research questions in the realm of intrinsic brain activity and thereby illustrates the broad range of topics pressing to be tackled by neuroscientists in the field. By examining (1) the perceptual relevance of slow fluctuations in intrinsic brain activity and (2) the non-invasive perturbation of intrinsic nested oscillations, relevant knowledge of this activity's EEG-assessed dynamics and neurophysiological functionality will be imparted and an incentive for future studies building on this knowledge provided. Both projects work toward a thorough understanding of the restless brain, which will eventually constitute a cornerstone for extensive advances in decoding healthy, diseased, as well as artificial neural systems.

2

Project I: The Evolution of Pre-Stimulus Slow Cortical Potentials is Associated with an Upcoming Stimulus' Access to Visual Consciousness

The current chapter depicts a research article entitled “The evolution of pre-stimulus slow cortical potentials is associated with an upcoming stimulus’ access to visual consciousness”. The article is authored by Sarah Glim, Anja Ries, Christian Sorg, and Afra M. Wohlschläger and is currently unpublished. In the presented research project, a visual backward-masking task was used to elicit perception near sensory threshold. It was demonstrated that the evolution of EEG-recorded SCPs can be related to the level of conscious stimulus perception seconds before the actual stimulus presentation, with this finding strengthening the link between slow fluctuations in intrinsic brain activity and essential perceptual functioning.

Contributions

The author of this thesis is the first author of the manuscript. A.M.W. and C.S. conceived the experiment. **S.G.**, C.S., and A.M.W. designed the experiment. **S.G.** and A.R. collected the data. **S.G.** and A.M.W. analyzed the data. **S.G.** wrote the manuscript. **S.G.**, C.S., and A.M.W. reviewed the manuscript.

**The evolution of pre-stimulus slow cortical potentials is associated
with an upcoming stimulus' access to visual consciousness**

Sarah Glim^{1,2,3}, Anja Ries^{1,2}, Christian Sorg^{1,2,4}, Afra M. Wohlschläger^{1,2,3,}*

¹Department of Neuroradiology, Technische Universität München, Munich, Germany; ²TUM-Neuroimaging Center, Technische Universität München, Munich, Germany; ³Graduate School of Systemic Neurosciences, Ludwig-Maximilians-Universität München, Planegg-Martinsried, Germany; ⁴Department of Psychiatry, Technische Universität München, Munich, Germany; *Corresponding author. Department of Neuroradiology, Neuro-Kopf-Zentrum, Klinikum rechts der Isar, Technische Universität München, Ismaninger Straße 22, 81675 Munich, Germany; e-mail: afra.wohlschlaeger@tum.de

Abstract

Slow cortical potentials (SCPs) have been proposed to be optimally positioned for neural processes leading up to the formation of conscious visual experience. While the sheer signal magnitude of SCPs can indeed influence the perception of a subsequently appearing visual stimulus, the role of their relative evolution toward stimulus presentation has so far received much less attention. To this end, we recorded direct-current electroencephalography during a visual backward-masking task, which required participants to localize the missing part of a briefly presented target stimulus. A subsequent confidence rating was used as a proxy for the target's access to conscious awareness. Broadband event-related potentials (ERPs) of all correct trials were determined relative to a short period immediately before the target and then compared among consciousness levels. From 2 s prior to target presentation up to this period, a negative relationship between ERPs and the level of consciousness became evident, with the grand average ERP slowly increasing toward the target when highest conscious awareness was about to be formed and slightly declining in all other cases. After target presentation, conscious awareness was characterized by an enhanced visual awareness negativity, an increased P3 component, and associated positive SCPs. By stressing the relevance of their intrinsic pre-stimulus evolution while also noting their occurrence during active stimulus processing, our findings support the proposed role of SCPs in the successful emergence of conscious visual perception.

Keywords

electroencephalography, slow cortical potentials, event-related potentials, visual perception, confidence

New & Noteworthy

We used a backward-masking paradigm to elicit visual perception near sensory threshold. The level of conscious target processing was found to be associated with the evolution of slow cortical potentials (SCPs) seconds before target presentation. After target presentation, visual consciousness was characterized by enhancements of the visual awareness negativity, the P3 component, and related positive SCPs. Results stress the importance of SCPs alongside faster neural processes for emerging visual consciousness.

Introduction

The same extrinsic stimulus can reach our conscious awareness in some moments and might fail to do so in others. Even though such perceptual variability has long been studied (e.g., Busch et al. 2009; Devrim et al. 1999; Ergenoglu et al. 2004; Linkenkaer-Hansen et al. 2004; Monto et al. 2008; Samaha et al. 2017), the neural mechanisms that determine whether an incoming piece of information will gain access to conscious processing are still insufficiently understood. Recently, slow fluctuations (frequency f typically ≤ 1 Hz) in brain activity, so-called slow cortical potentials (SCPs), have been put forward as a necessary condition or “neural predisposition” of consciousness (Northoff 2017; see also Birbaumer et al. 1990; He and Raichle 2009; Rutiku and Bachmann 2017). Due to their slow temporal dynamics, which are well suited for a large-scale synchronization of neural assemblies (He et al. 2008; von Stein and Sarnthein 2000), as well as their generation primarily by pyramidal cells with long-distance connections in upper cortical layers (Mitzdorf 1985), SCPs are believed to be optimally positioned for processes of global information integration (He and Raichle 2009). In a similar vein, other authors have associated variants of the SCP signal with consciousness-relevant processing properties such as network excitability (Devrim et al. 1999), perceptual anticipation (van Boxtel and Böcker 2004), and neural ignition (Dehaene and Changeux 2011), with the relevance of SCPs fitting well to recent theories of consciousness, including

the global neuronal workspace model (GNW model; Dehaene and Changeux 2011; Dehaene and Naccache 2001; Dehaene et al. 1998), the integrated information theory (IIT; Oizumi et al. 2014; Tononi 2004), and the temporo-spatial theory of consciousness (TTC; Northoff 2013, 2017; Northoff and Huang 2017). While the fundamental role of SCPs in the emergence of conscious awareness is thus generally agreed upon, knowledge of their precise shape and timing in empirical recordings of varying perceptual outcomes is still incomplete.

Empirically, SCPs can be observed in humans with a range of non-invasive recording techniques including direct-current (DC) electroencephalography (EEG; e.g., Vanhatalo et al. 2004, 2005). So far, a number of EEG studies have demonstrated the occurrence of SCPs during efficient processing and/or retention of sensory stimuli, particularly in the most commonly examined visual domain (Bosch et al. 2001; Pins and ffytche 2003; Pun et al. 2012). Only few studies, though, have also recognized the relevance of the intrinsic (ongoing) SCP state previous to stimulus presentation for an incoming stimulus' successful transfer to conscious awareness. In a seminal study, Devrim and colleagues (Devrim et al. 1999) demonstrated that the detection of visual stimuli near sensory threshold was better after negative relative to positive SCP magnitudes and thereby highlighted the relevance of spontaneous shifts in the EEG baseline for visual performance. Interestingly, evidence from other sensory modalities (Monto et al. 2008), recording techniques (see Wohlschläger et al. 2016, for a functional magnetic resonance imaging [fMRI] study), and signal frequency ranges (especially the alpha band [\sim 8-12 Hz]; Busch et al. 2009; Helfrich et al. 2014; Mathewson et al. 2009) indicates that not only sheer signal magnitude but also the signal's evolution, most often assessed via oscillatory phase analyses, prior to or right around stimulus presentation can be crucially involved in the stimulus' eventual fate. Of particular interest in this context is an EEG study by Monto and colleagues (Monto et al. 2008), which related an enhanced detection of somatosensory stimuli to stimulus presentation during the rising phase

of SCPs. It should be noted, though, that methodological criticism regarding such phase dependency has recently been raised, attributing effects in parts to a mere filtering artifact, namely the characteristic of acausal filters to smear post-stimulus differences into the pre-stimulus time interval (Zoefel and Heil 2013). While these studies thus hint, tentatively and with reservations, at a potential connection also between the pre-stimulus signal evolution of EEG-recorded SCPs on the one hand and upcoming consciousness in the visual domain on the other hand, the present study aims at providing direct and methodologically clean evidence for this relation.

To this end, we collected EEG inclusively DC signals from fifteen healthy participants while they were performing a demanding visual backward-masking task. In each trial of this task, the missing part of a target stimulus had to be localized within a binary-decision setting (“gap at top” or “gap at bottom”). A subsequent confidence rating (“not sure at all”, “slightly sure”, “quite sure”, or “very sure”) was used as a proxy for the target’s access to conscious awareness (Sandberg et al. 2010; Seth et al. 2008; Wohlschläger et al. 2016; Zehetleitner and Rausch 2013). It should be noted in this context that any operationalization of consciousness naturally emphasizes certain concept dimensions over others. With the selection of confidence ratings, our measure was targeted mainly at the “cognitive features of consciousness” (Northoff and Huang 2017) or the “ability to reflexively represent oneself”, typically referred to as self-monitoring, introspection, or meta-cognition (Dehaene et al. 2017). Yet, while we controlled for differences in objective performance by including only correct trials in the EEG analysis (e.g., Lamy et al. 2009), our measure was not generally aimed at isolating a particular concept dimension and adopted a rather comprehensive approach to consciousness (considering the typically good agreement between different behavioral measures including those not assessed here; see Dehaene and Changeux 2011). With respect to the conducted EEG analysis, an exploratory procedure was implemented with little a priori assumptions

about the precise profile (e.g., frequency structure and rhythmicity) of SCPs and other potentially relevant electrophysiological signals. We hence spared narrow band-pass filtering and involved artificial signal modifications and instead took advantage of the $1/f$ power relationship inherent to EEG data (Buzsáki and Draguhn 2004; Dehghani et al. 2010; see also Freeman et al. 2000; He 2014) by assessing SCP-dominated, broadband event-related potentials (ERPs). ERPs were computed relative to a 0.2 s window immediately before target onset and thereby satisfied our primary interest not in sheer signal magnitude but in the evolution of signals around the target stimulus. Subsequent statistical tests (Page 1963) were used to assess monotonic changes of voltage values with changing consciousness levels. As the analysis' main focus was on slowly changing pre-target differences in intrinsic activity fluctuations, the analysis window began 2 s before target onset. In addition, we also examined a corresponding post-target time interval, ending 2 s after target onset, with the intention to replicate previously established post-stimulation correlates of conscious processing (e.g., Koivisto et al. 2008; Lamy et al. 2009; Ojanen et al. 2003; Pins and ffytche 2003).

Materials and Methods

Participants

Fifteen healthy adults (ten females, five males, mean age \pm SD: 25.1 ± 3.3 years) took part in this study. One participant had to be excluded from data analysis because valid trials were lacking for the confidence rating “very sure”. The remaining fourteen participants (nine females, five males) had a mean age \pm SD of 25.4 ± 3.1 years. All participants were right-handed and had normal or corrected-to-normal vision. Participants gave written informed consent prior to experimentation and were paid a compensation of 8 € per hour. The experiment was approved by the Ethics Commission of the TUM School of Medicine and conducted in accordance with the Declaration of Helsinki.

Behavioral Task

An overview of the visual perception task is presented in Fig. 1. Stimuli and trial sequence were based on previously published tasks (Haynes et al. 2005; Wohlschläger et al. 2016), partially modified for the purpose of this study, and controlled with the Presentation stimulus delivery software (Neurobehavioral Systems, Inc., USA). Throughout the task, participants fixated a central white fixation cross on a black background. Each trial started with the presentation of just this fixation cross for 2,007 ms, after which a honeycomb-like grid was added as the target stimulus. This grid was composed of eighteen white hexagonal combs that were arranged to form a global hexagonal pattern with a missing comb either at the pattern's top or bottom. Each of the two possible gap locations was used in half of the trials in randomized order. We presented this target either in participants' upper or lower left visual field, with each visual field again selected in half of the trials in randomized order. In either case, the distance between the fixation cross and the closest and furthest grid point was 7° and 10.44° of visual angle, respectively. The target appeared for 34 ms and was followed by a fixation interval of 67 ms. Subsequently, a color-inverted image of the complete hexagonal honeycomb grid, consisting of all nineteen combs, was presented for 17 ms at the same location as the target, serving as the backward-masking stimulus. After the mask's disappearance, participants indicated, first, whether the target's missing comb had been located at its top or bottom and, second, how confident they were on a four-point scale from "not sure at all" over "slightly sure" and "quite sure" to "very sure" (e.g., Sandberg et al. 2010). Participants were instructed to respond as accurately as possible before the beginning of the subsequent trial without optimizing response speed. Judgments of the gap location were automatically considered incorrect if they were registered earlier than 200 ms after target onset or after the trial's ending. The next trial started after an inter-trial interval of 6,021 ms, 8,028 ms, or 10,035 ms, with the shortest interval having been used in 34/100 trials (17/50

trials), the middle interval in 33/100 trials (17/50 trials), and the longest interval in 33/100 trials (16/50 trials) of the actual experimental blocks (training blocks) in randomized order.

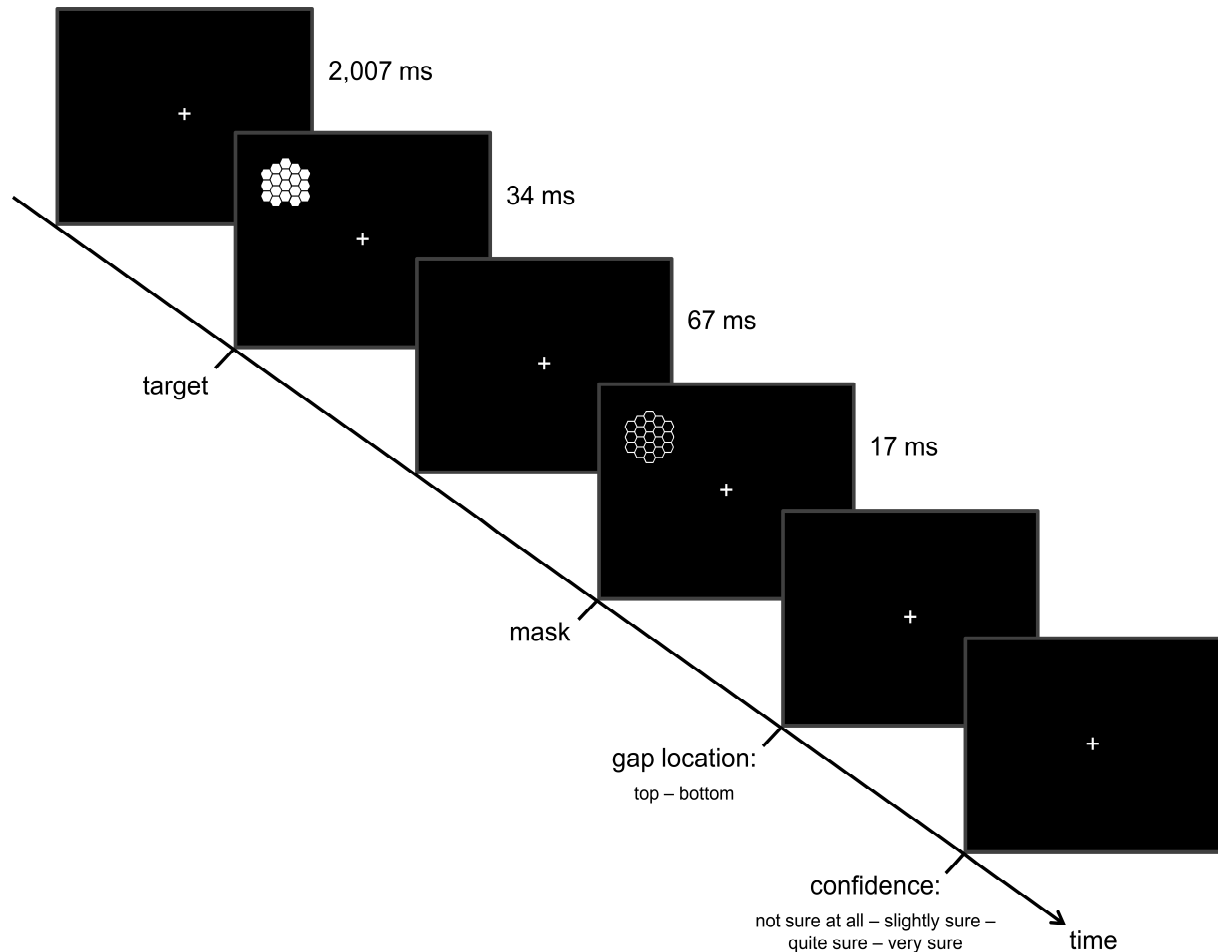


Fig. 1. Behavioral task. Throughout the task, participants fixated a white cross displayed centrally on a black computer screen. Following the presentation of just this fixation cross, each trial proceeded with the addition of a target stimulus, a honeycomb-like grid with a missing comb either at its top or bottom, in the upper or lower left visual field. After a fixed inter-stimulus interval, a negative image of the complete grid was presented at the same location, acting as a backward mask. Participants then had to indicate, first, the location of the target's missing comb and, second, their confidence on a four-point scale from "not sure at all" over "slightly sure" and "quite sure" to "very sure" via unspeeded button presses. After an inter-trial interval of 6,021 ms, 8,028 ms, or 10,035 ms, the next trial began automatically.

The visual perception task was implemented within the following testing procedure. To familiarize them with the task, participants first underwent a training session, in which at least two blocks of 50 trials each had to be completed. In the first training block, the white fixation cross turned either green or red for 500 ms after the first response to indicate a correct or an incorrect judgment, respectively. No confidence ratings had to be given. The second training block was identical to the actual experiment, as described above. Depending on a participant's performance and learning rate, further training blocks were optionally inserted. After this training session, participants completed 10 min of eyes-closed resting state, data of which were not analyzed in the context of the present study, followed by four blocks of 100 trials each of the visual perception task. Between blocks, participants could take short breaks.

Experimental Setup

While the experiment was run, participants were seated at a distance of 57 cm in front of a computer monitor in a darkened testing room and wore headphones over which white noise was played at an individually determined volume that was sufficient to eliminate any external noise while still being perceived as comfortable. Behavioral responses were registered via right-hand presses of neighboring keys on a standard computer keyboard with German layout (gap at top or bottom: "B" or "N"; confidence in increasing order: "V", "B", "N", "M"). During resting state and the four visual perception task blocks, EEG was recorded with the BrainVision Recorder software (Brain Products GmbH, Germany) from 63 scalp electrodes (EASYCAP GmbH, Germany). Electrodes were positioned according to the 10/20 system with all further electrodes inserted from the 10/10 system. In addition, we placed one electrode on participants' left torso to record electrocardiographic (ECG) activity as well as two electrodes below the outer canthi of the eyes to record electrooculography (EOG). For all recordings, electrode AFz served as ground while FCz was used as online reference. Signals from DC to 250 Hz were sampled at a rate of 5,000 Hz and amplified with the BrainAmp MR

plus system (Brain Products GmbH, Germany). Impedances between the skin and the electrodes were kept below 10 k Ω .

Behavioral Analysis

We examined participants' task behavior in order to confirm that the experimental design was suited well for the research question at hand. To this end, behavioral responses of all valid trials, as defined below, were analyzed in SPSS Statistics (IBM, USA) in the following manner. First, we checked whether setup and timing of the backward-masking paradigm were appropriate to avoid floor or ceiling effects in performance by computing the proportion of trials with a correct first response ("gap at top" or "gap at bottom") relative to the total trial number of each participant. Using a two-tailed one-sample Student's *t*-test over participants, we then tested statistically whether the observed performance differed significantly from chance performance, which was 50% correct in the present study. Second, we examined whether participants' confidence judgments reflected their objective performance to a reasonable extent by computing the proportion of correct trials relative to the total trial number within each of the four confidence categories separately. In this regard, an increasing proportion of correct trials with increasing confidence ratings would suggest that valid judgments were readily accessible and earnestly reported. As before, the observed proportions were tested against chance level with two-tailed one-sample Student's *t*-tests over participants. Additionally, we examined whether proportions differed among one another using a one-way repeated-measures analysis of variance (ANOVA) and subsequent two-tailed paired-sample Student's *t*-tests, with multiple comparisons accounted for with the Bonferroni correction. Third, as the present study was focused on contrasting trials that were assigned different confidence levels despite objectively correct visual perception, we took a closer look at the allocation of correct trials to the four confidence categories, i.e., at the relative sample sizes available for the EEG analysis. For that matter, we computed the proportion of correct

trials within each category relative to the total number of correct trials of a participant and then tested all proportions against the value of 0.25, representing the theoretical outcome of uniformly distributed confidence ratings, with two-tailed one-sample Student's *t*-tests over participants. The significance threshold for the conducted behavioral analyses was set at $p \leq .05$, unless stated otherwise.

EEG Preprocessing and Analysis

EEG data from the four visual perception task blocks were individually preprocessed with the BrainVision Analyzer software (Brain Products GmbH, Germany) in the following manner. First, the data were filtered using phase shift-free Butterworth filters with infinite impulse responses (IIR), implemented as a low-pass filter with a cutoff frequency at 70 Hz and a notch filter at $50 \text{ Hz} \pm 2.5 \text{ Hz}$. Next, global DC trend correction was performed to remove DC drift artifacts, e.g., originating from thermal and electrochemical changes in the skin and the electrolyte, by computing the linear trend over the average voltage values within all 1 s pre-target intervals and then subtracting this trend from the data (Hennighausen et al. 1993). To remove electrophysiological artifacts brought about by eye movements and eye blinks as well as by ECG activity and higher-frequency muscular activity, the following procedure was implemented. After applying a high-pass Butterworth filter with a cutoff frequency at 0.5 Hz and manually excluding data intervals that contained prominent, unsystematic noise in all electrodes, an independent component analysis (ICA; 64 components, classic sphering, restricted infomax algorithm) was performed. We carefully selected all components that captured the aforementioned artifacts (Hipp and Siegel 2013; Jung et al. 2000) and from these components reconstructed the corresponding time-domain signals with an inverse ICA. Lastly, difference waves between the reconstructed signals on the one hand and the original data before high-pass filtering on the other hand were computed to clean the original data of all identified artifacts. After this cleaning procedure, the data were re-referenced to the

average of electrodes TP9 and TP10 and subjected to a semi-automatic data inspection with the following criteria: maximal allowed voltage step: 50 $\mu\text{V}/\text{ms}$, maximal allowed difference of values in a 100 ms interval: 200 μV , lowest allowed activity (difference between maximum and minimum) in a 100 ms interval: 0.5 μV . Whenever a criterion was violated, an interval of ± 200 ms around the respective data point was marked as bad for later data rejection. Additional intervals were tagged upon visual inspection where required. At last, the preprocessed time-domain data as well as the computed ICA components were down-sampled to a sampling rate of 500 Hz and imported into MATLAB (The MathWorks, Inc., USA).

All following analyses were performed using the FieldTrip toolbox (Oostenveld et al. 2011) and custom-written MATLAB scripts. We segmented the imported time-domain EEG data into trials of ± 2 s around target onset and discarded all trials that met at least one of the following exclusion criteria. (1) Fewer or more than the required two responses were registered between the onset of the trial's target and the appearance of the next target, (2) invalid keys were pressed to respond, (3) the trial segment contained intervals previously marked as bad, and (4) an eye blink was registered closer than ± 100 ms around target emergence, indicating insufficient processing of the physical stimulus. Regarding the last criterion, data points were tagged as containing eye blinks whenever the time course of the ICA component capturing those blinks best within a particular task block exceeded ± 3 SD around its mean value. Out of 400 collected trials per participant, 383.93 ± 11.27 valid trials (mean \pm SD over participants) were retained. After this preparatory step, we examined whether the EEG signal evolution around target presentation was related to the level of confidence in objectively correct target percepts. For this purpose, the following analysis was performed successively for each available scalp electrode. We selected all correct trials, baseline-corrected them using a baseline window of -0.2 s to 0 s around target onset, and averaged the resulting time courses within each confidence category of each participant.

Separately for each trial time point, we then performed a pair of non-parametric significance tests for linear ranks (Page's trend tests; Page 1963), which allowed us to check the data for monotonic changes of voltage values with increasing levels of the ordinal confidence variable. To conduct these tests, we first ranked the trial-averaged voltage values of the different confidence categories separately for each participant, with the lowest value receiving the rank 1 and the highest value receiving the rank 4. Second, the test statistic L was computed as

$$L = \sum^n \left(Y_j \sum^m X_{ij} \right),$$

where $n = 4$ confidence categories, $m = 14$ participants, Y_j = hypothetical rank of the j th confidence category, and X_{ij} = observed rank of the j th confidence category within the i th participant. The test statistic L was computed twice, with the hypothetical ranking of confidence categories from "not sure at all" to "very sure" (Y) being 4, 3, 2, 1 when checking for a monotonic decrease and 1, 2, 3, 4 when checking for a monotonic increase of voltage values with increasing confidence. Third, statistical significance was determined by permutation testing. For each observed test statistic L , we computed 1,000 test statistics based on ranks that were permuted within participants. The p -value was defined as the proportion of permuted test statistics equal to or larger than the originally observed one. As we performed 4,002 such tests, two for each of 2,001 covered time points, p -values were subsequently adjusted for multiple comparisons with the false discovery rate (FDR) procedure (Benjamini and Hochberg 1995). The significance threshold was set at $p_{FDR} \leq .05$.

Results

Behavioral Results

The proportion of correct trials relative to all valid trials was 0.77 ± 0.11 (mean \pm SD over participants). This performance level differed significantly from a value of 0.5, which would have been expected for chance performance (two-tailed one-sample Student's t -test: $t(13) =$

8.92, $p < .001$), and attests that neither floor nor ceiling effects in performance prevailed. The implemented backward-masking paradigm was thus well suited to elicit visual perception near the threshold of conscious awareness. Broken down into the different confidence categories (Fig. 2A), the proportion of correct trials relative to the total trial number within a particular category was 0.63 ± 0.13 for “not sure at all”, 0.72 ± 0.13 for “slightly sure”, 0.83 ± 0.12 for “quite sure”, and 0.91 ± 0.12 for “very sure” (mean \pm SD over participants). All performance levels differed significantly from chance performance (two-tailed one-sample Student’s t -tests: $t(13) = 3.91$, $p = .002$ for “not sure at all”; $t(13) = 6.00$, $p < .001$ for “slightly sure”; $t(13) = 9.93$, $p < .001$ for “quite sure”; $t(13) = 12.46$, $p < .001$ for “very sure”). The presence of above-chance performance during apparent guessing (“not sure at all”) has been demonstrated previously and is considered an indication of unconscious stimulus knowledge according to the “guessing criterion” (e.g., Dienes et al. 1995; Sandberg et al. 2010). A one-way repeated-measures ANOVA furthermore yielded a significant main effect of confidence ($F(3,39) = 32.51$, $p < .001$). Subsequent pairwise comparisons revealed significant differences between all possible pairs of confidence categories but one, the pair “quite sure” vs. “very sure” (two-tailed paired-sample Student’s t -tests with a Bonferroni-corrected significance threshold at $p \leq .008$: $t(13) = -4.54$, $p = .001$ for “not sure at all” vs. “slightly sure”; $t(13) = -6.09$, $p < .001$ for “not sure at all” vs. “quite sure”; $t(13) = -7.80$, $p < .001$ for “not sure at all” vs. “very sure”; $t(13) = -4.79$, $p < .001$ for “slightly sure” vs. “quite sure”; $t(13) = -5.46$, $p < .001$ for “slightly sure” vs. “very sure”; $t(13) = -2.54$, $p = .025$ for “quite sure” vs. “very sure”). As objective performance thus increased with increasing confidence ratings, these results indicate that participants were able to readily access the higher-order judgments required for the task at hand, with conscious knowledge of their performance generally available according to the “zero-correlation criterion” (e.g., Dienes et al. 1995; Sandberg et al. 2010).

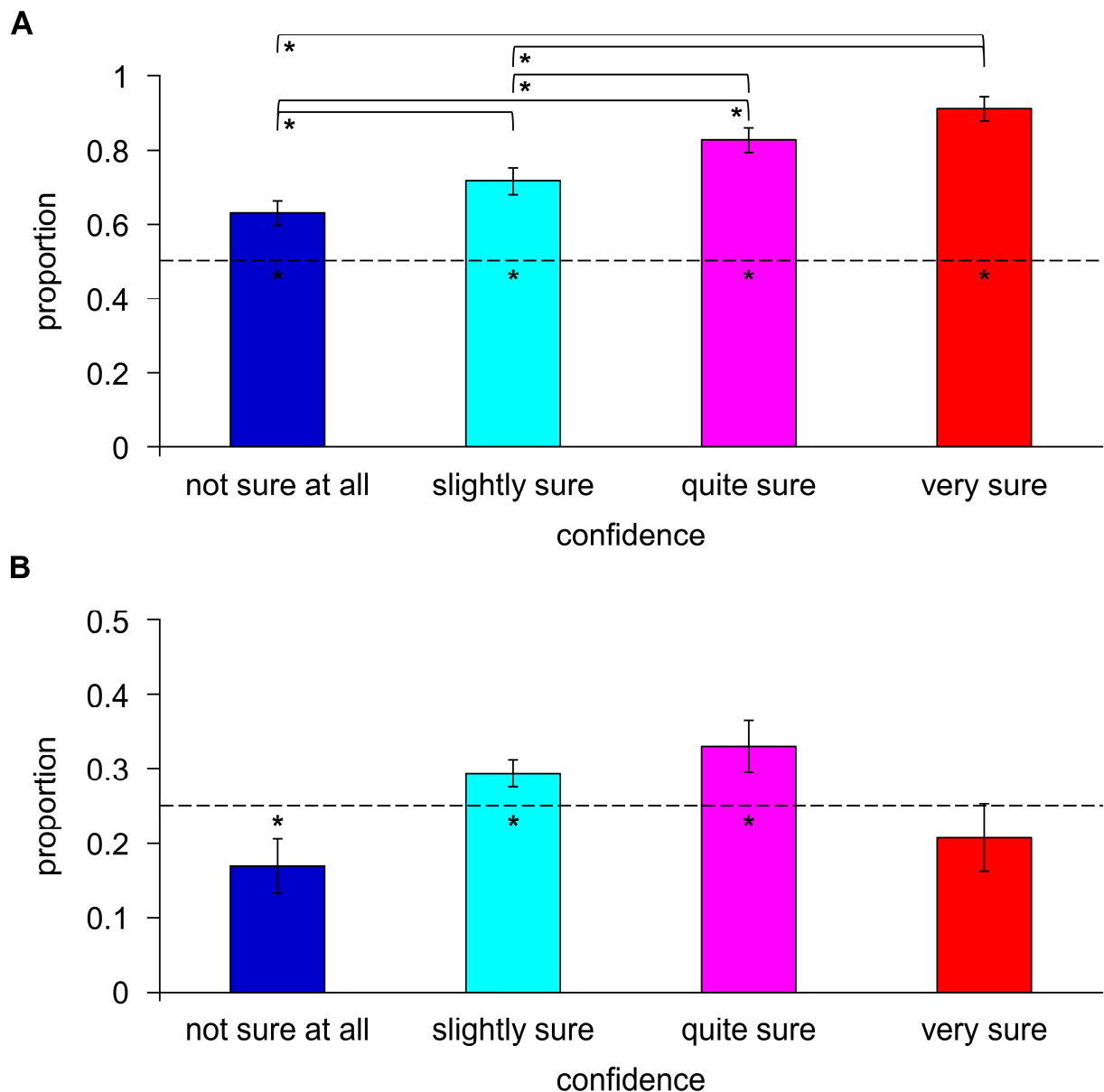


Fig. 2. Behavioral results. Bar charts show the proportion of correct trials in a particular confidence category relative to the total trial number in that category (A) and the total number of correct trials (B), respectively. Depicted are the mean proportion ± 1 SEM over $N = 14$ participants. Values are based on valid trials only, as defined in “Materials and Methods”. Statistical significance was examined with two-tailed one-sample Student’s *t*-tests against the values of 0.5 or 0.25 (see dashed lines in A and B: * $p \leq .05$) and two-tailed paired-sample Student’s *t*-tests between categories (see lines above the respective bars in A: * $p \leq .008$).

Next, we checked the allocation of correct trials to the different confidence categories in order to examine the relative sample sizes underlying the EEG analysis (Fig. 2B). The proportion of correct trials in a particular category relative to the total number of correct trials was 0.17 ± 0.14 for “not sure at all”, 0.29 ± 0.07 for “slightly sure”, 0.33 ± 0.13 for “quite sure”, and 0.21 ± 0.17 for “very sure” (mean \pm SD over participants), with the first three proportions differing significantly from a value of 0.25, the theoretical outcome of uniformly distributed confidence ratings (two-tailed one-sample Student’s t -tests: $t(13) = -2.20$, $p = .047$ for “not sure at all”; $t(13) = 2.39$, $p = .032$ for “slightly sure”; $t(13) = 2.29$, $p = .039$ for “quite sure”; $t(13) = -0.94$, $p = .362$ for “very sure”). Although correct trials were thus non-uniformly distributed among the different confidence categories, the ranking of their relative sample sizes (“not sure at all” < “very sure” < “slightly sure” < “quite sure”) differed from those rankings tested in the EEG analysis and was therefore unlikely to have confounded the following findings.

Event-Related Potentials

Since previous studies in the field had focused on local activity in visual cortical areas (Devrim et al. 1999; Wohlschläger et al. 2016) and since the target in our study was always presented in the left visual field and visual processing was thus handled primarily by the right visual cortex, ERPs at the nearby-located electrode O2 were of particular interest to us. As displayed in Fig. 3, three findings were striking at this location. First, the baseline-corrected EEG signal decreased significantly (Page’s trend tests: $p_{FDR} \leq .05$) with increasing confidence ratings at multiple time points across the entire pre-target interval (see green highlighting in Fig. 3). During this interval, the activity that eventually gave rise to a “very sure” rating of the upcoming perception diverged noticeably from the signal traces of the other three confidence categories. While low-frequency signals in the latter categories slightly declined toward target onset, they increased on average before the target’s appearance when high confidence was about to be reached. Second, a pronounced negativity associated with high confidence became

manifest also ~ 0.2 s after target presentation, but did not reach statistical significance at electrode O2. Third, the opposite pattern, i.e., significant signal increases with increasing confidence ratings, emerged in an interval of approximately 0.45-0.9 s after target onset (see yellow highlighting in Fig. 3). The signal modulation was again non-linear, with only little difference between the two lowest confidence categories and a conspicuous deviation of the “very sure” category.

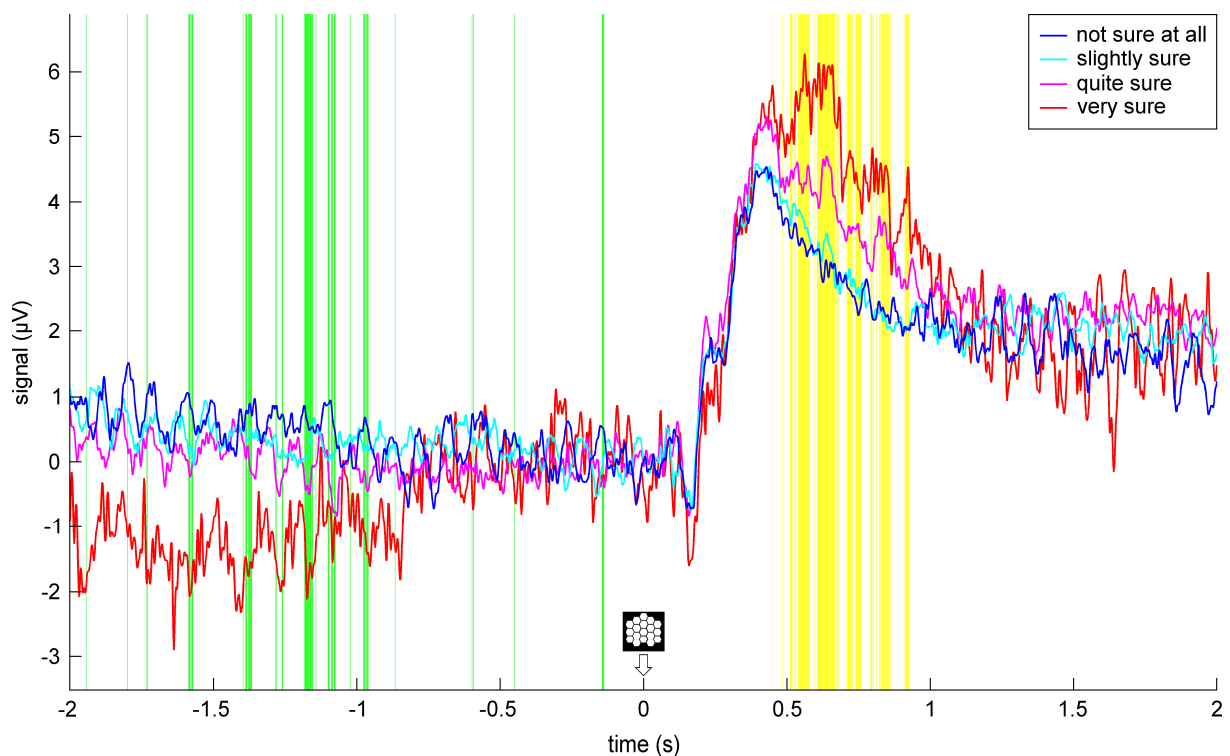


Fig. 3. Local event-related potentials (ERPs) at electrode O2. Grand average ERPs over $N = 14$ participants are displayed for the four utilized confidence categories as a function of trial time, ranging from -2 s to 2 s around target onset. Time points at which the signal decreased significantly with increasing confidence ratings are highlighted in green, time points of significant signal increase are marked in yellow (Page's trend tests: $p_{FDR} \leq .05$). Note that only correct valid trials were included in this analysis, with single-trial signal values computed relative to a window of -0.2 s to 0 s around target onset.

Next, we examined the topographic layout of the aforementioned three effects across all analyzed electrodes (Fig. 4). First, significant signal decreases with increasing confidence (see green highlighting in Fig. 4A) before target onset turned out to be concentrated on right occipital electrodes, with less prominent effects being observable at right parietal and fronto-temporal electrodes (see also Fig. 4B, for a different visualization of this topographic focus). As already observed at electrode O2, other electrodes' signal patterns likewise indicated that the effect was driven primarily by a deviation of the "very sure" category from the other categories' low-frequency signal traces. Second, several midline and right central electrodes showed significant signal decreases with increasing confidence around 0.2 s after target onset (see also Fig. 4C). Third, significant signal increases with increasing confidence ratings (see yellow highlighting in Fig. 4A) occurred in the post-target intervals of almost all electrodes. As can be easily appreciated via visual inspection, this effect was broadest at right frontal, fronto-central, and fronto-temporal electrodes, where it encompassed most of the post-target interval, and the least pronounced at corresponding electrodes of the left hemisphere (see also Fig. 4D).

Discussion

With the present study, we provide evidence that the evolution of SCPs seconds before the presentation of a visual target stimulus near sensory threshold is tightly linked to whether that stimulus will reach conscious awareness. In this regard, a negative relationship became manifest between the signal values of SCPs, determined relative to a brief period immediately before target presentation, on the one hand and the access to consciousness on the other hand, with a rising SCP signal preceding best conscious access and slightly declining signals in all other consciousness categories. The $1/f$ power relationship inherent to EEG data (Buzsáki and Draguhn 2004; Dehghani et al. 2010) allowed us to expose this connection without applying a narrow band-pass filter to the data. We thereby aimed at avoiding signal distortions associated

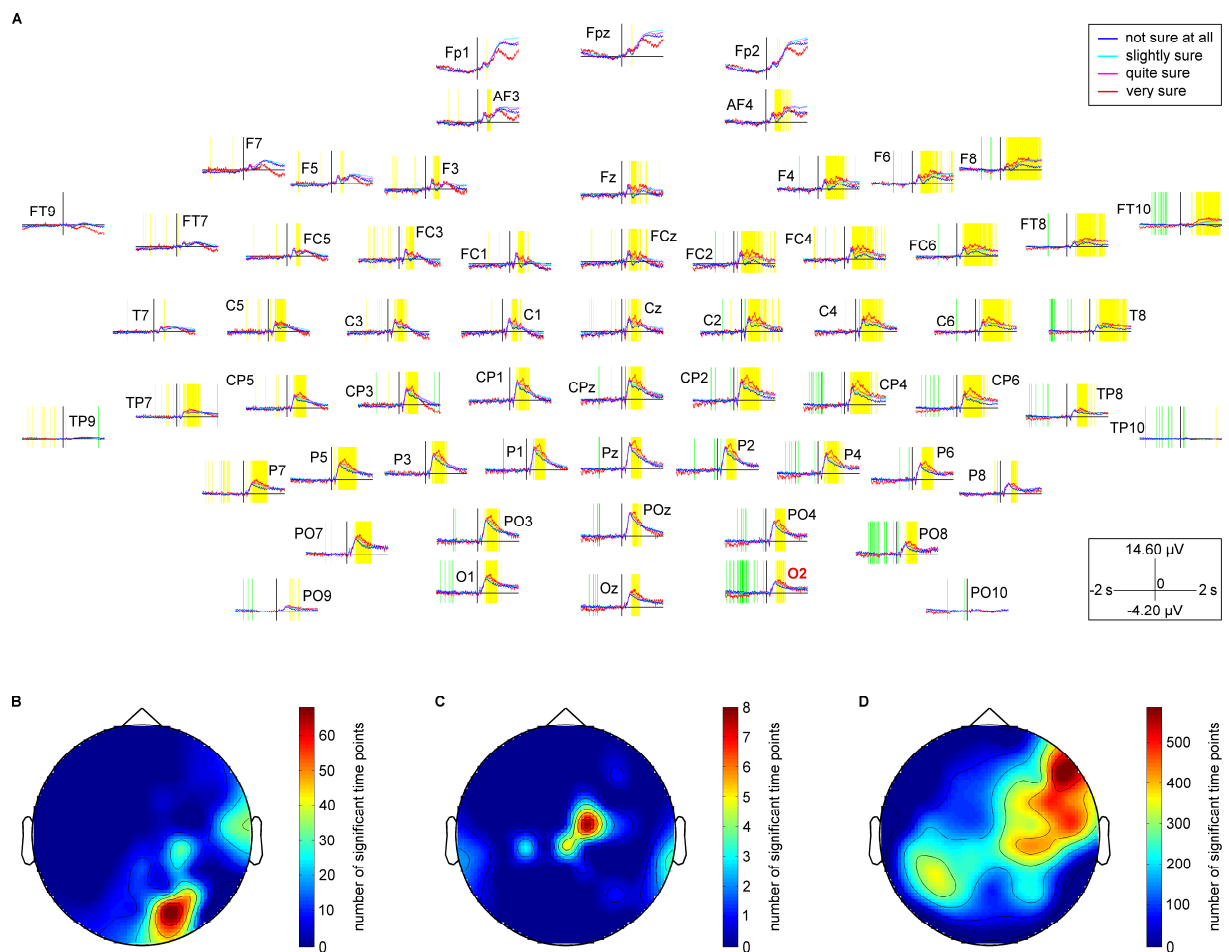


Fig. 4. Global topographic layout. (A) Grand average event-related potentials (ERPs) over $N = 14$ participants are displayed for the four utilized confidence categories and each available scalp electrode. Time points at which the signal decreased significantly with increasing confidence ratings are highlighted in green, time points of significant signal increase are marked in yellow (Page's trend tests: $p_{FDR} \leq .05$). (B-D) Topographic maps show the number of time points highlighted in green during the pre-target interval (B) and the entire interval after target onset (C) as well as the number of time points highlighted in yellow during this latter interval (D), with each interval containing 1,000 time points at a sampling rate of 500 Hz in total.

with both acausal and causal (high-pass) filters (Acunzo et al. 2012; Tanner et al. 2015, 2016; Zoefel and Heil 2013), including, but not limited to, the creation of artificial rhythmicity when

being actually interested in a largely arrhythmic fluctuation (He and Raichle 2009) with no a priori hypotheses about the contribution of phase and amplitude progressions within specific tight frequency limits. The observations made in this manner fit closely to previous studies in the field, which related enhanced somatosensory stimulus detection to the rising phase of SCP activity (Monto et al. 2008) and associated a lack of conscious access with a declining pre-stimulus blood-oxygen-level-dependent (BOLD) signal (Wohlschläger et al. 2016). The present result extends these previous studies into the domain of EEG-monitored visual perception, where the access to consciousness has been shown before to relate to low-frequency differences in sheer pre-stimulus signal magnitude, with cortical negativity accompanying better perception (Devrim et al. 1999), rather than to differences in relative signal evolution.

Together, these and other (e.g., Fox et al. 2007; Hesselmann et al. 2008a, 2008b; Schölvinck et al. 2012) studies draw a comprehensive picture of the pronounced influence that the brain's slowly fluctuating intrinsic state seems to exert on human perception, cognition, and behavior and thereby substantiate the proposed view of the brain as a proactive rather than reflexive organ (Bar 2007; Raichle 2010). This view, which advocates the continuous generation of top-down predictions about incoming sensory input as a major brain function (see also Clark 2013), is further supported by the highly structured organization of the awake brain's intrinsic activity (Raichle 2011; Raichle et al. 2001; see Fingelkurts et al. 2010, 2013, for a detailed discussion of the brain's and mind's space-time organization), to whose maintenance the vast majority of the brain's energy consumption is devoted (Raichle 2010; Raichle and Mintun 2006). In this context, the pre-target SCP fluctuations observed in the present study might reflect anticipatory adjustments of cortical excitability to tune the intrinsic system to the expected behaviorally relevant events, with conscious awareness of threshold stimuli indicating successfully configured settings for sensory information processing (see e.g.,

Ekman et al. 2012). As proposed by the recently introduced TTC (Northoff and Huang 2017), such favorable settings might be characterized by a temporo-spatial alignment or binding of intrinsic activity to the incoming stimuli. The long cycle duration of SCPs could in this regard provide a temporal window for the integration of stimuli into a cognitive unity of consciousness, with the proper correspondence between SCP timing and stimulus onset constituting the prerequisite for that stimulus' successful transfer to conscious awareness.

Topographically, the demonstrated relationship between pre-target EEG activity and conscious access was concentrated on electrodes over occipital and parietal sites of the right cerebral hemisphere, where the left-sided stimuli were primarily processed. This finding is consistent with previous work indicating that the connection between slow fluctuations in intrinsic brain activity and task performance is clearest in those brain regions pertaining to the task (Born et al. 1984) and, in the case of visual consciousness, stronger for the primary visual cortex, where bottom-up processing of the incoming stimulus dominates (Melloni et al. 2012), than for a later visual processing stage (Wohlschläger et al. 2016). Even though the spatial resolution of scalp EEG does not allow for a precise anatomical localization of effects, the topographic focus of our results together with these studies support the hypothesized role of intrinsic brain activity in the anticipatory fine-tuning of relevant processing capacities, with the stage for successful conscious access being set locally in brain regions involved in sensory stimulus processing.

By contrast, the access to conscious processing after target presentation became evident first through a negative EEG potential at (right) central electrodes. This finding is in line with studies suggesting that the earliest electrophysiological correlate of visual consciousness is the so-called visual awareness negativity (VAN) around 200-300 ms after stimulus onset, with the actually observed latency depending on a stimulus' precise nature and design (Koivisto et al.

2005, 2008; Ojanen et al. 2003; Wilenius-Emet et al. 2004). While the VAN might announce this stimulus' entry into phenomenal awareness (Koivisto and Revonsuo 2003), potential secondary conscious processes (Koivisto et al. 2008; Pins and ffytche 2003) manifested themselves in our study as subsequent positivity at almost all scalp electrodes. The topographic focus of this later positivity was on right frontal, fronto-central, and fronto-temporal sites, where the effect started the earliest and ended the latest. An enhanced positive potential emerging approximately 300-500 ms after stimulus presentation, typically termed the P3 component, has been consistently shown in the literature to accompany stimulus visibility (e.g., Dehaene and Changeux 2011; Koivisto et al. 2008; Lamy et al. 2009; Pins and ffytche 2003; Sergent et al. 2005) at the intersection of task-related activation and meta-cognitive experiences (Desender et al. 2016) and appears to be generated by activation in widespread brain areas including association cortices and the hippocampus (Halgren et al. 1998). The right-hemispheric dominance observed in our study is in accordance with the previously reported involvement of mainly the right brain side in meta-cognitive insights and reports (Fleming et al. 2012; Schmitz et al. 2006; Yokoyama et al. 2010). Still, the actual neural mechanisms underlying the P3 component are a matter of ongoing debate. According to the widely applied GNW model, incoming visual information gains access to consciousness when it is made globally available to multiple associative regions, which in turn trigger a top-down reactivation of early visual areas (Dehaene and Changeux 2011; Dehaene and Naccache 2001; Dehaene et al. 1998; Sergent et al. 2005). Several observations of the present study are consistent with the idea that the P3 event and therein included longer-lasting effects in the SCP range reflect this reverberant activation or global ignition. First, the hypothesized top-down-induced reactivation of visual areas is in line with the observed later P3 onset in occipital relative to more frontal electrodes. Second, the proposed ignition's all-or-none character fits well to the non-linear P3 changes emerging in our study (see also Sergent et al. 2005). And third, a suggested influence of highly structured intrinsic brain activity on whether

this ignition will arise or not (Dehaene and Changeux 2005) is in accordance with the demonstrated relationship between pre-target activity fluctuations and conscious access. While broad correspondence thus seems to exist between the observed data and established model concepts, it should be noted that other authors have objected to the interpretation of P3 and associated positive SCPs as reflecting global ignition and instead related these signals to a global inhibition of irrelevant information (Li et al. 2014). Notwithstanding these discrepancies, our results support the long-distance character innate to both approaches by emphasizing the role of far-ranging information processing rather than that of localized activity in single visual areas (e.g., ffytche and Zeki 1996; Zeki and Bartels 1998; Zeki and ffytche 1998) for a successful transfer of visual information to consciousness, with evidence for the supramodality of human meta-cognitive mechanisms having recently been provided (Faivre et al. 2018).

In the current study, this transfer was assessed via subjective confidence ratings in the face of objectively correct performance. To date, a wide variety of measures has been applied to quantify conscious access (see Seth et al. 2008, for a review). Because adopting an objective criterion, i.e., assuming consciousness whenever performance in a stimulus classification task surpasses chance level, has been criticized for overestimating conscious perception (among other points; see Dehaene and Changeux 2011), subjective measures are nowadays often the method of choice. In this context, confidence ratings are considered meta-cognitive judgments that test for “awareness of knowing” on a trial-by-trial basis, with their application based on the assumption that a mental state is conscious if the participant is aware of being in that state (Seth et al. 2008; note also Jachs et al. 2015, for an alternative view opposing the classically intimate link between meta-cognition and consciousness). Even though no subjective measure has proven itself to be clearly superior to all others, confidence ratings have been used in a number of studies on meta-cognition and/or conscious access so far (e.g., Cheesman and

Merikle 1986; Dienes et al. 1995; Fleming et al. 2012; Maniscalco and Lau 2012; Wohlschläger et al. 2016) and captured the emergence of visual consciousness sufficiently well in our study, as indicated by the broad correspondence of post-target effects with established correlates of conscious awareness (but see Li et al. 2014, for a dissociation of neural activity underlying confidence ratings and other measures of conscious access). Controlled experimental studies investigating the current findings with other behavioral measures are needed in the future to illuminate the precise interplay among the various theorized dimensions of consciousness inclusively (meta-)cognition that are potentially underlying them.

To summarize, we recorded DC-EEG during a demanding backward-masking task in which the visual target's access to conscious processing was assessed on a trial-by-trial basis via subjective confidence ratings. The evolution of slow EEG signals in the SCP range was associated with this access as early as ~2 s before target presentation. Even though no claim to direct causality is made, these results suggest that the brain's intrinsic state is critically involved in the perceptual fate of incoming sensory information. After target presentation, this fate was characterized by established neural correlates of consciousness, in particular the VAN, the P3 component, and related positive SCP shifts, with differences between consciousness categories lingering for at least 2 s post-target. Together, these findings add to our growing understanding of SCPs in the context of conscious awareness and encourage the routine inclusion and analysis of such low-frequency activity in future EEG studies.

Acknowledgments

The authors would like to thank Markus Ploner for providing EEG equipment and laboratory space as well as Laura Tiemann for valuable help with data collection.

Grants

S. Glim was supported by a scholarship of the Graduate School of Systemic Neurosciences (DFG - GSC 82/3). A. Ries was supported by the Studienstiftung des deutschen Volkes.

Disclosures

No conflicts of interest, financial or otherwise, are declared by the authors.

References

Acunzo DJ, MacKenzie G, van Rossum MCW. Systematic biases in early ERP and ERF components as a result of high-pass filtering. *J Neurosci Methods* 209: 212-218, 2012.

Bar M. The proactive brain: Using analogies and associations to generate predictions. *Trends Cogn Sci* 11: 280-289, 2007.

Benjamini Y, Hochberg Y. Controlling the false discovery rate: A practical and powerful approach to multiple testing. *J R Statist Soc B* 57: 289-300, 1995.

Birbaumer N, Elbert T, Canavan AGM, Rockstroh B. Slow potentials of the cerebral cortex and behavior. *Physiol Rev* 70: 1-41, 1990.

Born J, Whipple SC, Stamm J. Potential-related events: Reaction time tasks contingent upon frontal lobe slow potential shifts. *Ann N Y Acad Sci* 425: 667-670, 1984.

Bosch V, Mecklinger A, Friederici AD. Slow cortical potentials during retention of object, spatial, and verbal information. *Brain Res Cogn Brain Res* 10: 219-237, 2001.

Busch NA, Dubois J, VanRullen R. The phase of ongoing EEG oscillations predicts visual perception. *J Neurosci* 29: 7869-7876, 2009.

Buzsáki G, Draguhn A. Neuronal oscillations in cortical networks. *Science* 304: 1926-1929, 2004.

Cheesman J, Merikle PM. Distinguishing conscious from unconscious perceptual processes. *Can J Psychol* 40: 343-367, 1986.

Clark A. Whatever next? Predictive brains, situated agents, and the future of cognitive science. *Behav Brain Sci* 36: 181-204, 2013.

Dehaene S, Changeux J-P. Ongoing spontaneous activity controls access to consciousness: A neuronal model for inattention blindness. *PLoS Biol* 3: e141, 2005.

Dehaene S, Changeux J-P. Experimental and theoretical approaches to conscious processing. *Neuron* 70: 200-227, 2011.

Dehaene S, Kerszberg M, Changeux J-P. A neuronal model of a global workspace in effortful cognitive tasks. *Proc Natl Acad Sci U S A* 95: 14529-14534, 1998.

Dehaene S, Lau H, Kouider S. What is consciousness, and could machines have it? *Science* 358: 486-492, 2017.

Dehaene S, Naccache L. Towards a cognitive neuroscience of consciousness: Basic evidence and a workspace framework. *Cognition* 79: 1-37, 2001.

Dehghani N, Bédard C, Cash SS, Halgren E, Destexhe A. Comparative power spectral analysis of simultaneous electroencephalographic and magnetoencephalographic recordings in humans suggests non-resistive extracellular media. *J Comput Neurosci* 29: 405-421, 2010.

Desender K, Van Opstal F, Hughes G, Van den Bussche E. The temporal dynamics of metacognition: Dissociating task-related activity from later metacognitive processes. *Neuropsychologia* 82: 54-64, 2016.

Devrim M, Demiralp T, Kurt A, Yücesir I. Slow cortical potential shifts modulate the sensory threshold in human visual system. *Neurosci Lett* 270: 17-20, 1999.

Dienes Z, Altmann GTM, Kwan L, Goode A. Unconscious knowledge of artificial grammars is applied strategically. *J Exp Psychol Learn Mem Cogn* 21: 1322-1338, 1995.

Ekman M, Derrfuss J, Tittgemeyer M, Fiebach CJ. Predicting errors from reconfiguration patterns in human brain networks. *Proc Natl Acad Sci U S A* 109: 16714-16719, 2012.

Ergenoglu T, Demiralp T, Bayraktaroglu Z, Ergen M, Beydagi H, Uresin Y. Alpha rhythm of the EEG modulates visual detection performance in humans. *Brain Res Cogn Brain Res* 20: 376-383, 2004.

Faivre N, Filevich E, Solovey G, Kühn S, Blanke O. Behavioral, modeling, and electrophysiological evidence for supramodality in human metacognition. *J Neurosci* 38: 263-277, 2018.

ffytche DH, Zeki S. Brain activity related to the perception of illusory contours. *Neuroimage* 3: 104-108, 1996.

Fingelkurts AA, Fingelkurts AA, Neves CFH. Natural world physical, brain operational, and mind phenomenal space-time. *Phys Life Rev* 7: 195-249, 2010.

Fingelkurts AA, Fingelkurts AA, Neves CFH. Consciousness as a phenomenon in the operational architectonics of brain organization: Criticality and self-organization considerations. *Chaos Solitons Fractals* 55: 13-31, 2013.

Fleming SM, Huijgen J, Dolan RJ. Prefrontal contributions to metacognition in perceptual decision making. *J Neurosci* 32: 6117-6125, 2012.

Fox MD, Snyder AZ, Vincent JL, Raichle ME. Intrinsic fluctuations within cortical systems account for intertrial variability in human behavior. *Neuron* 56: 171-184, 2007.

Freeman WJ, Rogers LJ, Holmes MD, Silbergeld DL. Spatial spectral analysis of human electrocorticograms including the alpha and gamma bands. *J Neurosci Methods* 95: 111-121, 2000.

Halgren E, Marinkovic K, Chauvel P. Generators of the late cognitive potentials in auditory and visual oddball tasks. *Electroencephalogr Clin Neurophysiol* 106: 156-164, 1998.

Haynes J-D, Driver J, Rees G. Visibility reflects dynamic changes of effective connectivity between V1 and fusiform cortex. *Neuron* 46: 811-821, 2005.

He BJ. Scale-free brain activity: Past, present, and future. *Trends Cogn Sci* 18: 480-487, 2014.

He BJ, Raichle ME. The fMRI signal, slow cortical potential and consciousness. *Trends Cogn Sci* 13: 302-309, 2009.

He BJ, Snyder AZ, Zempel JM, Smyth MD, Raichle ME. Electrophysiological correlates of the brain's intrinsic large-scale functional architecture. *Proc Natl Acad Sci U S A* 105: 16039-16044, 2008.

Helfrich RF, Schneider TR, Rach S, Trautmann-Lengsfeld SA, Engel AK, Herrmann CS. Entrainment of brain oscillations by transcranial alternating current stimulation. *Curr Biol* 24: 333-339, 2014.

Hennighausen E, Heil M, Rösler F. A correction method for DC drift artifacts. *Electroencephalogr Clin Neurophysiol* 86: 199-204, 1993.

Hesselmann G, Kell CA, Eger E, Kleinschmidt A. Spontaneous local variations in ongoing neural activity bias perceptual decisions. *Proc Natl Acad Sci U S A* 105: 10984-10989, 2008a.

Hesselmann G, Kell CA, Kleinschmidt A. Ongoing activity fluctuations in hMT+ bias the perception of coherent visual motion. *J Neurosci* 28: 14481-14485, 2008b.

Hipp JF, Siegel M. Dissociating neuronal gamma-band activity from cranial and ocular muscle activity in EEG. *Front Hum Neurosci* 7: 338, 2013.

Jachs B, Blanco MJ, Grantham-Hill S, Soto D. On the independence of visual awareness and metacognition: A signal detection theoretic analysis. *J Exp Psychol Hum Percept Perform* 41: 269-276, 2015.

Jung T-P, Makeig S, Humphries C, Lee T-W, McKeown MJ, Iragui V, Sejnowski TJ.

Removing electroencephalographic artifacts by blind source separation. *Psychophysiology* 37: 163-178, 2000.

Koivisto M, Lähteenmäki M, Sørensen TA, Vangkilde S, Overgaard M, Revonsuo A.

The earliest electrophysiological correlate of visual awareness? *Brain Cogn* 66: 91-103, 2008.

Koivisto M, Revonsuo A. An ERP study of change detection, change blindness, and visual awareness. *Psychophysiology* 40: 423-429, 2003.

Koivisto M, Revonsuo A, Salminen N. Independence of visual awareness from attention at early processing stages. *Neuroreport* 16: 817-821, 2005.

Lamy D, Salti M, Bar-Haim Y. Neural correlates of subjective awareness and unconscious processing: An ERP study. *J Cogn Neurosci* 21: 1435-1446, 2009.

Li Q, Hill Z, He BJ. Spatiotemporal dissociation of brain activity underlying subjective awareness, objective performance and confidence. *J Neurosci* 34: 4382-4395, 2014.

Linkenkaer-Hansen K, Nikulin VV, Palva S, Ilmoniemi RJ, Palva JM. Prestimulus oscillations enhance psychophysical performance in humans. *J Neurosci* 24: 10186-10190, 2004.

Maniscalco B, Lau H. A signal detection theoretic approach for estimating metacognitive sensitivity from confidence ratings. *Conscious Cogn* 21: 422-430, 2012.

Mathewson KE, Gratton G, Fabiani M, Beck DM, Ro T. To see or not to see: Prestimulus α phase predicts visual awareness. *J Neurosci* 29: 2725-2732, 2009.

Melloni L, van Leeuwen S, Alink A, Müller NG. Interaction between bottom-up saliency and top-down control: How saliency maps are created in the human brain. *Cereb Cortex* 22: 2943-2952, 2012.

Mitzdorf U. Current source-density method and application in cat cerebral cortex: Investigation of evoked potentials and EEG phenomena. *Physiol Rev* 65: 37-100, 1985.

Monto S, Palva S, Voipio J, Palva JM. Very slow EEG fluctuations predict the dynamics of stimulus detection and oscillation amplitudes in humans. *J Neurosci* 28: 8268-8272, 2008.

Northoff G. What the brain's intrinsic activity can tell us about consciousness? A tri-dimensional view. *Neurosci Biobehav Rev* 37: 726-738, 2013.

Northoff G. "Paradox of slow frequencies" - Are slow frequencies in upper cortical layers a neural predisposition of the level/state of consciousness (NPC)? *Conscious Cogn* 54: 20-35, 2017.

Northoff G, Huang Z. How do the brain's time and space mediate consciousness and its different dimensions? Temporo-spatial theory of consciousness (TTC). *Neurosci Biobehav Rev* 80: 630-645, 2017.

Oizumi M, Albantakis L, Tononi G. From the phenomenology to the mechanisms of consciousness: Integrated information theory 3.0. *PLoS Comput Biol* 10: e1003588, 2014.

Ojanen V, Revonsuo A, Sams M. Visual awareness of low-contrast stimuli is reflected in event-related brain potentials. *Psychophysiology* 40: 192-197, 2003.

Oostenveld R, Fries P, Maris E, Schoffelen J-M. FieldTrip: Open source software for advanced analysis of MEG, EEG, and invasive electrophysiological data. *Comput Intell Neurosci* 2011: 156869, 2011.

Page EB. Ordered hypotheses for multiple treatments: A significance test for linear ranks. *J Am Stat Assoc* 58: 216-230, 1963.

Pins D, ffytche D. The neural correlates of conscious vision. *Cereb Cortex* 13: 461-474, 2003.

Pun C, Emrich SM, Wilson KE, Stergiopoulos E, Ferber S. In and out of consciousness: Sustained electrophysiological activity reflects individual differences in perceptual awareness. *Psychon Bull Rev* 19: 429-435, 2012.

Raichle ME. Two views of brain function. *Trends Cogn Sci* 14: 180-190, 2010.

Raichle ME. The restless brain. *Brain Connect* 1: 3-12, 2011.

Raichle ME, MacLeod AM, Snyder AZ, Powers WJ, Gusnard DA, Shulman GL. A default mode of brain function. *Proc Natl Acad Sci U S A* 98: 676-682, 2001.

Raichle ME, Mintun MA. Brain work and brain imaging. *Annu Rev Neurosci* 29: 449-476, 2006.

Rutiku R, Bachmann T. Juxtaposing the real-time unfolding of subjective experience and ERP neuromarker dynamics. *Conscious Cogn* 54: 3-19, 2017.

Samaha J, Iemi L, Postle BR. Prestimulus alpha-band power biases visual discrimination confidence, but not accuracy. *Conscious Cogn* 54: 47-55, 2017.

Sandberg K, Timmermans B, Overgaard M, Cleeremans A. Measuring consciousness: Is one measure better than the other? *Conscious Cogn* 19: 1069-1078, 2010.

Schmitz TW, Rowley HA, Kawahara TN, Johnson SC. Neural correlates of self-evaluative accuracy after traumatic brain injury. *Neuropsychologia* 44: 762-773, 2006.

Schölvinck ML, Friston KJ, Rees G. The influence of spontaneous activity on stimulus processing in primary visual cortex. *Neuroimage* 59: 2700-2708, 2012.

Sergent C, Baillet S, Dehaene S. Timing of the brain events underlying access to consciousness during the attentional blink. *Nat Neurosci* 8: 1391-1400, 2005.

Seth AK, Dienes Z, Cleeremans A, Overgaard M, Pessoa L. Measuring consciousness: Relating behavioural and neurophysiological approaches. *Trends Cogn Sci* 12: 314-321, 2008.

Tanner D, Morgan-Short K, Luck SJ. How inappropriate high-pass filters can produce artifactual effects and incorrect conclusions in ERP studies of language and cognition. *Psychophysiology* 52: 997-1009, 2015.

Tanner D, Norton JJS, Morgan-Short K, Luck SJ. On high-pass filter artifacts (they're real) and baseline correction (it's a good idea) in ERP/ERMF analysis. *J Neurosci Methods* 266: 166-170, 2016.

Tononi G. An information integration theory of consciousness. *BMC Neurosci* 5: 42, 2004.

van Boxtel GJM, Böcker KBE. Cortical measures of anticipation. *J Psychophysiol* 18: 61-76, 2004.

Vanhatalo S, Palva JM, Holmes MD, Miller JW, Voipio J, Kaila K. Infralow oscillations modulate excitability and interictal epileptic activity in the human cortex during sleep. *Proc Natl Acad Sci U S A* 101: 5053-5057, 2004.

Vanhatalo S, Voipio J, Kaila K. Full-band EEG (FbEEG): An emerging standard in electroencephalography. *Clin Neurophysiol* 116: 1-8, 2005.

von Stein A, Sarnthein J. Different frequencies for different scales of cortical integration: From local gamma to long range alpha/theta synchronization. *Int J Psychophysiol* 38: 301-313, 2000.

Wilenius-Emet M, Revonsuo A, Ojanen V. An electrophysiological correlate of human visual awareness. *Neurosci Lett* 354: 38-41, 2004.

Wohlschläger AM, Glim S, Shao J, Draheim J, Köhler L, Lourenço S, Riedl V, Sorg C.

Ongoing slow fluctuations in V1 impact on visual perception. *Front Hum Neurosci* 10: 411, 2016.

Yokoyama O, Miura N, Watanabe J, Takemoto A, Uchida S, Sugiura M, Horie K, Sato

S, Kawashima R, Nakamura K. Right frontopolar cortex activity correlates with reliability of retrospective rating of confidence in short-term recognition memory performance. *Neurosci Res* 68: 199-206, 2010.

Zehetleitner M, Rausch M. Being confident without seeing: What subjective measures of

visual consciousness are about. *Atten Percept Psychophys* 75: 1406-1426, 2013.

Zeki S, Bartels A. The asynchrony of consciousness. *Proc Biol Sci* 265: 1583-1585, 1998.

Zeki S, ffytche DH. The Riddoch syndrome: Insights into the neurobiology of conscious

vision. *Brain* 121: 25-45, 1998.

Zoefel B, Heil P. Detection of near-threshold sounds is independent of EEG phase in

common frequency bands. *Front Psychol* 4: 262, 2013.

3

Project II: Phase-Amplitude Coupling of Neural Oscillations can be Effectively Probed with Concurrent TMS-EEG

The current chapter depicts a research article entitled “Phase-amplitude coupling of neural oscillations can be effectively probed with concurrent TMS-EEG”. The article is authored by Sarah Glim, Yuka O. Okazaki, Yumi Nakagawa, Yuji Mizuno, Takashi Hanakawa, and Keiichi Kitajo and has been submitted for publication. In the presented research project, concurrent TMS-EEG was used to demonstrate that both single-pulse TMS (sTMS) and repetitive TMS (rTMS) can transiently enhance the macroscopic phase-amplitude coupling of neural oscillations, presumably by synchronizing underlying neural oscillators. It was concluded that TMS-EEG constitutes an effective experimental technique to probe intrinsic phase-amplitude coupling in humans.

Contributions

The author of this thesis is the first author of the manuscript. Y.N., T.H., and K.K. conceived and designed the experiment. Y.N., Y.O.O., Y.M., T.H., and K.K. collected the data. S.G., Y.N., Y.O.O., and K.K. analyzed the data. S.G., Y.O.O., and K.K. wrote the manuscript. All authors reviewed the manuscript.

**Phase-amplitude coupling of neural oscillations can be effectively
probed with concurrent TMS-EEG**

*Sarah Glim^{1,2,3}, Yuka O. Okazaki¹, Yumi Nakagawa¹, Yuji Mizuno^{1,4},
Takashi Hanakawa^{1,4}, Keiichi Kitajo^{1,4,*}*

¹RIKEN BSI-TOYOTA Collaboration Center, RIKEN Brain Science Institute, Wako, Japan;
²Department of Neuroradiology, Technische Universität München, Munich, Germany;
³Graduate School of Systemic Neurosciences, Ludwig-Maximilians-Universität München,
Planegg-Martinsried, Germany; ⁴National Center of Neurology and Psychiatry, Kodaira,
Japan; *Corresponding author. Rhythm-Based Brain Information Processing Unit, RIKEN
BSI-TOYOTA Collaboration Center, RIKEN Brain Science Institute, 2-1 Hirosawa, Wako,
Saitama 351-0198, Japan; e-mail: kkitajo@brain.riken.jp

Abstract

Despite the widespread use of transcranial magnetic stimulation (TMS), knowledge of its neurophysiological mode of action is still incomplete. Recently, TMS has been proposed to synchronise neural oscillators, and to thereby increase the detectability of corresponding oscillations at the population level. As oscillations in the human brain are known to interact within nested hierarchies via phase-amplitude coupling, TMS might also be able to increase the macroscopic detectability of such coupling. In a concurrent TMS-electroencephalography study, we therefore examined the technique's influence on theta-gamma, alpha-gamma and beta-gamma phase-amplitude coupling by delivering single-pulse TMS (sTMS) and repetitive TMS (rTMS) over the left motor cortex and right visual cortex of healthy participants. The rTMS pulse trains were of 5 Hz, 11 Hz and 23 Hz for the three coupling variations, respectively. Relative to sham stimulation, all conditions showed transient but significant increases in phase-amplitude coupling at the stimulation site. In addition, we observed enhanced coupling over various other cortical sites, with a more extensive propagation during rTMS than during sTMS. By indicating that scalp-recorded phase-amplitude coupling can be effectively probed with TMS, these findings open the door to the technique's application in manipulative dissections of such coupling during human cognition and behaviour.

Introduction

Due to its extensive effects on human perception, cognition and action, transcranial magnetic stimulation (TMS) is nowadays widely used in both basic neuroscientific research (e.g., during investigations of visual awareness¹, attention², speech³ and motor processing⁴) and in clinical practice (with potential treatment domains [see guidelines on therapeutic use⁵] including medication-resistant major depressive disorder⁶, post-stroke motor impairment⁷, aphasia⁸ and schizophrenia⁹). Despite this broad scope of application, knowledge of the precise neurophysiological effects of TMS is still incomplete.

Over the past decade, interest has arisen in the effects of TMS on macroscopic neural oscillations, as measured with non-invasive recording techniques such as electroencephalography (EEG)^{10,11,12,13,14}. In this context, Kawasaki and colleagues¹³ demonstrated a direct modulation of the temporal dynamics of these oscillations by showing that the consistency of oscillatory phases across stimulation trials, so-called phase locking, is transiently enhanced after single-pulse TMS (sTMS). Even though this effect can occur within a wide oscillatory spectrum, sTMS is assumed to act on intrinsic neural systems, and thus to be most effective for those frequencies that arise naturally within particular cortico-thalamic modules¹⁵. Accordingly, a highly probable candidate mechanism behind the observed increase in macroscopic across-trial phase locking is the phase resetting of underlying intrinsic oscillators (but see Sauseng and colleagues¹⁶ for a critical discussion of phase locking). Considering that such resets would simultaneously pertain to a multitude of coexistent oscillators, transiently enhanced synchronisation would also unfold within stimulation trials. As Thut and colleagues^{12,17} argued, rhythmic stimulation via repetitive TMS (rTMS) can foster such a synchronisation through neural entrainment, during which individual oscillators start to cycle with the same period as pulses delivered at their eigenfrequency, and thus become more and more aligned to such pulses, and consequently also to each other. Interestingly, this synchronisation or alignment of coexistent neural oscillators has been argued to prevent population-level signal nullifications, and to thereby enhance the detectability of macroscopic oscillations with scalp-based measurement techniques¹⁷. Associated EEG-recorded oscillatory power increases have de facto been reported for both sTMS^{15,18} and rTMS¹².

To fully appreciate the neurophysiological effects of TMS, it is necessary to consider that the human brain is unlikely to be a composition of neatly separated neural modules whose oscillatory signatures can be manipulated independently from each other. Rather, its essence

lies in a myriad of dynamic neural interactions that serve the integration of information across various temporal and spatial processing scales¹⁹. One promising mechanism for how such integration may be implemented in the brain is through a nested hierarchy of neural oscillations²⁰. In particular, studies have shown that the phase of oscillations arising from slower global computations can flexibly modulate the amplitude of faster local oscillations^{21,22,23,24,25}, a mechanism that might enable the coordination of multiple specialised processing nodes across large-scale brain networks. The functional relevance of such phase-amplitude coupling is supported by findings associating its strength with behavioural outcomes, e.g., success in a visual motion discrimination task²⁶. Given that phase-amplitude coupling is an inherent property of neural systems, the alignment of oscillators by TMS should enhance not only the detectability of individual macroscopic oscillations, but also the detectability of their coupling to other oscillations. As this feature would greatly facilitate the investigation of phase-amplitude coupling with non-invasive measurement techniques such as scalp EEG, which often require extensive recordings to cope with only moderate signal-to-noise ratios, its clear demonstration would be of high relevance for both TMS methodologists and cognitive neuroscientists.

Attempts have already been made to demonstrate an enhancement of EEG-recorded phase-amplitude coupling by TMS²⁷ and other non-invasive brain stimulation techniques, specifically transcranial alternating current stimulation (tACS)²⁸. Even though Noda and colleagues²⁷ demonstrated increased theta-gamma coupling within an offline paradigm following several sessions of rTMS in patients with depression, conclusive evidence from a sham-controlled examination of online EEG recordings during TMS in the healthy population is still missing. With the present study, we set out to provide such evidence, thereby using TMS to shed light on the transient modulation of the human brain's nested oscillations. To this end, we delivered both sTMS and rTMS over the left motor cortex and right visual cortex

of healthy participants while simultaneously collecting EEG. To ensure coverage of a wide range of the oscillatory nesting observable in neural systems^{20,29,30}, the enhancement of phase-amplitude coupling relative to sham stimulation was assessed separately for theta-gamma, alpha-gamma and beta-gamma coupling, with the rTMS frequency always equalling the frequency of the slower modulating oscillation to allow for this oscillation's direct entrainment. The experiments were designed to evaluate the following theoretical reasoning. As enhanced oscillatory power has been reported for both sTMS^{15,18} and rTMS¹², scalp-recorded phase-amplitude coupling should likewise be transiently enhanced for both stimulation paradigms. As both paradigms were further shown to modulate phase dynamics not only locally at the stimulation site, but also with network-wide signal propagation^{13,14}, the enhancement of phase-amplitude coupling might likewise propagate across the cortex. Finally, we directly compared the neurophysiological effects of sTMS and rTMS by examining whether an rTMS-induced entrainment of neural oscillators can induce a locally stronger and/or globally more widespread enhancement of phase-amplitude coupling relative to sTMS.

Methods

Participants

Fourteen right-handed healthy participants (two females, twelve males; mean age \pm SD, 30.8 \pm 5.5 years) were recruited to this study. Written informed consent was obtained from all participants prior to experimentation. The study was approved by the RIKEN Ethics Committee and was conducted in accordance with the code of ethics of the World Medical Association for research involving humans (Declaration of Helsinki).

TMS Design

TMS pulses were delivered through a figure-of-eight coil with a 70 mm wing diameter, connected to a biphasic magnetic stimulator unit (Magstim Rapid, The Magstim Company Ltd, UK). Stimulation intensity was fixed at 90% of a participant's active motor threshold, which was determined for the right first dorsal interosseous (FDI) muscle. During the entire experimental procedure, participants fixated on a central grey cross on a black computer monitor background and wore earplugs to reduce stimulation-evoked auditory potentials in neural activity.

An overview of the experimental design is presented in Fig. 1. Each participant received stimulation at three different sites in randomly ordered sessions. In one session, TMS was applied over the left motor cortex (approximately between electrodes C1 and C3, with the exact position being determined by the individual hotspot of the right FDI muscle stimulation; coil handle perpendicular to the central sulcus) and in a second session, it was applied over the right visual cortex (between electrodes Oz and O2; coil handle perpendicular to the midsagittal plane). In a third session, sham stimulation was delivered at a location 10 cm above the vertex of the head (electrode Cz; coil handle directed posteriorly). Each of these sessions comprised four different blocks, with each block consisting of 30 trials with inter-trial intervals of $10 \text{ s} \pm 15\%$. Depending on the block, trials contained either single TMS pulses or trains of five consecutive pulses delivered at 5 Hz, 11 Hz or 23 Hz.

EEG Recording and Preprocessing

During the entire stimulation procedure, EEG (left earlobe reference; AFz as ground) was recorded from 63 TMS-compatible Ag/AgCl scalp electrodes (EASY CAP, EASYCAP GmbH, Germany; see Fig. 1a for the electrode layout), which were positioned according to the international 10/10 system with lead wires rearranged orthogonally to the TMS coil handle

to reduce TMS-induced artefacts³¹. In addition, horizontal and vertical electrooculography (EOG) was recorded to monitor eye movements and blinks. All signals were sampled at a rate of 5,000 Hz, filtered online from DC to 1,000 Hz and amplified using the TMS-compatible BrainAmp MR plus system (Brain Products GmbH, Germany). Impedances were kept below 10 k Ω .

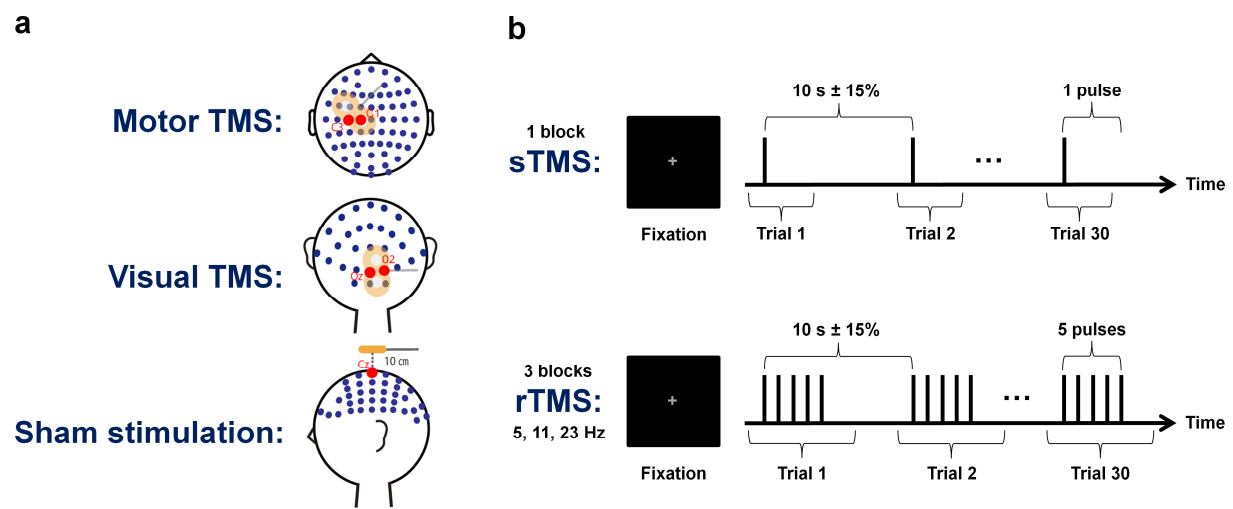


Figure 1: Experimental design. (a) The EEG electrode layout used in the present study is displayed along with the different stimulation sites. In separate sessions, TMS was applied over the left motor cortex (first row), over the right visual cortex (second row) and as sham stimulation 10 cm above the vertex of the head (third row). (b) Each session contained four blocks of 30 trials each, in which we performed sTMS (first row) as well as 5 Hz, 11 Hz and 23 Hz rTMS (second row). During rTMS trials, stimulation was delivered in trains of five consecutive pulses.

We preprocessed the EEG data by first segmenting it into epochs starting 2 s before the first (or single) TMS pulse and ending 3 s after the last (or single) pulse of a train, and then re-referencing these epochs to the averaged recordings from electrodes positioned on the left and right earlobe. To remove the TMS-induced ringing artefact in the EEG signals, we substituted

all values within an interval of 0–8 ms after each pulse with replacement values estimated using linear interpolation. In those cases where the interval was deemed to be too short, it was manually extended to 12 ms after the pulse. The longer-lasting exponential decay artefact was attenuated by identifying components capturing this artefact with an independent component analysis (ICA), and then removing them from the data^{18,32}. Next, we rejected trials with signal values exceeding $\pm 200 \mu\text{V}$ within an interval of -1 s to $+1 \text{ s}$ around the stimulation to exclude any remaining artefacts. After performing a current source density (CSD) transformation of the surface voltage distribution using spherical splines to reduce the effects of volume conduction^{33,34}, the data were down-sampled to a rate of 1,000 Hz.

EEG Analysis

To compute phase-amplitude coupling, we first convolved the preprocessed time series with complex Morlet wavelets $w(t, f)$ ^{35,36}:

$$w(t, f) = \sqrt{f} \exp\left(-\frac{t^2}{2\sigma_t^2}\right) \exp(i2\pi ft),$$

with t denoting time, f denoting the central frequency of interest, σ_t denoting the SD of the Gaussian window and the number of wavelet cycles within a $6\sigma_t$ interval $n_{co} = 3$ determining the approximate width of the frequency bands³⁷:

$$\left[f - \frac{4f}{n_{co}}, f + \frac{4f}{n_{co}} \right].$$

The central frequencies f were chosen to be 5 Hz, 11 Hz and 23 Hz for phase extraction and 30 Hz to 45 Hz in 1 Hz steps for amplitude extraction. The upper limit was fixed at 45 Hz to diminish potential artefacts from muscular activity and power line noise. The instantaneous phase ϕ at each time point was then defined as the angle of the resulting complex-plane vector with respect to the positive real axis, while the magnitude of this vector was utilised as a measure of instantaneous amplitude a . For each combination of phase and amplitude

frequency and for each trial time point, we separately computed the event-related phase-amplitude coupling (ERPAC) $\rho_{\phi a}$, which was defined as the circular-linear correlation of phase and amplitude values across stimulation trials^{38,39}:

$$\rho_{\phi a} = \sqrt{\frac{r_{ca}^2 + r_{sa}^2 - 2r_{ca}r_{sa}r_{cs}}{1 - r_{cs}^2}},$$

where $r_{ca} = c(\cos\phi[n], a[n])$, $r_{sa} = c(\sin\phi[n], a[n])$ and $r_{cs} = c(\sin\phi[n], \cos\phi[n])$ with $c(x, y)$ being the Pearson correlation between x and y .

As the sixteen amplitude frequencies were pooled together in each ERPAC analysis, three different phase-amplitude combinations existed (5 Hz, 11 Hz or 23 Hz phase coupled to amplitudes at 30–45 Hz, i.e., theta-gamma coupling, alpha-gamma coupling and beta-gamma coupling), which were examined separately for motor and visual TMS. Analyses of the resulting six conditions focused on contrasting motor or visual TMS with sham stimulation to account for any indirect effects of stimulation and were performed either individually for sTMS and rTMS (first and third analysis) or directly compared the two stimulation paradigms (second and fourth analysis), as detailed below. Whenever statistical tests were performed, the (multiple-comparison-corrected) significance level was set at $p \leq .05$. With regard to rTMS, it is important to note that the frequency of a condition's respective phase angle time series always corresponded to the applied stimulation frequency. This approach allowed us to directly assess how targeting a particular oscillation via repetitive stimulation affected this oscillation's scalp-recorded coupling to faster oscillations.

We first examined whether sTMS and rTMS led to an increase in phase-amplitude coupling at the stimulation site by analysing ERPAC as a function of amplitude frequency and time, spanning -0.5 cycles to $+4.5$ cycles of a condition's phase-providing oscillation around the onset of the first (or single) pulse. Statistically significant enhancements of ERPAC were

determined via nonparametric permutation testing in the following way. To evaluate the observed set of time-frequency representations encompassing the ERPAC data from the two local electrodes of interest (C1 and C3 for motor TMS; Oz and O2 for visual TMS), the two modes of stimulation (TMS and sham) and each of the fourteen participants, we created 500 sets of corresponding surrogate representations by computing ERPAC between the unchanged phase values and the trial-shuffled amplitude values. As we randomised the relative trial structure between phase and amplitude while maintaining the temporal structure, and thus left any pulse-evoked changes intact, significant differences to the observed data could not arise from spurious stimulus-evoked relationships between phase and amplitude values³⁹. We next averaged each set's ERPAC data over the electrodes of interest, then took the difference between motor or visual TMS and sham stimulation and averaged resulting values over participants. One observed time-frequency representation and a distribution of 500 surrogate representations emerged, all of which were subsequently binarised by thresholding them with the 95th percentile of the surrogate distribution at each time-frequency point. Contiguous suprathreshold points were clustered and the sum of ERPAC values within each cluster was determined. To account for multiple comparisons, we removed from the observed time-frequency representation those clusters whose cluster sum of ERPAC values was below the 95th percentile of the distribution of maximum cluster sums, obtained by taking the highest sum within each surrogate representation.

Second, to investigate whether the local enhancement of phase-amplitude coupling differed between sTMS and rTMS, we took the mean ERPAC over the local electrodes of interest (C1 and C3 for motor TMS; Oz and O2 for visual TMS), subtracted corresponding mean data obtained from sham stimulation and averaged values over a time window of interest, covering $\pm 1/10^{\text{th}}$ of the respective phase-providing oscillation's cycle around either the sTMS pulse or the last pulse of the rTMS trains, as well as over the sixteen amplitude frequencies. By

selecting a narrow time window around the last rTMS pulse, we aimed at minimising the potential contamination of the rTMS data from surrounding pulses. Resulting values were then compared between sTMS and rTMS using a two-tailed paired-sample Student's *t*-test over participants.

Third, we assessed whether an enhancement of phase-amplitude coupling by sTMS and rTMS was observable not only at the stimulation site, but also over other cortical regions. ERPAC was therefore computed at all scalp electrodes for each time point within nine different time windows of interest, centred at -2 cycles to $+6$ cycles of a condition's phase-providing oscillation in 1-cycle steps around the onset of the first (or single) pulse and spanning $\pm 1/10^{\text{th}}$ of this cycle. Topographic maps were created by taking the difference between motor or visual TMS and sham stimulation, and then averaging the resulting values over time points within the respective window of interest, over the sixteen amplitude frequencies as well as over participants.

Fourth, to analyse whether the global propagation of phase-amplitude coupling differed between sTMS and rTMS, we counted the number of electrodes that showed significantly higher ERPAC during motor or visual TMS than during sham stimulation using one-tailed paired-sample Student's *t*-tests over participants. Tests were performed for windows of $\pm 1/10^{\text{th}}$ of a condition's phase-providing oscillation's cycle around the sTMS pulse and each of the five rTMS pulses, with ERPAC values averaged over the respective time points as well as over amplitude frequencies. The extent of propagation induced by each of the five rTMS pulses was then compared to the sTMS-induced extent of propagation using exact binomial tests with parameters n_{el_1} = number of electrodes with a significant TMS-sham difference during a particular rTMS pulse but not the sTMS pulse, n_{el_2} = number of electrodes with a significant TMS-sham difference during the sTMS pulse but not a particular rTMS pulse and

the total number of discordant electrodes $n_{el} = n_{el_1} + n_{el_2}$. As the assignment of these electrodes to either n_{el_1} or n_{el_2} would have happened with equal probability under the null hypothesis of no sTMS-rTMS difference, the p -value was defined as the probability of n_{el_1} reaching the observed or a higher value. Since we performed five tests per condition, multiple comparisons were subsequently accounted for by adjusting p -values with the false discovery rate (FDR) procedure⁴⁰.

All analyses were performed in MATLAB (The MathWorks, Inc., USA), using the CSD toolbox³⁴, the CircStat toolbox³⁸, the FieldTrip toolbox⁴¹ and custom-written scripts.

Data Availability

The dataset analysed in the current study is available from the corresponding author on reasonable request.

Results

Local Modulation of Phase-Amplitude Coupling

Time-frequency representations of the local change in ERPAC relative to the sham stimulation revealed that both motor TMS, analysed at electrodes C1 and C3, and visual TMS, analysed at electrodes Oz and O2, led to an enhancement of phase-amplitude coupling in all assessed phase-amplitude combinations (Fig. 2). For sTMS (Fig. 2a), significant time-frequency clusters ($p \leq .05$, one-tailed cluster-based permutation tests) were found around the onset of the single pulse at 0 ms in all conditions but one: The ERPAC increase around the time of the pulse did not reach significance for the effect of visual sTMS on alpha-gamma coupling. However, later clusters of significant increases suggested an effect of sTMS on local ERPAC in this condition as well. For rTMS (Fig. 2b), significant time-frequency clusters of increased ERPAC could likewise be observed around the onset times of almost all

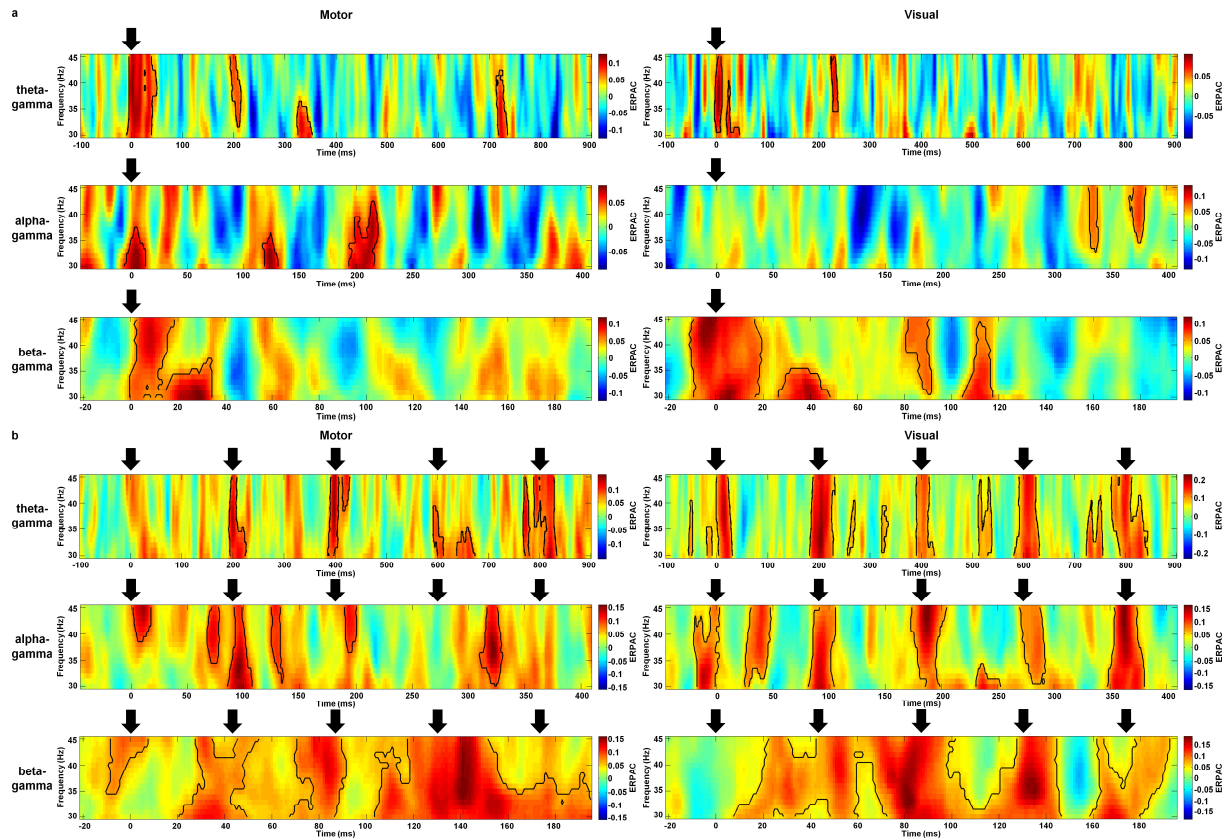


Figure 2: Grand average time-frequency representations of phase-amplitude coupling. Plots show the strength of motor-TMS-induced (left column) and visual-TMS-induced (right column) theta-gamma (first row), alpha-gamma (second row) and beta-gamma (third row) event-related phase-amplitude coupling (ERPAC) as a function of trial time and amplitude frequency. Stimulation paradigms are (a) sTMS and (b) rTMS, with the rTMS frequency always corresponding to the frequency of the phase series. We extracted TMS effects by averaging ERPAC over electrodes C1 and C3 for motor TMS and electrodes Oz and O2 for visual TMS, subtracting corresponding mean data obtained during sham stimulation and averaging the resulting values over the fourteen assessed participants. Time points of pulses are indicated by black arrows and significant time-frequency clusters ($p \leq .05$, one-tailed cluster-based permutation tests) by black contours.

pulses. Interestingly, whereas the ERPAC increases induced by the individual pulses were clearly separated in time in the 5 Hz and 11 Hz stimulation, which related to theta-gamma and

alpha-gamma coupling, respectively, the effects were more strongly merged for the beta-gamma coupling occurring during the faster 23 Hz stimulation. Although clusters in all conditions could spread out symmetrically in time because of the temporal smoothing introduced by the wavelet convolution, it should be noted that their spreading was generally biased towards post-stimulation rather than pre-stimulation time points. While the ERPAC enhancement induced by the present TMS design thus seemed to linger for some tens of milliseconds, it was still transient in nature, with individual effects typically lasting for less than 50 ms.

A comparison of the local change in phase-amplitude coupling induced by sTMS and rTMS revealed that in all but one condition, the mean ERPAC increase relative to the sham stimulation was higher for the last rTMS pulse than for the sTMS pulse, with the opposite pattern being observable for beta-gamma coupling during visual TMS (Fig. 3). However, because of high variability over participants, the p -values from two-tailed paired-sample Student's t -tests did not reach statistical significance (all $p > .05$), there being merely a statistical trend ($t(13) = -1.93, p = .076$) observable for alpha-gamma coupling during visual TMS, suggesting stronger ERPAC enhancement by rTMS than by sTMS.

Global Modulation of Phase-Amplitude Coupling

To illustrate the change in ERPAC relative to the sham stimulation at all 63 scalp electrodes, nine topographic maps were computed for each condition and stimulation paradigm (Fig. 4). The first two maps represented pre-stimulation time windows, the next one (sTMS) or next five (rTMS) represented windows centred on the individual pulses and all remaining maps represented post-stimulation time windows. In accordance with the transient character of the assessed effects, an enhancement of ERPAC was most noticeable within the topographic maps centred on the pulses. Visual inspection further revealed that sTMS-induced increases in

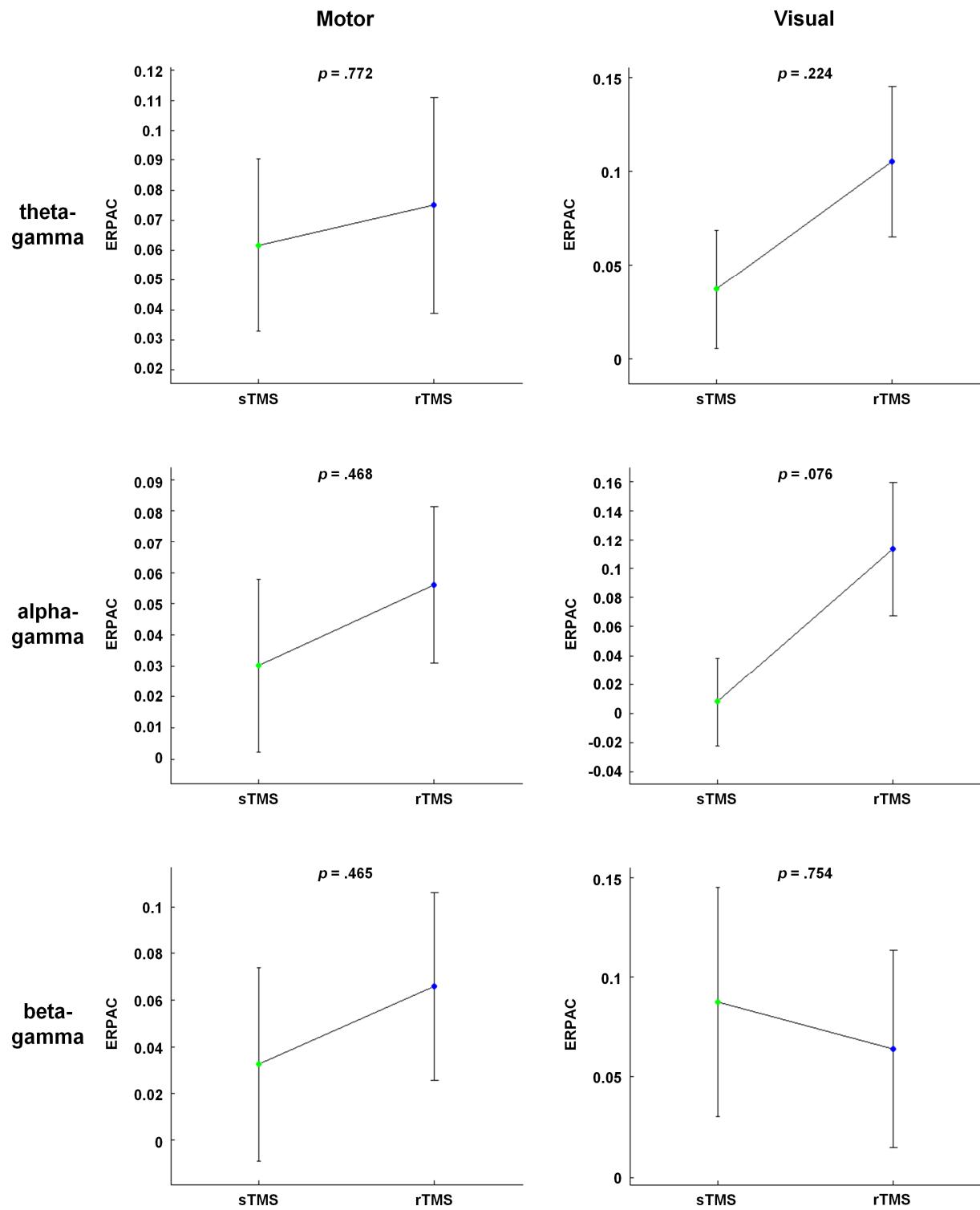


Figure 3: Local comparisons of phase-amplitude coupling between sTMS and rTMS. Plots show the strength of motor-TMS-induced (left column) and visual-TMS-induced (right column) theta-gamma (first row), alpha-gamma (second row) and beta-gamma (third row) event-related phase-amplitude coupling (ERPAC) during the sTMS pulse in green and the last rTMS pulse in blue, with the rTMS frequency always corresponding to the frequency of the

phase series. We extracted TMS effects by averaging ERPAC over electrodes C1 and C3 for motor TMS and electrodes Oz and O2 for visual TMS, subtracting corresponding mean data obtained during sham stimulation and averaging the resulting values over predefined time windows of interest around the respective pulses and over the sixteen amplitude frequencies. Bars of sTMS and rTMS represent mean values ± 1 SEM over the fourteen assessed participants; each displayed p -value is based on a two-tailed paired-sample Student's t -test between the stimulation paradigms.

ERPAC were prominent primarily over the site of stimulation, with sporadic enhancements also occurring at other sites (Fig. 4a). By contrast, the effects of rTMS within the five topographic maps centred on the five pulses appeared to be more strongly distributed over the entire cortex (Fig. 4b).

We quantified this observation by determining the number of electrodes with significantly higher ERPAC during motor or visual TMS than during sham stimulation ($p \leq .05$, one-tailed paired-sample Student's t -tests), and then comparing the electrode numbers between sTMS and the five rTMS pulses (Fig. 5). As expected, in most cases, the number of significant electrodes was larger for a particular rTMS pulse than for the sTMS pulse of the same condition. With regard to motor stimulation, this difference was statistically significant ($p_{FDR} \leq .05$, exact binomial tests) for three out of five rTMS pulses when investigating alpha-gamma coupling (pulses 1, 2, 3: each $p_{FDR} = .041$) and for one rTMS pulse when investigating beta-gamma coupling (pulse 3: $p_{FDR} = .019$). With regard to visual stimulation, three out of five rTMS pulses showed a significantly larger propagation when investigating theta-gamma coupling (pulse 1: $p_{FDR} = .019$, pulse 4: $p_{FDR} = .009$, pulse 5: $p_{FDR} = .006$), whereas two rTMS pulses were significant for beta-gamma coupling (pulses 2, 3: each $p_{FDR} = .021$). Thus, while significant sTMS-sham differences were still found at five or more electrodes in all

conditions, indicating a certain extent of propagation in this stimulation paradigm as well, rTMS induced a considerably more widespread propagation of ERPAC enhancement overall.

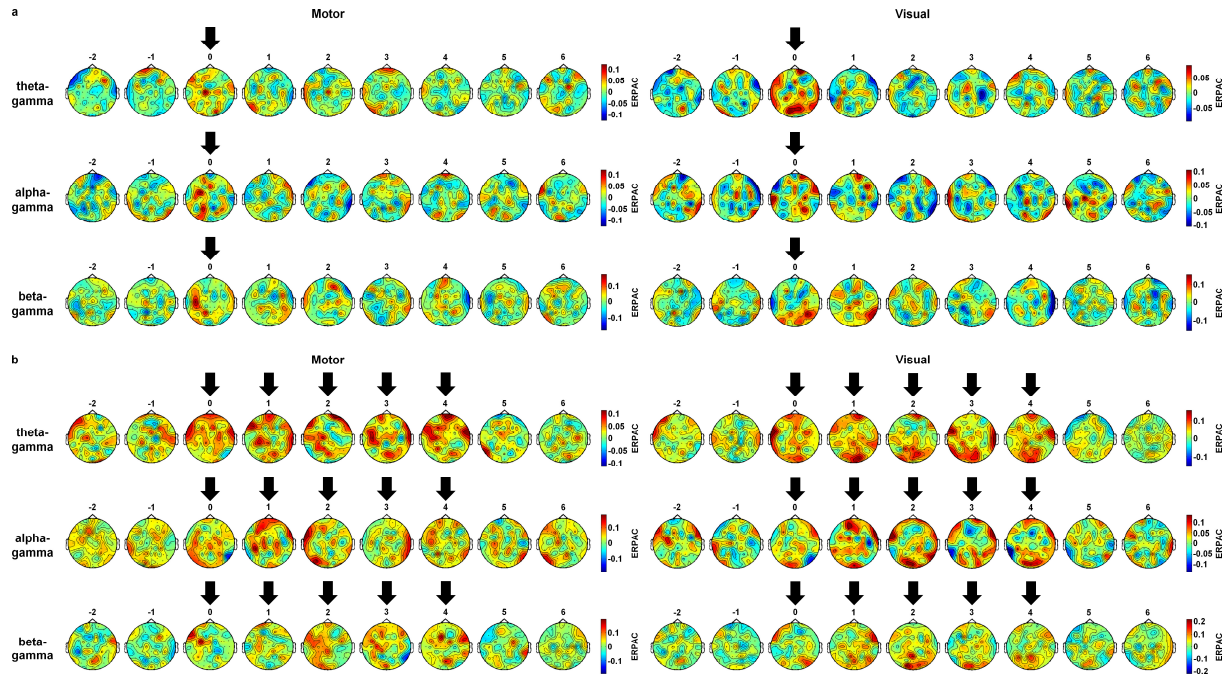


Figure 4: Grand average topographic maps of phase-amplitude coupling. Plots show the strength of motor-TMS-induced (left column) and visual-TMS-induced (right column) theta-gamma (first row), alpha-gamma (second row) and beta-gamma (third row) event-related phase-amplitude coupling (ERPAC) at all scalp electrodes within nine time windows of interest. Stimulation paradigms are (a) sTMS and (b) rTMS, with the rTMS frequency always corresponding to the frequency of the phase series. We extracted TMS effects by subtracting ERPAC obtained during sham stimulation from that obtained during motor or visual TMS and averaging the resulting values over predefined time windows of interest, positioned at -2 cycles to $+6$ cycles of a condition's phase-providing oscillation around the onset of the first (or single) pulse, over the sixteen amplitude frequencies and fourteen assessed participants. Topographic maps centred on pulses are indicated by black arrows.

Discussion

With the present study, we provide compelling evidence that both sTMS and rTMS can transiently enhance phase-amplitude coupling of neural oscillations, as measured with concurrent EEG. This enhancement was found not only locally at the stimulation site, but also over various other cortical sites, with the propagation induced by rTMS outperforming that induced by sTMS. By demonstrating enhanced theta-gamma, alpha-gamma and beta-gamma phase-amplitude coupling during motor and visual TMS, our results have relevance for a wide range of the nested oscillatory signatures inherent to neural processing^{20,21,42,43} and are highly consistent with the hypothesised population-level increase in intrinsic coupling brought about by oscillatory phase alignment. We hence propose that concurrent TMS-EEG can be utilised to effectively probe such coupling in humans, a feature making it a highly promising technique for future non-invasive investigations of this important mechanism.

At the site of stimulation, all of the assessed conditions showed significant increases in phase-amplitude coupling strength during or slightly after TMS. As the phase-amplitude coupling in the present study was operationalised as the circular-linear correlation of phase and amplitude values at each time point across stimulation trials^{38,39}, changes in coupling strength could be assessed without the loss of temporal resolution inherent to most other coupling measures^{21,22,29}. Given that the enhancement of local phase-amplitude coupling typically lasted for less than 50 ms around the pulse, a finding consistent with the previously reported short-lived character of TMS-induced phase dynamics¹³, this approach was vital to quantify transient effects that would otherwise be barely detectable in scalp EEG recordings. We took the following steps to ensure that the observed effects did indeed reflect a direct enhancement of macroscopic phase-amplitude coupling by TMS. First, to account for any indirect effects of stimulation, particularly for auditory-evoked changes in brain activity including cross-modally triggered phase locking after salient sounds⁴⁴, phase-amplitude coupling was always

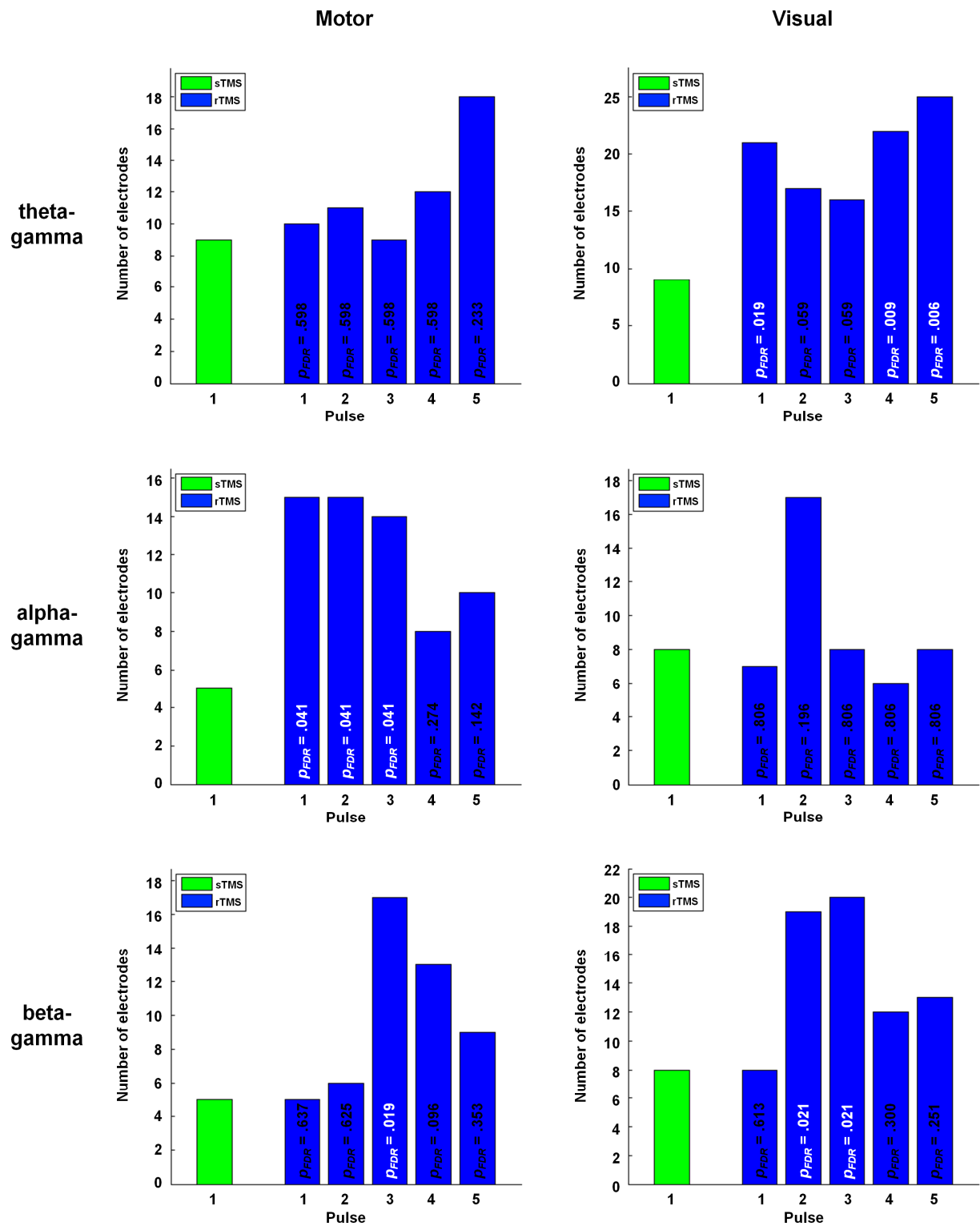


Figure 5: Global comparisons of phase-amplitude coupling between sTMS and rTMS. Plots show the spatial extent of motor-TMS-induced (left column) and visual-TMS-induced (right column) theta-gamma (first row), alpha-gamma (second row) and beta-gamma (third row) event-related phase-amplitude coupling (ERPAC) during the sTMS pulse in green and the five

rTMS pulses in blue, with the rTMS frequency always corresponding to the frequency of the phase series. We extracted TMS effects by averaging ERPAC at all electrodes over predefined time windows of interest around the respective pulses and over the sixteen amplitude frequencies, comparing the resulting values between motor or visual TMS and sham stimulation with one-tailed paired-sample Student's t-tests and counting the number of electrodes with a statistically significant difference ($p \leq .05$; drawn on y-axis). The spatial extent of TMS effects was subsequently compared between the sTMS pulse and each of the five rTMS pulses with exact binomial tests. Corresponding p-values, adjusted for multiple comparisons with the false discovery rate (FDR) procedure, are superimposed onto the rTMS bars in all plots; significant p-values ($p_{FDR} \leq .05$) are displayed in white, all other p-values in black.

assessed relative to the sham stimulation, which was applied over the vertex of the head. Second, by statistically comparing the observed TMS-sham differences to surrogate distributions of trial-shuffled data with unmodified temporal structure³⁹, we confirmed that the observed enhancement of phase-amplitude coupling was based on a specific statistical relationship between phase and amplitude values across trials, rather than on spurious relationships induced by unrelated neural effects of the pulse or any sharp edge artefacts⁴⁵. Thanks to these methodological approaches, a clear demonstration of TMS-induced changes in phase-amplitude coupling was made possible. Even though such changes seemed to be stronger for the last pulse of the delivered rTMS trains (targeted at the phase-providing lower-frequency oscillations) than for the sTMS pulse in almost all conditions, the statistical power was not high enough to enable a conclusion regarding local phase-amplitude coupling differences between stimulation paradigms. Notably, a slight modification of the rTMS paradigm could potentially facilitate the detection of such differences. Successful neural entrainment, which might underlie a potential rTMS benefit by enabling stronger oscillatory

phase alignment relative to sTMS, requires the existence of a neural population that can oscillate at the stimulation frequency under natural conditions¹⁷. As such eigenfrequencies differ between cortical regions¹⁵ and individuals⁴⁶, the entrainment capability of rTMS should be enhanced by tuning its frequency to the local power spectrum peak frequencies of participants. Recent evidence has indeed demonstrated the benefits of such an individualised targeting of intrinsic oscillations by rTMS¹⁴, making a comparison of local phase-amplitude coupling strength between this rTMS paradigm and sTMS promising. Importantly, even though the perturbation of intrinsic oscillations is potentially stronger in the case of individualised rTMS frequencies, previously reported effects of non-individualised stimulation on human cognition⁴⁷ suggest successful entrainment in this case as well. As Thut and colleagues¹² noted, such effects might be enabled by intra-individual frequency fluctuations as well as a loosening relationship between eigenfrequency and effective stimulation frequency at higher stimulation intensities (see also Gouwens and colleagues⁴⁸). A decision in favour of non-individualised stimulation paradigms may eventually also be driven by the increased expenditure of time and resources associated with the pre-experimental determination of individual peak frequencies, especially when testing clinical populations.

Alongside the described local effects of sTMS and rTMS, we found that TMS can enhance population-level measures of phase-amplitude coupling over various other cortical sites. In line with this finding, propagation of neural activation related to either sTMS or rTMS has been shown in a number of previous studies^{13,14,49,50,51,52,53,54}. In particular, Kawasaki and colleagues¹³ demonstrated an sTMS-induced large-scale propagation of oscillatory phase locking, which was accompanied by increased directional information flow of phase dynamics from the occipital stimulation site to an examined distant site over the motor cortex, as assessed by transfer entropy. Since the therein suggested alignment of phases of individual oscillators should increase the detectability of intrinsic phase-amplitude coupling at the

population level, the propagation of enhanced coupling observed here is highly consistent with this report. However, knowledge of any propagation differences between sTMS and rTMS is sparse. In the present study, rTMS enhanced scalp-recorded phase-amplitude coupling at considerably more sites than sTMS. This difference was particularly pronounced for alpha-gamma coupling during 11 Hz motor stimulation and theta-gamma coupling during 5 Hz visual stimulation, with three out of five rTMS pulses outperforming the respective sTMS pulse in each case. As (nested) intrinsic oscillations are believed to play an important role in neural signal transmission^{42,55}, their entrainment by rTMS may again be at the bottom of the observed benefit. In accordance with this idea, Romei and colleagues¹⁴ demonstrated that rTMS pulses propagate from the sensorimotor cortex to spinal levels only when sensorimotor oscillations are specifically targeted via their eigenfrequency, with stimulation at other frequencies having little impact on cortico-spinal signal interactions. Likewise, the impact of sTMS on relevant oscillations might have been too weak to reach the extent of propagation achieved by rTMS in the present study. Before alternatively ascribing the observed propagation benefit of rTMS to a methodological contamination of rTMS pulses by surrounding pulses, it should be noted that during rTMS, both local alpha-gamma coupling and local theta-gamma coupling typically returned to baseline long before the next pulse arrived. Still, one could argue that we had already observed a more widespread distribution of enhanced phase-amplitude coupling during the first rTMS pulse in several conditions. As an rTMS-induced synchronisation of neural oscillators might have progressively strengthened within entire rTMS blocks, including multiple stimulation trials, in these cases, the assessed correlation of phase and amplitude values could have been driven by the intensified entrainment present only in later trials. Nonetheless, conclusive evidence on this matter is so far missing and future studies are needed to shed light on the exact cause of the observed sTMS-rTMS differences in phase-amplitude coupling propagation.

As phase-amplitude coupling is believed to play a fundamental role in the transfer of neural information across diverse spatial and temporal processing scales, thereby serving the dynamic integration of global computations with fast local processing, it may be extremely relevant for cognitive functioning⁴². Recent evidence has started to support this claim by hinting at its functional significance for visual perception²⁶, feedback processing⁵⁶, memory recall⁵⁷, visuomotor mapping⁵⁸ and movement planning and execution⁵⁹. Accordingly, a dysfunction in phase-amplitude coupling has been identified in several clinical conditions such as Parkinson's disease⁶⁰, autism spectrum disorders⁶¹ and epilepsy⁶². Still, our current understanding of this intriguing mechanism is far from exhaustive. Investigations of phase-amplitude coupling in the human population are hampered by the inherent shortcomings of established non-invasive measurement techniques. As methods such as EEG capture the summed potentials of tens of thousands of synchronously activated neurons, scalp-recorded oscillations inevitably reflect the summation of multiple underlying neural oscillators. Consequently, even strong phase-amplitude coupling can only be detected with EEG if a considerable quantity of those oscillators are in phase, and thus are not cancelling out at the population level. We suggest that by aligning the phases of individual oscillators, TMS fosters this setting, and thereby facilitates the non-invasive detection of intrinsic phase-amplitude coupling with an improved signal-to-noise ratio. The proposed perturbational approach therefore holds great promise for future investigations aimed at further unravelling the association between such oscillatory nesting on the one hand, and healthy or pathological human functioning on the other hand. By probing the intrinsic capacity of individuals for phase-amplitude coupling, concurrent TMS-EEG might, in this regard, prove particularly useful for the reliable development of coupling-based biomarkers, as have already been presented for amnesic mild cognitive impairment⁶³. Besides opening the door to a deeper understanding of the functional role of phase-amplitude coupling, the present results add to the constantly growing body of knowledge regarding the neurophysiological mode of action

underlying TMS (see Klomjai and colleagues⁶⁴ for a review). By actively modulating nested intrinsic oscillations, TMS impacts on the gating of information along interconnected neural ensembles, and consequently affects a fundamental property of neural processing in the human brain.

In conclusion, we used a concurrent TMS-EEG study design to demonstrate that TMS can transiently enhance scalp-recorded phase-amplitude coupling. This enhancement was found for both sTMS and rTMS, with a more widespread propagation of effects being observed during the latter stimulation paradigm. We thus recommend the perturbational approach of concurrent TMS-EEG as a novel experimental technique to effectively probe intrinsic phase-amplitude coupling in humans. The utility of this design for future studies investigating the functional roles of phase-amplitude coupling in the healthy population, as well as phase-amplitude coupling changes in pathological conditions, awaits confirmation.

Acknowledgements

K.K. was supported by JST PRESTO, MEXT Grants-in-Aid for Scientific Research 26282169, 15H05877 and a research grant from Toyota Motor Corporation.

Competing Financial Interests

The authors declare no competing financial interests.

References

1. de Graaf, T. A., Koivisto, M., Jacobs, C. & Sack, A. T. The chronometry of visual perception: Review of occipital TMS masking studies. *Neurosci. Biobehav. Rev.* **45**, 295-304 (2014).
2. Olk, B., Peschke, C. & Hilgetag, C. C. Attention and control of manual responses in cognitive conflict: Findings from TMS perturbation studies. *Neuropsychologia* **74**, 7-20 (2015).
3. Murakami, T., Ugawa, Y. & Ziemann, U. Utility of TMS to understand the neurobiology of speech. *Front. Psychol.* **4**, 446; 10.3389/fpsyg.2013.00446 (2013).
4. Volz, L. J., Hamada, M., Rothwell, J. C. & Grefkes, C. What makes the muscle twitch: Motor system connectivity and TMS-induced activity. *Cereb. Cortex* **25**, 2346-2353 (2015).
5. Lefaucheur, J.-P. *et al.* Evidence-based guidelines on the therapeutic use of repetitive transcranial magnetic stimulation (rTMS). *Clin. Neurophysiol.* **125**, 2150-2206 (2014).
6. Perera, T. *et al.* The Clinical TMS Society consensus review and treatment recommendations for TMS therapy for major depressive disorder. *Brain Stimul.* **9**, 336-346 (2016).
7. Di Pino, G. *et al.* Modulation of brain plasticity in stroke: A novel model for neurorehabilitation. *Nat. Rev. Neurol.* **10**, 597-608 (2014).
8. Chrysikou, E. G. & Hamilton, R. H. Noninvasive brain stimulation in the treatment of aphasia: Exploring interhemispheric relationships and their implications for neurorehabilitation. *Restor. Neurol. Neurosci.* **29**, 375-394 (2011).
9. Cole, J. C., Green Bernacki, C., Helmer, A., Pinninti, N. & O'Reardon, J. P. Efficacy of transcranial magnetic stimulation (TMS) in the treatment of schizophrenia: A review of the literature to date. *Innov. Clin. Neurosci.* **12**, 12-19 (2015).

10. Fuggetta, G., Fiaschi, A. & Manganotti, P. Modulation of cortical oscillatory activities induced by varying single-pulse transcranial magnetic stimulation intensity over the left primary motor area: A combined EEG and TMS study. *Neuroimage* **27**, 896-908 (2005).
11. Taylor, P. C. J., Walsh, V. & Eimer, M. Combining TMS and EEG to study cognitive function and cortico-cortico interactions. *Behav. Brain Res.* **191**, 141-147 (2008).
12. Thut, G. *et al.* Rhythmic TMS causes local entrainment of natural oscillatory signatures. *Curr. Biol.* **21**, 1176-1185 (2011).
13. Kawasaki, M., Uno, Y., Mori, J., Kobata, K. & Kitajo, K. Transcranial magnetic stimulation-induced global propagation of transient phase resetting associated with directional information flow. *Front. Hum. Neurosci.* **8**, 173; 10.3389/fnhum.2014.00173 (2014).
14. Romei, V. *et al.* Causal evidence that intrinsic beta-frequency is relevant for enhanced signal propagation in the motor system as shown through rhythmic TMS. *Neuroimage* **126**, 120-130 (2016).
15. Rosanova, M. *et al.* Natural frequencies of human corticothalamic circuits. *J. Neurosci.* **29**, 7679-7685 (2009).
16. Sauseng, P. *et al.* Are event-related potential components generated by phase resetting of brain oscillations? A critical discussion. *Neuroscience* **146**, 1435-1444 (2007).
17. Thut, G., Schyns, P. G. & Gross, J. Entrainment of perceptually relevant brain oscillations by non-invasive rhythmic stimulation of the human brain. *Front. Psychol.* **2**, 170; 10.3389/fpsyg.2011.00170 (2011).
18. Herring, J. D., Thut, G., Jensen, O. & Bergmann, T. O. Attention modulates TMS-locked alpha oscillations in the visual cortex. *J. Neurosci.* **35**, 14435-14447 (2015).
19. Tononi, G. Information integration: Its relevance to brain function and consciousness. *Arch. Ital. Biol.* **148**, 299-322 (2010).

20. Lakatos, P. *et al.* An oscillatory hierarchy controlling neuronal excitability and stimulus processing in the auditory cortex. *J. Neurophysiol.* **94**, 1904-1911 (2005).
21. Canolty, R. T. *et al.* High gamma power is phase-locked to theta oscillations in human neocortex. *Science* **313**, 1626-1628 (2006).
22. Tort, A. B. L., Komorowski, R., Eichenbaum, H. & Kopell, N. Measuring phase-amplitude coupling between neuronal oscillations of different frequencies. *J. Neurophysiol.* **104**, 1195-1210 (2010).
23. Roux, F., Wibral, M., Singer, W., Aru, J. & Uhlhaas, P. J. The phase of thalamic alpha activity modulates cortical gamma-band activity: Evidence from resting-state MEG recordings. *J. Neurosci.* **33**, 17827-17835 (2013).
24. Bonnefond, M. & Jensen, O. Gamma activity coupled to alpha phase as a mechanism for top-down controlled gating. *PLoS ONE* **10**, e0128667; 10.1371/journal.pone.0128667 (2015).
25. Kajihara, T. *et al.* Neural dynamics in motor preparation: From phase-mediated global computation to amplitude-mediated local computation. *Neuroimage* **118**, 445-455 (2015).
26. Händel, B. & Haarmeier, T. Cross-frequency coupling of brain oscillations indicates the success in visual motion discrimination. *Neuroimage* **45**, 1040-1046 (2009).
27. Noda, Y. *et al.* Resting-state EEG gamma power and theta-gamma coupling enhancement following high-frequency left dorsolateral prefrontal rTMS in patients with depression. *Clin. Neurophysiol.* **128**, 424-432 (2017).
28. Helfrich, R. F., Herrmann, C. S., Engel, A. K. & Schneider, T. R. Different coupling modes mediate cortical cross-frequency interactions. *Neuroimage* **140**, 76-82 (2016).
29. Voytek, B. *et al.* Shifts in gamma phase-amplitude coupling frequency from theta to alpha over posterior cortex during visual tasks. *Front. Hum. Neurosci.* **4**, 191; 10.3389/fnhum.2010.00191 (2010).

30. Wang, L., Saalman, Y. B., Pinsk, M. A., Arcaro, M. J. & Kastner, S. Electrophysiological low-frequency coherence and cross-frequency coupling contribute to BOLD connectivity. *Neuron* **76**, 1010-1020 (2012).
31. Sekiguchi, H., Takeuchi, S., Kadota, H., Kohno, Y. & Nakajima, Y. TMS-induced artifacts on EEG can be reduced by rearrangement of the electrode's lead wire before recording. *Clin. Neurophysiol.* **122**, 984-990 (2011).
32. Korhonen, R. J. *et al.* Removal of large muscle artifacts from transcranial magnetic stimulation-evoked EEG by independent component analysis. *Med. Biol. Eng. Comput.* **49**, 397-407 (2011).
33. Perrin, F., Pernier, J., Bertrand, O. & Echallier, J. F. Spherical splines for scalp potential and current density mapping. *Electroencephalogr. Clin. Neurophysiol.* **72**, 184-187 (1989).
34. Kayser, J. & Tenke, C. E. Principal components analysis of Laplacian waveforms as a generic method for identifying ERP generator patterns: I. Evaluation with auditory oddball tasks. *Clin. Neurophysiol.* **117**, 348-368 (2006).
35. Kronland-Martinet, R., Morlet, J. & Grossmann, A. Analysis of sound patterns through wavelet transforms. *Intern. J. Pattern Recognit. Artif. Intell.* **1**, 273-302 (1987).
36. Tallon-Baudry, C., Bertrand, O., Delpuech, C. & Pernier, J. Stimulus specificity of phase-locked and non-phase-locked 40 Hz visual responses in human. *J. Neurosci.* **16**, 4240-4249 (1996).
37. Lachaux, J.-P. *et al.* Studying single-trials of phase synchronous activity in the brain. *Int. J. Bifurc. Chaos* **10**, 2429-2439 (2000).
38. Berens, P. CircStat: A MATLAB toolbox for circular statistics. *J. Stat. Softw.* **31**, 10; 10.18637/jss.v031.i10 (2009).
39. Voytek, B., D'Esposito, M., Crone, N. & Knight, R. T. A method for event-related phase/amplitude coupling. *Neuroimage* **64**, 416-424 (2013).

40. Benjamini, Y. & Hochberg, Y. Controlling the false discovery rate: A practical and powerful approach to multiple testing. *J. R. Statist. Soc. B* **57**, 289-300 (1995).
41. Oostenveld, R., Fries, P., Maris, E. & Schoffelen, J.-M. FieldTrip: Open source software for advanced analysis of MEG, EEG, and invasive electrophysiological data. *Comput. Intell. Neurosci.* **2011**, 156869; 10.1155/2011/156869 (2011).
42. Canolty, R. T. & Knight, R. T. The functional role of cross-frequency coupling. *Trends Cogn. Sci.* **14**, 506-515 (2010).
43. Sotero, R. C. Modeling the generation of phase-amplitude coupling in cortical circuits: From detailed networks to neural mass models. *Biomed Res. Int.* **2015**, 915606; 10.1155/2015/915606 (2015).
44. Romei, V., Gross, J. & Thut, G. Sounds reset rhythms of visual cortex and corresponding human visual perception. *Curr. Biol.* **22**, 807-813 (2012).
45. Kramer, M. A., Tort, A. B. L. & Kopell, N. J. Sharp edge artifacts and spurious coupling in EEG frequency comodulation measures. *J. Neurosci. Methods* **170**, 352-357 (2008).
46. Haegens, S., Cousijn, H., Wallis, G., Harrison, P. J. & Nobre, A. C. Inter- and intra-individual variability in alpha peak frequency. *Neuroimage* **92**, 46-55 (2014).
47. Sauseng, P. *et al.* Brain oscillatory substrates of visual short-term memory capacity. *Curr. Biol.* **19**, 1846-1852 (2009).
48. Gouwens, N. W. *et al.* Synchronization of firing in cortical fast-spiking interneurons at gamma frequencies: A phase-resetting analysis. *PLoS Comput. Biol.* **6**, e1000951; 10.1371/journal.pcbi.1000951 (2010).
49. Ilmoniemi, R. J. *et al.* Neuronal responses to magnetic stimulation reveal cortical reactivity and connectivity. *Neuroreport* **8**, 3537-3540 (1997).
50. Massimini, M. *et al.* Breakdown of cortical effective connectivity during sleep. *Science* **309**, 2228-2232 (2005).

51. Morishima, Y. *et al.* Task-specific signal transmission from prefrontal cortex in visual selective attention. *Nat. Neurosci.* **12**, 85-91 (2009).
52. Casali, A. G., Casarotto, S., Rosanova, M., Mariotti, M. & Massimini, M. General indices to characterize the electrical response of the cerebral cortex to TMS. *Neuroimage* **49**, 1459-1468 (2010).
53. Parks, N. A. *et al.* Examining cortical dynamics and connectivity with simultaneous single-pulse transcranial magnetic stimulation and fast optical imaging. *Neuroimage* **59**, 2504-2510 (2012).
54. Zanon, M., Battaglini, P. P., Jarmolowska, J., Pizzolato, G. & Busan, P. Long-range neural activity evoked by premotor cortex stimulation: A TMS/EEG co-registration study. *Front. Hum. Neurosci.* **7**, 803; 10.3389/fnhum.2013.00803 (2013).
55. Akam, T. & Kullmann, D. M. Oscillations and filtering networks support flexible routing of information. *Neuron* **67**, 308-320 (2010).
56. Cohen, M. X., Elger, C. E. & Fell, J. Oscillatory activity and phase-amplitude coupling in the human medial frontal cortex during decision making. *J. Cogn. Neurosci.* **21**, 390-402 (2009).
57. Tort, A. B. L., Komorowski, R. W., Manns, J. R., Kopell, N. J. & Eichenbaum, H. Theta-gamma coupling increases during the learning of item-context associations. *Proc. Natl. Acad. Sci. U.S.A.* **106**, 20942-20947 (2009).
58. Tzvi, E., Verleger, R., Münte, T. F. & Krämer, U. M. Reduced alpha-gamma phase amplitude coupling over right parietal cortex is associated with implicit visuomotor sequence learning. *Neuroimage* **141**, 60-70 (2016).
59. Combrisson, E. *et al.* From intentions to actions: Neural oscillations encode motor processes through phase, amplitude and phase-amplitude coupling. *Neuroimage* **147**, 473-487 (2017).

60. de Hemptinne, C. *et al.* Exaggerated phase-amplitude coupling in the primary motor cortex in Parkinson disease. *Proc. Natl. Acad. Sci. U.S.A.* **110**, 4780-4785 (2013).
61. Khan, S. *et al.* Local and long-range functional connectivity is reduced in concert in autism spectrum disorders. *Proc. Natl. Acad. Sci. U.S.A.* **110**, 3107-3112 (2013).
62. Edakawa, K. *et al.* Detection of epileptic seizures using phase-amplitude coupling in intracranial electroencephalography. *Sci. Rep.* **6**, 25422; 10.1038/srep25422 (2016).
63. Dimitriadis, S. I., Laskaris, N. A., Bitzidou, M. P., Tarnanas, I. & Tsolaki, M. N. A novel biomarker of amnesic MCI based on dynamic cross-frequency coupling patterns during cognitive brain responses. *Front. Neurosci.* **9**, 350; 10.3389/fnins.2015.00350 (2015).
64. Klomjai, W., Katz, R. & Lackmy-Vallée, A. Basic principles of transcranial magnetic stimulation (TMS) and repetitive TMS (rTMS). *Ann. Phys. Rehabil. Med.* **58**, 208-213 (2015).

4

Discussion: Decoding the Restless Brain

The current thesis is aimed at drawing a detailed picture of intrinsic brain activity, one of the indispensable neural foundations of low- and high-level mental functioning (see e.g., Sadaghiani and Kleinschmidt 2013). Existing knowledge of this activity's dynamic temporo-spatial layout, especially with respect to its spectral characteristics, and of its essential impact on human perception, cognition, and behavior has been extended by means of two main projects. While the first project took an interest in the relation between slow fluctuations in intrinsic brain activity and the emergence of conscious visual perception, the second project laid its focus on the development of a methodological tool to advance the reliable assessment of similar relations in future non-invasive studies. The two conducted projects are exemplary for a wide range of topics pressing to be addressed in this rapidly developing research field and promote the overall appreciation of the so-called restless brain (Raichle 2011) as the basic state of human neural processing. In this chapter, the key findings from both projects are summarized, interpreted, and integrated into the current state of research, taking into account also methodological limitations and (in parts already implemented) conceivable future research steps, to allow for the assessment of their usefulness in understanding elementary brain mechanisms and functions.

4.1 Advancing Research on Intrinsic Brain Activity

Two original research articles were presented, entitled (1) “The evolution of pre-stimulus slow cortical potentials is associated with an upcoming stimulus’ access to visual consciousness” and (2) “Phase-amplitude coupling of neural oscillations can be effectively

probed with concurrent TMS-EEG”. In the current section, the key attributes of each of these projects are summarized and integrated into a common frame of advancements in understanding the dynamics of intrinsic brain activity with scalp EEG.

The first main project was dedicated to the functional relevance of intrinsic brain activity, in particular concerning the relation between slow fluctuations in such activity and the access of incoming visual information to conscious awareness. This relation had been tackled previously in an fMRI study by the group around the current thesis’ author (Wohlschläger et al. 2016), with the present project aimed at finding a potential electrophysiological analog of the therein emphasized meaningful evolution of slow pre-stimulus BOLD signals. SCPs, which reside at the low-frequency end of electrophysiological activity measures and thus in a frequency range similar to that of BOLD activity, seem to be optimally positioned for large-scale information integration (He and Raichle 2009) and have been proposed to constitute a neural predisposition of integrated conscious experience (Northoff 2017). While a relation between the magnitude of intrinsic SCPs on the one hand and the detection of visual stimuli near sensory threshold on the other hand had indeed been demonstrated experimentally (Devrim et al. 1999), the role of their relative evolution toward stimulus presentation remained to be understood. We therefore conducted a visual backward-masking task, during each trial of which healthy participants had to, first, identify a given property of a briefly presented target stimulus and to, second, indicate their confidence on a four-point scale from “not sure at all” up to “very sure” as a proxy for the target’s access to conscious awareness. Direct-current (DC) EEG was recorded throughout the task. The inspection of correct-trials-only event-related potentials (ERPs), which were generated relative to a brief period immediately before target presentation, revealed that the grand average signal slowly increased toward target presentation when highest awareness was about to arise and slightly decreased in all other conditions. The presented EEG project thus successfully demonstrated

the functional relevance of slowly evolving intrinsic brain activity, a finding in close correspondence with the fMRI study of Wohlschläger and colleagues (Wohlschläger et al. 2016) and in support of a recent theoretical account according to which incoming stimuli bind to slow intrinsic activity - accessible either via SCPs or the BOLD signal - as a function of the degree of temporal correspondence between the stimuli and such activity's ongoing cycles (Northoff and Huang 2017). In addition, we identified well-known post-target correlates of conscious awareness, including enhancements of the visual awareness negativity and the P3 component (see e.g., Koivisto et al. 2008). While it therefore seemed that slow activity fluctuations acted alongside faster neural processes to offer incoming information access to higher-level neural processing and ultimately conscious experience, any attempts to quantify such interplay of slow and fast neural processes were unsuccessful in the context of the conducted study.

With the second main project, we aimed at bringing forward a novel experimental technique to enhance the detectability of such interactions, in the form of intrinsic phase-amplitude coupling, in non-invasive scalp recordings. Given that the perturbational method of TMS had been proposed to synchronize individual neural oscillators by means of phase alignment and to thereby attenuate population-level signal nullifications (Thut et al. 2011a, 2011b), concurrent TMS-EEG was considered a promising yet untested candidate to accomplish this objective. In separate sessions, we consequently delivered sTMS as well as rTMS at 5, 11, and 23 Hz over the left motor cortex, over the right visual cortex, and as sham stimulation above the vertex of the head while simultaneously collecting EEG data. Changes relative to sham stimulation were assessed for theta-gamma, alpha-gamma, and beta-gamma phase-amplitude coupling, with the rTMS frequency always corresponding to the frequency of the phase-providing slower oscillation (which means that we assessed changes in theta-gamma coupling, e.g., during motor and visual sTMS and 5 Hz rTMS). An in-depth analysis of the

collected EEG data revealed that TMS pulses of all conditions induced transient increases in phase-amplitude coupling at the respective stimulation site. In addition, phase-amplitude coupling was found to be enhanced also over other cortical sites. A direct comparison of sTMS and rTMS showed in this context that the latter stimulation paradigm induced a significantly more extensive propagation of coupling enhancement than the former paradigm. Together, these results indicate that TMS can be successfully applied to increase the detectability of phase-amplitude coupling in scalp recordings of neural activity. They thereby open the door to the method's application in various lines of research revolving around intrinsic brain activity, e.g., concerning a tentative relationship between the strength of intrinsic oscillatory nesting and healthy or pathological mental functioning. Explicitly probing an individual's inherent capacity for such nesting has the potential to uncover the neural basis of particular psychological traits and states and to provide an apt biomarker of neurological or psychiatric disease.

While the two main projects of the current thesis tackled different subtopics in the realm of intrinsic brain activity, they both help toward a better understanding of this activation mode. Both projects focused on the puzzling temporo-spatial dynamics of such activity, with the temporal signal evolution having been assessed either via slow fluctuations (first project) or faster oscillatory phases (second project). The inherent properties, settings, and consequences of the addressed neural fluctuations and oscillations were spotlighted as these phenomena might lie at the very core of human functional brain organization. Evidence for the functional relevance of dynamic intrinsic brain activity, which can range from contributions to basic perception or action up to interactions with high-level mental processes such as decision-making, cognitive control, and the formation of unified conscious experiences, is an essential advocate for its right to exist. Such evidence, though, can only be provided with sensitive measures of brain activity, which need to be non-invasive in order to be applicable to broad

and representative samples of the human population. EEG is a feasible and widely-used method in this regard, since it is relatively inexpensive, mobile, and can generate data at a high temporal resolution on the order of milliseconds. Even though notable discoveries have indeed been made with EEG, the method's power is undoubtedly limited by its low spatial resolution, with the captured electrophysiological signal reflecting not single neuronal sources but the summed, and in the process partly nullified, potentials of tens of thousands of active neurons. The ability to measure the mechanisms of intrinsic brain activity without this limitation or with it at least being diminished (and without raising new limitations by switching to entirely different methods such as fMRI) constitutes a valuable asset to understanding the activity's functional relevance. Concurrent TMS-EEG, as brought forward in the second main project, can fulfill this demand and pave the way for comprehensive examinations of intrinsic brain activity and its relation to mental functioning, with an exemplary research question behind such examinations having been presented in the first main project. Although intrinsic brain activity is not understood in its entirety yet, a solid fundament has thus been built for future discoveries in the field.

4.2 Methodological Considerations

Nonetheless, a number of methodological considerations concerning the two presented research projects can be brought up and will be discussed in detail in the current section.

A major challenge with regard to the first main project has been the adequate operationalization of a concept as abstract as conscious awareness, with such an operationalization being required to make the concept measurable in empirical observations. So what is the best way to quantify the extent to which participants become aware of a sensory stimulus? There is an ongoing debate about the most suitable approach to access conscious experience in cognitive neuroscience and experimental psychology (see Sandberg

et al. 2010; Seth et al. 2008; Zehetleitner and Rausch 2013) and a generally agreed-upon answer is still pending. Several behavioral measures of consciousness have been proposed, among them objective measures such as performance accuracy and subjective measures such as ratings of the clarity of sensory experiences or ratings of confidence, as used here (for a comparison of subjective consciousness measures, see Zehetleitner and Rausch 2013). The choice of a particular empirical measure is often driven by a particular theoretical understanding of what consciousness actually is, with views again diverging among different scientists and philosophers: While a mental state might already be considered conscious if it can express its content in behavior, other approaches require a person to be aware of being in that state (see Seth et al. 2008, for an insightful review of relevant theories and associated behavioral measures). Confidence ratings reflect an implementation of the latter notion, with consciousness being characterized by self-monitoring or “the ability to conceive and make use of internal representations of one’s own knowledge and abilities” (Dehaene et al. 2017). The results of the first main project thus need to be understood in terms of this meta-cognitive interpretation of conscious visual perception and provide only limited insight into other, potentially distinguishable forms of consciousness.

A further debatable issue of the first main project concerns the mode of action through which slow fluctuations in intrinsic brain activity ultimately impact on the fast local processing associated with moment-to-moment perception. While a nested hierarchy of oscillations in the traditional frequency bands has been found by others to control neuronal excitability and thus stimulus-related responses via cross-frequency interactions and in particular phase-amplitude coupling (e.g., Canolty et al. 2006; Lakatos et al. 2005; Tort et al. 2010), a corresponding mechanism incorporating SCPs could not be detected in the current project. Slow activity fluctuations have been shown to exhibit phase-amplitude coupling among their own subfrequency bands (Huang et al. 2017) and may thus be suited to also modulate activity in

faster bands such as the alpha and/or gamma band (see Monto et al. 2008; Vanhatalo et al. 2004) in order to control local visual processing. The (unreported) null result of the presented research project does by no means exclude this possibility and might be simply caused by an insufficient signal-to-noise ratio within the artifact-prone frequency range of SCPs (for a description of relevant artifacts, see Birbaumer et al. 1990). As long as evidence for this mechanism or a different process is missing though, the underlying mode of action of SCPs remains only incompletely understood. Such understanding is further limited by the low spatial resolution of scalp EEG, with any statements about top-down global-to-local modulations of neural activity being merely tentative (e.g., regarding the exact brain areas that generate and drive relevant fluctuations in SCPs).

The second main project faced an entirely different set of challenges, centered on our hypothesis that TMS can enhance the detectability of intrinsic phase-amplitude coupling by synchronizing natural neural oscillators. While this hypothesis is highly compatible with the findings presented by us and others (Thut et al. 2011b), irrevocable evidence for it, based on the direct observation of modulated oscillators, is still missing. Alternatively to the hypothesized mechanism, one might ascribe the observed increase in macroscopic phase-amplitude coupling to the generation of entirely novel coupling overlaid on top of intrinsic brain activity. Given that different cortical regions exhibit different oscillatory profiles (Rosanova et al. 2009), a TMS-induced modulation of intrinsic phase-amplitude coupling should entail differences in phase-amplitude coupling enhancement between motor and visual stimulation. While such differences were not apparent in the current project and could have been obscured by the relatively high stimulation intensity, a quantitative investigation targeted at particular intrinsic modules, present already before stimulation and altered afterwards, may be able to reveal regionally distinct effects of TMS in the future, with a conclusive answer in this matter still being pending. Apart from this objection, one might be inclined to attribute

the reported effects to no neural mechanism at all but simply to artifacts brought about by the TMS pulses. TMS has indeed been shown to produce a number of artifacts in EEG recordings, which originate, e.g., from interactions between the magnetic field and the recording equipment (Herring et al. 2015; Ilmoniemi and Kičić 2010; Rogasch et al. 2017). In the current project, established techniques to attenuate these artifacts have been applied, including the linear-interpolation-based substitution of affected data segments and the removal of artifact components via independent component analyses. The occurrence of spurious phase-amplitude coupling has been further reduced by assessing all effects relative to sham stimulation and by determining significance via surrogate-based permutation testing. It has to be acknowledged, though, that TMS-related artifacts cannot be entirely eliminated from EEG data, especially not within the analyzed period directly enclosing the pulses, and that neither sham stimulation (which did not control for TMS-induced somatosensory inputs in the presented project) nor surrogate analyses can preclude their influence completely. As there is currently no technique available to entirely prevent TMS artifacts in the EEG signal during data recording or analysis, any findings resulting from concurrent TMS-EEG need to be critically evaluated against this background. However, given that novel technological and analytical advancements are brought up regularly, future investigations are likely to reduce this concern, with evidence that TMS does in fact interact with intrinsic brain activity already now accumulating (e.g., Eldaief et al. 2011; Kundu et al. 2014; van der Werf et al. 2010).

4.3 Future Directions and Already Accomplished Steps

As foreshadowed in the previous section, research on intrinsic brain activity, and in particular on the two topics addressed by the current thesis' two main projects, is not completed yet. While a number of relevant future research projects are conceivable, including the targeted and more fine-grained investigation of cross-frequency interactions between SCPs and faster neural oscillations, the comparison of such interactions between different behavioral measures

of conscious awareness, and their modulation by TMS, the current section focuses on one project in particular. This project addresses the limited spatial resolution of scalp (DC-)EEG in a different manner, by combining the method with simultaneous fMRI, and has already been initialized by the current thesis' author and colleagues (i.e., by Sarah Glim, Anja Ries, Cristiana Dimulescu, Christian Sorg, and Afra M. Wohlschläger). In the following, the rationale behind this project is presented, together with an overview of the already completed data collection and (pre-)processing steps. Even though final results are still pending, the project should be able to convey a sound impression of how concurrent fMRI-EEG can be utilized in the future to advance research on intrinsic brain activity.

Slow electrophysiological fluctuations in brain activity, generally known as SCPs, have been ascribed a particularly prominent role in neural information integration (He and Raichle 2009). While we were able to show in the current thesis' first main project that the intrinsic evolution of SCPs is related to the emergence of conscious visual perception, the precise integrative mechanisms underlying this relationship remained partly elusive, owing to the low spatial resolution of the obtained EEG measurements. As mentioned above though, SCPs seem to be accessible not only via electrophysiology but might constitute a direct correlate of the fMRI BOLD signal with its equally slow temporal dynamics (He and Raichle 2009; Khader et al. 2008). This hypothesis, for which evidence is more and more accumulating (He et al. 2008; Hiltunen et al. 2014; note also the close correspondence of findings obtained in the current thesis' first main project and by Wohlschläger et al. 2016), opens up the possibility to examine intrinsic SCPs, their relation to faster neural oscillations (which have been associated with the BOLD signal via power fluctuations; Goldman et al. 2002; Mantini et al. 2007; Sadaghiani et al. 2010), and to behavior at both a high temporal and a high spatial resolution. With the initialized fMRI-EEG project, we aim at (1) providing further evidence for a direct mapping of electrophysiological SCPs and the hemodynamic BOLD signal in its

raw fluctuations and at (2) characterizing the precise temporo-spatial layout of functionally relevant intrinsic brain activity in the context of SCPs and emerging visual consciousness. In particular, we are interested in the dynamic configuration of brain areas and networks that drive the modulation and integration of incoming visual information - before, during, and after local visual processing - and in the oscillatory mechanisms reflecting such proceedings.

To pursue this research interest, the following measurements were conducted. 25 healthy adults were assessed on two testing days each. The first day started with a training session of the same visual backward-masking task that was applied already in the current thesis' first main project and, in a modified form, by Wohlschläger and colleagues (Wohlschläger et al. 2016; with each trial requiring the localization of the missing part of a briefly presented target stimulus, followed by a confidence rating). After this behavioral training, participants underwent 10 min of eyes-closed resting state fMRI with an occipital field of view, inclusively measurements of their electrodermal activity, heart rate, oxygen saturation, and respiration, as well as a retinotopy fMRI session, during which an expanding and rotating checkerboard stimulus had to be observed while maintaining central fixation. Both fMRI measurements were performed to enable an exact delineation of early visual areas during later data processing (see Engel et al. 1994; Sereno et al. 1995; Wig et al. 2014). The first testing day was concluded with a T1-weighted anatomical MRI scan and a routine clinical scan employed to check for incidental clinical findings. On the second testing day, participants started again by training the visual backward-masking task and then carried out one block of 100 trials of this task with concurrent EEG. The latter measurement was conducted to obtain electrophysiological data free from fMRI artifacts for subsequent data quality checks. Afterwards, whole-brain fMRI-EEG was recorded during (1) 10 min of eyes-closed resting state and (2) 4 blocks of 100 trials each of the visual task. These measurements were again accompanied by the simultaneous recording of a number of physiological parameters, namely

electrodermal activity, heart rate, oxygen saturation, and respiration, which provide valuable information for the reduction of non-neuronal noise in the signals of interest (see e.g., Birn et al. 2008; Chang et al. 2009). Finally, participants completed the “Student Opinion Scale” (with the word “test” replaced by “task”; Sundre 2007) as a measure of their overall study motivation. After the data acquisition phase had been completed, the collected data were preprocessed, which - for the task fMRI data - corresponded to slice timing correction, realignment and unwarping, co-registration of the anatomical image, segmentation, normalization, and spatial smoothing. With regard to the concurrent task EEG data, preprocessing comprised the correction of scanner and cardioballistic artifacts specific to combined fMRI-EEG recordings (Allen et al. 1998, 2000), therein included low-pass filtering, DC detrending (Hennighausen et al. 1993), the independent-component-analysis-based removal of artifacts originating from eye movements, eye blinks, and other muscular activity (Hipp and Siegel 2013; Jung et al. 2000), re-referencing, as well as down-sampling. As to all data, trials were rejected if they contained any remaining artifacts in the collected signals, if the presented target stimulus was obscured by an eye blink occurring immediately around it, or if participants’ button presses were invalid, regarding either the number of presses or the used buttons. Besides these routines, further processing steps are currently being implemented or planned, including the integration of retinotopic maps and of the recorded physiological parameters.

With this comprehensive, ready-to-use data set at hand, manifold analyses are possible in future research projects, targeting the abovementioned study aims and numerous others. Concurrent fMRI-EEG, albeit being a technologically and methodologically demanding method, offers the valuable possibility to examine neural mechanisms and processes non-invasively at a high spatial and high temporal resolution and should thereby enable novel insights into intrinsic brain activity that are barely achievable otherwise. An essential first step

toward such insights has been made with the preparation of the presented task and rest fMRI-EEG data set, which will be made available upon reasonable request.

4.4 Conclusions

Intrinsic brain activity is widely accepted these days as the basic scaffold of human neural functioning. The restless brain is believed to set the stage for survival by predicting environmental changes; it processes and maintains behaviorally relevant information and tunes its internal structures to enhance responses and improve performance (Raichle 2011, 2015). Accordingly, intrinsic brain activity commands the majority of the brain's energy resources (Raichle and Mintun 2006) and is engaging an ever-growing research community. Much insight has been gained already on the dynamic temporo-spatial layout of this activity, on its (non-invasive) measurability, and on its significance for human perception, cognition, and behavior. Nonetheless, the precise mechanisms underlying its generation and evolution, ranging from the level of cell biology to network-level neuroscience, are not understood in their entirety yet and more work is required to illuminate the importance of intrinsic brain activity for healthy and diseased mental functioning.

With the current thesis, a relevant step is made toward a more complete understanding of a number of these topics. The thesis offers original findings on (1) the functional relevance of EEG-recorded intrinsic brain activity, specifically with regard to the relation between slowly evolving fluctuations in such activity and the emergence of conscious visual perception, and on (2) its non-invasive detection, which has been shown by us to improve - in the case of intrinsic phase-amplitude coupling - with concurrent TMS-EEG. These findings can open the door for future studies aimed at examining the functional relevance of (nested) oscillatory mechanisms at an enhanced signal-to-noise ratio. An enhanced spatial resolution can be

furthermore achieved with concurrent fMRI-EEG, a large data set of which was additionally outlined above.

In conclusion, the current thesis provides novel content-related and methodology-related insights into the dynamics of intrinsic brain activity, as recorded non-invasively with scalp EEG, and thereby complements existing literature on this critical subject of modern neuroscience. The aspired comprehensive decoding of intrinsic brain activity might be able to advance personalized medicine in the field of neurological and psychiatric disorders and to serve as a model for artificial neural systems in the conceivable future, with exciting developments lying ahead of us.

REFERENCES

- Alahmadi N, Evdokimov SA, Kropotov Y, Müller AM, Jäncke L.** Different resting state EEG features in children from Switzerland and Saudi Arabia. *Front Hum Neurosci* 10: 559, 2016.
- Allen EA, Damaraju E, Plis SM, Erhardt EB, Eichele T, Calhoun VD.** Tracking whole-brain connectivity dynamics in the resting state. *Cereb Cortex* 24: 663-676, 2014.
- Allen PJ, Josephs O, Turner R.** A method for removing imaging artifact from continuous EEG recorded during functional MRI. *Neuroimage* 12: 230-239, 2000.
- Allen PJ, Polizzi G, Krakow K, Fish DR, Lemieux L.** Identification of EEG events in the MR scanner: The problem of pulse artifact and a method for its subtraction. *Neuroimage* 8: 229-239, 1998.
- Berger H.** Über das Elektrenkephalogramm des Menschen. *Archiv für Psychiatrie und Nervenkrankheiten* 87: 527-570, 1929.
- Birbaumer N, Elbert T, Canavan AGM, Rockstroh B.** Slow potentials of the cerebral cortex and behavior. *Physiol Rev* 70: 1-41, 1990.
- Birn RM, Smith MA, Jones TB, Bandettini PA.** The respiration response function: The temporal dynamics of fMRI signal fluctuations related to changes in respiration. *Neuroimage* 40: 644-654, 2008.
- Biswal B, Yetkin FZ, Haughton VM, Hyde JS.** Functional connectivity in the motor cortex of resting human brain using echo-planar MRI. *Magn Reson Med* 34: 537-541, 1995.
- Bonnefond M, Jensen O.** Gamma activity coupled to alpha phase as a mechanism for top-down controlled gating. *PLoS One* 10: e0128667, 2015.

Britz J, Díaz Hernández L, Ro T, Michel CM. EEG-microstate dependent emergence of perceptual awareness. *Front Behav Neurosci* 8: 163, 2014.

Brueggen K, Fiala C, Berger C, Ochmann S, Babiloni C, Teipel SJ. Early changes in alpha band power and DMN BOLD activity in Alzheimer's disease: A simultaneous resting state EEG-fMRI study. *Front Aging Neurosci* 9: 319, 2017.

Buckner RL, Andrews-Hanna JR, Schacter DL. The brain's default network: Anatomy, function, and relevance to disease. *Ann N Y Acad Sci* 1124: 1-38, 2008.

Busch NA, Dubois J, VanRullen R. The phase of ongoing EEG oscillations predicts visual perception. *J Neurosci* 29: 7869-7876, 2009.

Canolty RT, Edwards E, Dalal SS, Soltani M, Nagarajan SS, Kirsch HE, Berger MS, Barbaro NM, Knight RT. High gamma power is phase-locked to theta oscillations in human neocortex. *Science* 313: 1626-1628, 2006.

Canolty RT, Knight RT. The functional role of cross-frequency coupling. *Trends Cogn Sci* 14: 506-515, 2010.

Chang C, Cunningham JP, Glover GH. Influence of heart rate on the BOLD signal: The cardiac response function. *Neuroimage* 44: 857-869, 2009.

Clark A. Whatever next? Predictive brains, situated agents, and the future of cognitive science. *Behav Brain Sci* 36: 181-204, 2013.

Dawson GD. A summation technique for the detection of small evoked potentials. *Electroencephalogr Clin Neurophysiol* 6: 65-84, 1954.

de Pasquale F, Corbetta M, Betti V, Della Penna S. Cortical cores in network dynamics. *Neuroimage* (September 30, 2017). doi: 10.1016/j.neuroimage.2017.09.063.

de Vos F, Koini M, Schouten TM, Seiler S, van der Grond J, Lechner A, Schmidt R, de Rooij M, Rombouts SARB. A comprehensive analysis of resting state fMRI measures to classify individual patients with Alzheimer's disease. *Neuroimage* 167: 62-72, 2018.

Deco G, Cabral J, Woolrich MW, Stevner ABA, van Hartevelt TJ, Kringelbach ML. Single or multiple frequency generators in on-going brain activity: A mechanistic whole-brain model of empirical MEG data. *Neuroimage* 152: 538-550, 2017.

Dehaene S, Lau H, Kouider S. What is consciousness, and could machines have it? *Science* 358: 486-492, 2017.

Devrim M, Demiralp T, Kurt A, Yücesir I. Slow cortical potential shifts modulate the sensory threshold in human visual system. *Neurosci Lett* 270: 17-20, 1999.

Dong D, Wang Y, Chang X, Luo C, Yao D. Dysfunction of large-scale brain networks in schizophrenia: A meta-analysis of resting-state functional connectivity. *Schizophr Bull* 44: 168-181, 2018.

Ekman M, Derrfuss J, Tittgemeyer M, Fiebach CJ. Predicting errors from reconfiguration patterns in human brain networks. *Proc Natl Acad Sci U S A* 109: 16714-16719, 2012.

Eldaief MC, Halko MA, Buckner RL, Pascual-Leone A. Transcranial magnetic stimulation modulates the brain's intrinsic activity in a frequency-dependent manner. *Proc Natl Acad Sci U S A* 108: 21229-21234, 2011.

Engel SA, Rumelhart DE, Wandell BA, Lee AT, Glover GH, Chichilnisky E-J, Shadlen MN. fMRI of human visual cortex. *Nature* 369: 525, 1994.

Ergenoglu T, Demiralp T, Bayraktaroglu Z, Ergen M, Beydagi H, Uresin Y. Alpha rhythm of the EEG modulates visual detection performance in humans. *Brain Res Cogn Brain Res* 20: 376-383, 2004.

Fox MD, Snyder AZ, Vincent JL, Raichle ME. Intrinsic fluctuations within cortical systems account for intertrial variability in human behavior. *Neuron* 56: 171-184, 2007.

Fox MD, Snyder AZ, Zacks JM, Raichle ME. Coherent spontaneous activity accounts for trial-to-trial variability in human evoked brain responses. *Nat Neurosci* 9: 23-25, 2006.

Friston KJ, Kahan J, Biswal B, Razi A. A DCM for resting state fMRI. *Neuroimage* 94: 396-407, 2014.

Goldman RI, Stern JM, Engel J Jr, Cohen MS. Simultaneous EEG and fMRI of the alpha rhythm. *Neuroreport* 13: 2487-2492, 2002.

Greicius M. Resting-state functional connectivity in neuropsychiatric disorders. *Curr Opin Neurol* 21: 424-430, 2008.

Greicius MD, Krasnow B, Reiss AL, Menon V. Functional connectivity in the resting brain: A network analysis of the default mode hypothesis. *Proc Natl Acad Sci U S A* 100: 253-258, 2003.

He BJ, Raichle ME. The fMRI signal, slow cortical potential and consciousness. *Trends Cogn Sci* 13: 302-309, 2009.

He BJ, Snyder AZ, Zempel JM, Smyth MD, Raichle ME. Electrophysiological correlates of the brain's intrinsic large-scale functional architecture. *Proc Natl Acad Sci U S A* 105: 16039-16044, 2008.

Hennighausen E, Heil M, Rösler F. A correction method for DC drift artifacts. *Electroencephalogr Clin Neurophysiol* 86: 199-204, 1993.

Henrie JA, Shapley R. LFP power spectra in V1 cortex: The graded effect of stimulus contrast. *J Neurophysiol* 94: 479-490, 2005.

Herring JD, Thut G, Jensen O, Bergmann TO. Attention modulates TMS-locked alpha oscillations in the visual cortex. *J Neurosci* 35: 14435-14447, 2015.

Hesselmann G, Kell CA, Eger E, Kleinschmidt A. Spontaneous local variations in ongoing neural activity bias perceptual decisions. *Proc Natl Acad Sci U S A* 105: 10984-10989, 2008a.

Hesselmann G, Kell CA, Kleinschmidt A. Ongoing activity fluctuations in hMT+ bias the perception of coherent visual motion. *J Neurosci* 28: 14481-14485, 2008b.

Hiltunen T, Kantola J, Abou Elseoud A, Lepola P, Suominen K, Starck T, Nikkinen J, Remes J, Tervonen O, Palva S, Kiviniemi V, Palva JM. Infra-slow EEG fluctuations are correlated with resting-state network dynamics in fMRI. *J Neurosci* 34: 356-362, 2014.

Hipp JF, Siegel M. Dissociating neuronal gamma-band activity from cranial and ocular muscle activity in EEG. *Front Hum Neurosci* 7: 338, 2013.

Huang Z, Zhang J, Longtin A, Dumont G, Duncan NW, Pokorny J, Qin P, Dai R, Ferri F, Weng X, Northoff G. Is there a nonadditive interaction between spontaneous and evoked activity? Phase-dependence and its relation to the temporal structure of scale-free brain activity. *Cereb Cortex* 27: 1037-1059, 2017.

Huster RJ, Debener S, Eichele T, Herrmann CS. Methods for simultaneous EEG-fMRI: An introductory review. *J Neurosci* 32: 6053-6060, 2012.

Ilmoniemi RJ, Kičić D. Methodology for combined TMS and EEG. *Brain Topogr* 22: 233-248, 2010.

Jensen O, Mazaheri A. Shaping functional architecture by oscillatory alpha activity: Gating by inhibition. *Front Hum Neurosci* 4: 186, 2010.

- Jung T-P, Makeig S, Humphries C, Lee T-W, McKeown MJ, Iragui V, Sejnowski TJ.** Removing electroencephalographic artifacts by blind source separation. *Psychophysiology* 37: 163-178, 2000.
- Karbasforoushan H, Woodward ND.** Resting-state networks in schizophrenia. *Curr Top Med Chem* 12: 2404-2414, 2012.
- Khader P, Schicke T, Röder B, Rösler F.** On the relationship between slow cortical potentials and BOLD signal changes in humans. *Int J Psychophysiol* 67: 252-261, 2008.
- Khan AJ, Nair A, Keown CL, Datko MC, Lincoln AJ, Müller R-A.** Cerebro-cerebellar resting-state functional connectivity in children and adolescents with autism spectrum disorder. *Biol Psychiatry* 78: 625-634, 2015.
- Kirino E, Tanaka S, Fukuta M, Inami R, Arai H, Inoue R, Aoki S.** Simultaneous resting-state functional MRI and electroencephalography recordings of functional connectivity in patients with schizophrenia. *Psychiatry Clin Neurosci* 71: 262-270, 2017.
- Klimesch W, Sauseng P, Hanslmayr S.** EEG alpha oscillations: The inhibition-timing hypothesis. *Brain Res Rev* 53: 63-88, 2007.
- Koivisto M, Lähteenmäki M, Sørensen TA, Vangkilde S, Overgaard M, Revonsuo A.** The earliest electrophysiological correlate of visual awareness? *Brain Cogn* 66: 91-103, 2008.
- Kundu B, Johnson JS, Postle BR.** Prestimulation phase predicts the TMS-evoked response. *J Neurophysiol* 112: 1885-1893, 2014.
- Kwong KK, Belliveau JW, Chesler DA, Goldberg IE, Weisskoff RM, Poncelet BP, Kennedy DN, Hoppel BE, Cohen MS, Turner R, Cheng H-M, Brady TJ, Rosen BR.** Dynamic magnetic resonance imaging of human brain activity during primary sensory stimulation. *Proc Natl Acad Sci U S A* 89: 5675-5679, 1992.

Lakatos P, Shah AS, Knuth KH, Ulbert I, Karmos G, Schroeder CE. An oscillatory hierarchy controlling neuronal excitability and stimulus processing in the auditory cortex. *J Neurophysiol* 94: 1904-1911, 2005.

Lee MH, Hacker CD, Snyder AZ, Corbetta M, Zhang D, Leuthardt EC, Shimony JS. Clustering of resting state networks. *PLoS One* 7: e40370, 2012.

Mantini D, Perrucci MG, Del Gratta C, Romani GL, Corbetta M. Electrophysiological signatures of resting state networks in the human brain. *Proc Natl Acad Sci U S A* 104: 13170-13175, 2007.

Massimini M, Ferrarelli F, Huber R, Esser SK, Singh H, Tononi G. Breakdown of cortical effective connectivity during sleep. *Science* 309: 2228-2232, 2005.

Mathewson KE, Gratton G, Fabiani M, Beck DM, Ro T. To see or not to see: Prestimulus α phase predicts visual awareness. *J Neurosci* 29: 2725-2732, 2009.

Mazaheri A, Jensen O. Rhythmic pulsing: Linking ongoing brain activity with evoked responses. *Front Hum Neurosci* 4: 177, 2010.

Melloni L, Molina C, Pena M, Torres D, Singer W, Rodriguez E. Synchronization of neural activity across cortical areas correlates with conscious perception. *J Neurosci* 27: 2858-2865, 2007.

Menon V. Large-scale brain networks and psychopathology: A unifying triple network model. *Trends Cogn Sci* 15: 483-506, 2011.

Mitra A, Snyder AZ, Blazey T, Raichle ME. Lag threads organize the brain's intrinsic activity. *Proc Natl Acad Sci U S A* 112: E2235-E2244, 2015.

Monto S, Palva S, Voipio J, Palva JM. Very slow EEG fluctuations predict the dynamics of stimulus detection and oscillation amplitudes in humans. *J Neurosci* 28: 8268-8272, 2008.

Murphy K, Birn RM, Bandettini PA. Resting-state fMRI confounds and cleanup. *Neuroimage* 80: 349-359, 2013.

Niessing J, Ebisch B, Schmidt KE, Niessing M, Singer W, Galuske RAW. Hemodynamic signals correlate tightly with synchronized gamma oscillations. *Science* 309: 948-951, 2005.

Northoff G. “Paradox of slow frequencies” - Are slow frequencies in upper cortical layers a neural predisposition of the level/state of consciousness (NPC)? *Conscious Cogn* 54: 20-35, 2017.

Northoff G, Huang Z. How do the brain’s time and space mediate consciousness and its different dimensions? Temporo-spatial theory of consciousness (TTC). *Neurosci Biobehav Rev* 80: 630-645, 2017.

Ogawa S, Lee TM, Kay AR, Tank DW. Brain magnetic resonance imaging with contrast dependent on blood oxygenation. *Proc Natl Acad Sci U S A* 87: 9868-9872, 1990.

Osipova D, Hermes D, Jensen O. Gamma power is phase-locked to posterior alpha activity. *PLoS One* 3: e3990, 2008.

Papagiannopoulou EA, Lagopoulos J. Resting state EEG hemispheric power asymmetry in children with dyslexia. *Front Pediatr* 4: 11, 2016.

Pesaran B, Pezaris JS, Sahani M, Mitra PP, Andersen RA. Temporal structure in neuronal activity during working memory in macaque parietal cortex. *Nat Neurosci* 5: 805-811, 2002.

Raichle ME. Two views of brain function. *Trends Cogn Sci* 14: 180-190, 2010.

Raichle ME. The restless brain. *Brain Connect* 1: 3-12, 2011.

Raichle ME. The restless brain: How intrinsic activity organizes brain function. *Philos Trans R Soc Lond B Biol Sci* 370: 20140172, 2015.

Raichle ME, MacLeod AM, Snyder AZ, Powers WJ, Gusnard DA, Shulman GL. A default mode of brain function. *Proc Natl Acad Sci U S A* 98: 676-682, 2001.

Raichle ME, Mintun MA. Brain work and brain imaging. *Annu Rev Neurosci* 29: 449-476, 2006.

Ritter P, Moosmann M, Villringer A. Rolandic alpha and beta EEG rhythms' strengths are inversely related to fMRI-BOLD signal in primary somatosensory and motor cortex. *Hum Brain Mapp* 30: 1168-1187, 2009.

Rogasch NC, Sullivan C, Thomson RH, Rose NS, Bailey NW, Fitzgerald PB, Farzan F, Hernandez-Pavon JC. Analysing concurrent transcranial magnetic stimulation and electroencephalographic data: A review and introduction to the open-source TESA software. *Neuroimage* 147: 934-951, 2017.

Rosanova M, Casali A, Bellina V, Resta F, Mariotti M, Massimini M. Natural frequencies of human corticothalamic circuits. *J Neurosci* 29: 7679-7685, 2009.

Sacchet MD, Ho TC, Connolly CG, Tymofiyeva O, Lewinn KZ, Han LKM, Blom EH, Tapert SF, Max JE, Frank GKW, Paulus MP, Simmons AN, Gotlib IH, Yang TT. Large-scale hypoconnectivity between resting-state functional networks in unmedicated adolescent major depressive disorder. *Neuropsychopharmacology* 41: 2951-2960, 2016.

Sadaghiani S, Kleinschmidt A. Functional interactions between intrinsic brain activity and behavior. *Neuroimage* 80: 379-386, 2013.

Sadaghiani S, Scheeringa R, Lehongre K, Morillon B, Giraud A-L, Kleinschmidt A. Intrinsic connectivity networks, alpha oscillations, and tonic alertness: A simultaneous electroencephalography/functional magnetic resonance imaging study. *J Neurosci* 30: 10243-10250, 2010.

Samaha J, Iemi L, Postle BR. Prestimulus alpha-band power biases visual discrimination confidence, but not accuracy. *Conscious Cogn* 54: 47-55, 2017.

Sandberg K, Timmermans B, Overgaard M, Cleeremans A. Measuring consciousness: Is one measure better than the other? *Conscious Cogn* 19: 1069-1078, 2010.

Scheeringa R, Koopmans PJ, van Mourik T, Jensen O, Norris DG. The relationship between oscillatory EEG activity and the laminar-specific BOLD signal. *Proc Natl Acad Sci USA* 113: 6761-6766, 2016.

Scheeringa R, Mazaheri A, Bojak I, Norris DG, Kleinschmidt A. Modulation of visually evoked cortical fMRI responses by phase of ongoing occipital alpha oscillations. *J Neurosci* 31: 3813-3820, 2011.

Scheeringa R, Petersson KM, Kleinschmidt A, Jensen O, Bastiaansen MCM. EEG alpha power modulation of fMRI resting-state connectivity. *Brain Connect* 2: 254-264, 2012.

Schölvinck ML, Friston KJ, Rees G. The influence of spontaneous activity on stimulus processing in primary visual cortex. *Neuroimage* 59: 2700-2708, 2012.

Sereno MI, Dale AM, Reppas JB, Kwong KK, Belliveau JW, Brady TJ, Rosen BR, Tootell RBH. Borders of multiple visual areas in humans revealed by functional magnetic resonance imaging. *Science* 268: 889-893, 1995.

Seth AK, Dienes Z, Cleeremans A, Overgaard M, Pessoa L. Measuring consciousness: Relating behavioural and neurophysiological approaches. *Trends Cogn Sci* 12: 314-321, 2008.

Sherman MT, Kanai R, Seth AK, VanRullen R. Rhythmic influence of top-down perceptual priors in the phase of prestimulus occipital alpha oscillations. *J Cogn Neurosci* 28: 1318-1330, 2016.

Shulman GL, Fiez JA, Corbetta M, Buckner RL, Miezin FM, Raichle ME, Petersen SE. Common blood flow changes across visual tasks: II. Decreases in cerebral cortex. *J Cogn Neurosci* 9: 648-663, 1997.

Smith SM, Vidaurre D, Beckmann CF, Glasser MF, Jenkinson M, Miller KL, Nichols TE, Robinson EC, Salimi-Khorshidi G, Woolrich MW, Barch DM, Uğurbil K, Van Essen DC. Functional connectomics from resting-state fMRI. *Trends Cogn Sci* 17: 666-682, 2013.

Sundre DL. *The Student Opinion Scale (SOS): A measure of examinee motivation.* Harrisonburg, VA: Center for Assessment & Research Studies, 2007.

Thut G, Schyns PG, Gross J. Entrainment of perceptually relevant brain oscillations by non-invasive rhythmic stimulation of the human brain. *Front Psychol* 2: 170, 2011a.

Thut G, Veniero D, Romei V, Miniussi C, Schyns P, Gross J. Rhythmic TMS causes local entrainment of natural oscillatory signatures. *Curr Biol* 21: 1176-1185, 2011b.

Tort ABL, Komorowski R, Eichenbaum H, Kopell N. Measuring phase-amplitude coupling between neuronal oscillations of different frequencies. *J Neurophysiol* 104: 1195-1210, 2010.

van den Heuvel MP, Hulshoff Pol HE. Exploring the brain network: A review on resting-state fMRI functional connectivity. *Eur Neuropsychopharmacol* 20: 519-534, 2010.

van der Werf YD, Sanz-Arigita EJ, Menning S, van den Heuvel OA. Modulating spontaneous brain activity using repetitive transcranial magnetic stimulation. *BMC Neurosci* 11: 145, 2010.

van Dijk H, Schoffelen J-M, Oostenveld R, Jensen O. Prestimulus oscillatory activity in the alpha band predicts visual discrimination ability. *J Neurosci* 28: 1816-1823, 2008.

Vanhatalo S, Palva JM, Holmes MD, Miller JW, Voipio J, Kaila K. Infraslow oscillations modulate excitability and interictal epileptic activity in the human cortex during sleep. *Proc Natl Acad Sci U S A* 101: 5053-5057, 2004.

Wang J, Fang Y, Wang X, Yang H, Yu X, Wang H. Enhanced gamma activity and cross-frequency interaction of resting-state electroencephalographic oscillations in patients with Alzheimer's disease. *Front Aging Neurosci* 9: 243, 2017.

Wang J, Zuo X, He Y. Graph-based network analysis of resting-state functional MRI. *Front Syst Neurosci* 4: 16, 2010.

Wig GS, Laumann TO, Petersen SE. An approach for parcellating human cortical areas using resting-state correlations. *Neuroimage* 93: 276-291, 2014.

Wohlschläger AM, Glim S, Shao J, Draheim J, Köhler L, Lourenço S, Riedl V, Sorg C. Ongoing slow fluctuations in V1 impact on visual perception. *Front Hum Neurosci* 10: 411, 2016.

Workman CI, Lythe KE, McKie S, Moll J, Gethin JA, Deakin JFW, Elliott R, Zahn R. A novel resting-state functional magnetic resonance imaging signature of resilience to recurrent depression. *Psychol Med* 47: 597-607, 2017.

Ye AX, Leung RC, Schäfer CB, Taylor MJ, Doesburg SM. Atypical resting synchrony in autism spectrum disorder. *Hum Brain Mapp* 35: 6049-6066, 2014.

Yerys BE, Herrington JD, Satterthwaite TD, Guy L, Schultz RT, Bassett DS. Globally weaker and topologically different: Resting-state connectivity in youth with autism. *Mol Autism* 8: 39, 2017.

Zehetleitner M, Rausch M. Being confident without seeing: What subjective measures of visual consciousness are about. *Atten Percept Psychophys* 75: 1406-1426, 2013.

Zhou M, Hu X, Lu L, Zhang L, Chen L, Gong Q, Huang X. Intrinsic cerebral activity at resting state in adults with major depressive disorder: A meta-analysis. *Prog Neuropsychopharmacol Biol Psychiatry* 75: 157-164, 2017.

ACKNOWLEDGMENTS

I would like to thank all those people without whom this thesis would not have been possible.

First and foremost, my thanks go to my supervisor Afra Wohlschläger, whose continuous excitement and tireless enthusiasm about science has become the fundament of all our joint research projects. Yet, these projects could not have been completed the way they have been without invaluable advice also from Christian Sorg, with whom I have enjoyed countless inspiring discussions. I am grateful as well to all my other colleagues at the Technical University of Munich, for having been part of this exciting journey and for making every working day an enjoyable and delightful one.

In addition, I would like to thank my colleagues at the RIKEN Brain Science Institute, especially Keiichi Kitajo and Yuka Okazaki, for the amazing summer that I was allowed to spend in their lab and for the stimulating collaboration that followed. Not only did they enable me to broaden my knowledge and skills, but they made me feel welcome from the very first minute and they showed me the beauty of international exchange - in science and beyond.

Last but not least, I am deeply grateful to my family and friends for bearing with me during this eventful chapter of my life. I would like to thank my brother Sebastian, who has always supported and encouraged me and helped me through all struggles, and my parents, for the same reasons and many more.

CURRICULUM VITAE

EDUCATION

- Since 2014: *PhD in Systemic Neurosciences*
Ludwig-Maximilians-Universität München, Germany
- 2012 - 2014: *MSc in Neuro-Cognitive Psychology*
Ludwig-Maximilians-Universität München, Germany
- 2009 - 2012: *BSc in Psychology*
Georg-August-Universität Göttingen, Germany
- 2006 - 2009: *Abitur*
Geschwister-Scholl-Schule Melsungen, Germany

RESEARCH POSITIONS

- Since 2016: *Student Trainee*
RIKEN Brain Science Institute, Japan
- Since 2014: *Research Associate*
Department of Neuroradiology
Technische Universität München, Germany
- 2013: *Research Intern*
Department of Experimental Psychology
University of Oxford, United Kingdom
- 2013: *Research Intern*
Chair of Developmental Psychology
Ludwig-Maximilians-Universität München, Germany
- 2011 - 2012: *Research Assistant*
German Primate Center, Germany

LIST OF PUBLICATIONS

Published:

Wohlschläger AM, Glim S, Shao J, Draheim J, Köhler L, Lourenço S, Riedl V, Sorg C. Ongoing slow fluctuations in V1 impact on visual perception. *Front Hum Neurosci* 10: 411, 2016.

Unpublished:

Glim S, Okazaki YO, Nakagawa Y, Mizuno Y, Hanakawa T, Kitajo K. Phase-amplitude coupling of neural oscillations can be effectively probed with concurrent TMS-EEG. Unpublished manuscript.

Glim S, Ries A, Sorg C, Wohlschläger AM. The evolution of pre-stimulus slow cortical potentials is associated with an upcoming stimulus' access to visual consciousness. Unpublished manuscript.

EIDESSTATTLICHE VERSICHERUNG/AFFIDAVIT

Hiermit versichere ich an Eides statt, dass ich die vorliegende Dissertation „Decoding the Functional Relevance of Intrinsic Brain Activity with (TMS-)EEG“ selbstständig angefertigt habe, mich außer der angegebenen keiner weiteren Hilfsmittel bedient und alle Erkenntnisse, die aus dem Schrifttum ganz oder annähernd übernommen sind, als solche kenntlich gemacht und nach ihrer Herkunft unter Bezeichnung der Fundstelle einzeln nachgewiesen habe.

I hereby confirm that the dissertation “Decoding the Functional Relevance of Intrinsic Brain Activity with (TMS-)EEG” is the result of my own work and that I have only used sources or materials listed and specified in the dissertation.

Munich, 14.03.19

Place, date

Sarah Glim

DECLARATION OF AUTHOR CONTRIBUTIONS

Project I: The Evolution of Pre-Stimulus Slow Cortical Potentials is Associated with an Upcoming Stimulus' Access to Visual Consciousness

Authors: Sarah Glim, Anja Ries, Christian Sorg, Afra M. Wohlschläger

Contributions: The author of this thesis is the first author of the manuscript. A.M.W. and C.S. conceived the experiment. **S.G.**, C.S., and A.M.W. designed the experiment. **S.G.** and A.R. collected the data. **S.G.** and A.M.W. analyzed the data. **S.G.** wrote the manuscript. **S.G.**, C.S., and A.M.W. reviewed the manuscript.

Project II: Phase-Amplitude Coupling of Neural Oscillations can be Effectively Probed with Concurrent TMS-EEG

Authors: Sarah Glim, Yuka O. Okazaki, Yumi Nakagawa, Yuji Mizuno, Takashi Hanakawa, Keiichi Kitajo

Contributions: The author of this thesis is the first author of the manuscript. Y.N., T.H., and K.K. conceived and designed the experiment. Y.N., Y.O.O., Y.M., T.H., and K.K. collected the data. **S.G.**, Y.N., Y.O.O., and K.K. analyzed the data. **S.G.**, Y.O.O., and K.K. wrote the manuscript. All authors reviewed the manuscript.

Munich, 14.03.19

Place, date

Sarah Glim

Afra M. Wohlschläger

(Supervisor)